

Influence of Airborne Ocularly Assessed Stand Density on Wildfire Escapes and Containment Challenges

by

Andrew Peter Stack

A thesis submitted in partial fulfillment of the requirements for the degree of

Master of Science

in

Forest Biology and Management

Department of Renewable Resources

University of Alberta

© Andrew Peter Stack, 2024

Abstract

The relationship between increasing forest density and increasing wildfire behaviour is well established. However, in the unique case of initial attack wildfire operations, traditional data collection methods to measure forest density are both impractical and unsafe. As an alternative approach, aerial ocular assessment to rapidly determine forest density and its impacts on wildfire behaviour is examined. Wildfire assessment photography, taken during the initial action phase of wildfire suppression in pure boreal spruce (*Picea mariana*) forests, served as an excellent opportunistic dataset to develop a series of ordinal wildfire behaviour and forest density metrics for testing. This approach explored two scenarios: 1) the effects of forest density on containment escapes, where suppression efforts failed to contain a wildfire to less than 2 hectares before being classified as “being held,” and 2) the effects of forest density on wildfire containment challenges, where crews arrived at an incident where the wildfire had already exceeded 0.5 hectares before suppression began. The ocularly assessed metrics were merged with recorded weather and Fire Weather Index System values from nearby fire weather stations (altogether totaling 33 variables) and analyzed using logistic regression in the form of bi-directional generalized linear models. A parallel study, using LiDAR classification of forest structure in lieu of forest density assessed in wildfire photographs, was also performed.

Results of this study indicate that in three of the four tested scenarios (ocularly assessed density and fire escapes, LiDAR classified forest structure and fire escapes, and LiDAR classified forest structure and containment challenges), forest structure and increasing density were found to be significant with respect to an increase in wildfire behaviour. Further results also highlight the significance of wildfire smoke column attributes in scenario outcomes. The selected models all performed well with C-statistics >0.75, however lacked predictive capability.

Preface

This thesis is an original work was completed without the requirement for ethics approval. All personal and other identifiable information discernable from wildfire photography included herein has been redacted.

Acknowledgements

One sunny day in 1826, French inventor Joseph Nicéphore Niépce pointed a pewter plate covered in lavender oil out his window overlooking his villa for 8 straight hours. The result, entitled “View from the Window at Le Gras,” is credited as the world’s first photograph. It is through Joseph’s accomplishment that this thesis ultimately became possible almost 200 years later.

I wish to express my sincere gratitude to my supervisor, Dr. Jennifer Beverly, who has provided her guidance and expertise in the development of this thesis. Her input has helped shape me as a researcher and driven me to strive for nothing less than the highest quality standard for this work. Thank you as well to the other members of my committee, Daniel Perrakis, and Brad Pinno for their feedback, guidance, and suggestions.

I wish to extend my gratitude to the exclusive funding provided by Alberta Agriculture and Forestry, through the Canadian Partnership for Wildland Fire Science, grant number 18GRWMB06. Thank you also to the Coops Lab at the University of British Columbia, who provided the LiDAR data used in the parallel study of this Thesis.

To the immense help and support provided to me by Alberta Wildfire, who provided the incredible wildfire photos and supplemental data that I used to develop the database used in this thesis, thank you. Thank you also to the members of Alberta Wildfire and the Canadian Forest Service, notably Dave Schroeder, Brett Moore, Dan Thompson, Kelsey Gibos, and everyone else who offered their opinions, guidance, support, and helped foster turning my inner child into a professional that gets paid to light stuff on fire.

To my friends, colleagues, and lab mates, thank you for your incredible support and the invaluable discussions we had as we embarked on our journey as wildfire scientists, most notably Hilary Cameron,

Kate Bezooyen, Air Forbes, Denyse Dawe, Keira Smith, and Olivia Aftergood. Thank you also to Mark Soares, Brian Cechmanek, Robert Campeau, David Gust, and Adam Urkow; you may not be wildfire scientists, but you were with me the whole time.

I cannot understate the challenge that this thesis was to research, develop, and write. It has been undoubtedly the most difficult project I've ever undertaken, but I'm glad I stuck with it, because it's also among the most fulfilling. So last, but definitely not least, saying thank you to my incredible family who supported me the entire time during the ups and downs of this project, does not do you all justice. To my Parents, Monica and Peter, and my Brother, Evan, thank you so much for everything, from helping me learn to turn my nerdy pyrotechnical jargon into Bill Nye-esque science communication, and providing me continuous support as I worked my way to the rank of Master. I cannot thank you enough. Finally, saving the most important for last, my unfathomable gratitude and love to my incredible wife, Dr. Christine Sosiak. My Love, without you, whether in the same room or 9000 km away, this project would not have happened without you. Your endless love, support, and brilliant mind has always been there for me, pushing me forward, and catching me when I fall. Thank you.

Now, without further ado...

STAND BACK



**I'M GOING TO TRY
SCIENCE**

Credit: Randall Munroe/XKCD Comics

Table of Contents

CHAPTER 1: INTRODUCTION	1
1.1 FIRE IN CANADA’S BOREAL FOREST	1
1.2 A BRIEF SUMMARY OF WILDFIRE MANAGEMENT IN ALBERTA	2
1.3 THE CANADIAN FOREST FIRE DANGER RATING SYSTEM	3
1.4 EFFECTS OF FOREST DENSITY ON FIRE BEHAVIOUR	5
1.5 A BRIEF OVERVIEW OF INITIAL ATTACK WILDFIRE FIGHTING IN ALBERTA	6
1.6 THESIS OVERVIEW	8
CHAPTER 2: METHODS	12
2.1 STUDY AREA	12
2.1.1 <i>The Boreal Forest and Foothills Natural Regions</i>	12
2.1.2 <i>Climate</i>	13
2.1.3 <i>Vegetation Composition</i>	14
2.2 FIRE REGIME	15
2.3 HISTORICAL FIRE DATABASE	18
2.4 FIRE WEATHER DATABASE	19
2.5 RESEARCH QUESTIONS	22
2.6 OBLIQUE AERIAL PHOTO SCREENING	23
2.7 FIRE AND FIRE ENVIRONMENT ATTRIBUTES DERIVED FROM OBLIQUE AERIAL IMAGERY	25
2.7.1 <i>Stand Density</i>	26
2.7.2 <i>Perimeter Surface Flame</i>	29
2.7.3 <i>Crown Involvement</i>	31
2.7.4 <i>Smoke Colour</i>	34
2.7.5 <i>Smoke Continuity</i>	37
2.7.6 <i>Smoke Angle</i>	39
2.8 DATA ANALYSIS: PROBABILITY OF ESCAPED FIRE AND CHALLENGE FIRE	41
2.8.1 <i>Simplifying Test GLMs</i>	43
2.8.2 <i>Model Building</i>	44
2.8.3 <i>Comparing Photograph Density Estimations Against LIDAR-Derived Forest Structure</i>	44
CHAPTER 3: RESULTS	46
3.1 MODELING THE PROBABILITY OF FIRE ESCAPE WITH OCULARLY ASSESSED FOREST DENSITY	46
3.1.1 <i>Comparing Attributes of Contained and Escaped Fire Groups</i>	46
3.1.2 <i>Logistic Regression Analysis</i>	49
3.1.3 <i>Contribution of Stand Density Attributes to the Probability of a Fire Escaping Containment</i>	50
3.2 MODELING THE PROBABILITY OF FIRE ESCAPE WITH FOREST LIDAR STRUCTURE CLASSIFICATION	51
3.2.1 <i>Comparing Contained and Escaped Fire Groups</i>	51
3.2.2 <i>Logistic Regression Analysis</i>	55
3.2.3 <i>Contribution of Stand Structure to the Probability of a Fire Exceeding 2.0 Hectares</i>	55
3.3 PROBABILITY OF A CREW ARRIVING TO A CHALLENGE FIRE USING OCULARLY ASSESSED FOREST DENSITY	58
3.3.1 <i>Comparison of Attributes Between Challenge and No-Challenge Fire Groups</i>	58
3.3.2 <i>Logistic Regression Analysis</i>	62
3.3.3 <i>Contribution of Stand Structure to the Probability of Containment Challenge</i>	62

3.4 PROBABILITY OF A CREW ARRIVING TO A CHALLENGE FIRE USING LIDAR-BASED FOREST STRUCTURE	64
3.4.1 <i>Comparing Challenging and Non-Challenging Fire Groups</i>	64
3.4.2 <i>Logistic Regression Analysis</i>	68
3.4.3 <i>Contribution of LiDAR Structure Attributes to Predictive Models</i>	69
CHAPTER 4: DISCUSSION	73
4.1 OBLIQUE IMAGERY MODEL PERFORMANCE	73
4.2 LIDAR CLASSIFICATION MODEL PERFORMANCE	74
4.3 MODEL CHALLENGES AND DATA LIMITATIONS	78
4.3.1 <i>Input Weather</i>	78
4.3.2 <i>Photograph Quality</i>	79
4.4 IMPLICATIONS FOR WILDFIRE MANAGEMENT	81
4.5 AREAS FOR FUTURE RESEARCH	84
4.6 CONCLUSION	86
WORKS CITED	88
APPENDIX	103

List of Figures

FIGURE 1 TOTAL HECTARES BURNT EACH YEAR WITHIN ALBERTA’S FOREST PROTECTION AREA, FROM 2006-2018, INCLUSIVE, SORTED BY IGNITION CAUSE.	2
FIGURE 2 EXAMPLE OBLIQUE AERIAL PHOTO SHOWCASING DIVERSITY OF ALBERTA’S FORESTS, OBSERVED WILDFIRE BEHAVIOUR, AND IA PHOTOGRAPHY. PHOTO COURTESY OF ALBERTA WILDFIRE.	7
FIGURE 3 EXAMPLE OBLIQUE AERIAL PHOTO SHOWCASING DIVERSITY OF ALBERTA’S FORESTS, OBSERVED WILDFIRE BEHAVIOUR, AND IA PHOTOGRAPHY. PHOTO COURTESY OF ALBERTA WILDFIRE.	8
FIGURE 4 THE GEOGRAPHICAL EXTENT OF THE BOREAL FOREST AND FOOTHILLS NATURAL REGIONS ACROSS ALBERTA AND LOCATIONS OF THE FIRES USED IN THE ESCAPE FIRE AND THE CHALLENGING FIRE OBLIQUE PHOTO ANALYSIS. NOTE THAT SOME FIRES WERE USED FOR IN BOTH ANALYSES.	12
FIGURE 5 DISTRIBUTION OF WILDFIRE IGNITION SOURCES IN THE STUDY AREA AND THEIR CUMULATIVE AREAS BURNT FROM 2006-2018. 15	
FIGURE 6 DISTRIBUTION OF WILDFIRES AND THEIR RESPECTIVE SIZE CLASSIFICATIONS WITHIN THE STUDY AREA BETWEEN 2006 AND 2018, INCLUSIVE. 1	16
FIGURE 7 THE FIRE WEATHER INDEX (FWI) SYSTEM INPUTS AND OUTPUTS USED TO FORECAST FIRE BEHAVIOUR. DIAGRAM ADAPTED FROM NATURAL RESOURCES CANADA (VAN WAGNER, 1987).	20
FIGURE 8 FWI SYSTEM RANKING ADAPTED FROM ALBERTA WILDFIRE (ALBERTA WILDFIRE, 2023).	21
FIGURE 9 AN EXAMPLE ARRIVAL PHOTO TAKEN BY SUPPRESSION CREWS DURING INITIAL ASSESSMENT, PRIOR TO THE WILDFIRE EXCEEDING 2.0 HA. PHOTO COURTESY OF ALBERTA WILDFIRE.	24
FIGURE 10 VISUAL EXAMPLES OF FOREST DENSITY: SPARSE (A), MODERATE (B), AND DENSE (C). PHOTOS COURTESY OF ALBERTA WILDFIRE.	28
FIGURE 11 VISUAL EXAMPLES OF PERIMETER SURFACE FLAME: SMOULDERING (A), SPRITES (B), ISOLATED (C), AND CONTINUOUS FLAME (D). PHOTOS COURTESY OF ALBERTA WILDFIRE.	30
FIGURE 12 EXAMPLE PHOTOGRAPHS ASSOCIATED WITH CROWN INVOLVEMENT CATEGORIES: (A) LIGHT CANDLING; (B) HEAVY TORCHING; (C) INTERMITTENT CROWNING; AND (D) CONTINUOUS CROWNING. PHOTOS COURTESY OF ALBERTA WILDFIRE.	33
FIGURE 13 EXAMPLE PHOTOS ASSOCIATED WITH SMOKE COLOUR CATEGORIES: (A) LIGHT GREY, (B) BROWN GREY, AND (C) BLACK GREY. PHOTOS COURTESY OF ALBERTA WILDFIRE.	36
FIGURE 14 VISUAL EXAMPLES OF SMOKE CONTINUITY: PUFFER (A), CONTINUOUS (B), AND HEAVY (B).	38
FIGURE 15 VISUAL EXAMPLES OF COLUMN ANGLE: VERTICAL (A), LIGHT (B), MODERATE (C), AND STEEP (D). PHOTOS COURTESY OF ALBERTA WILDFIRE.	40
FIGURE 16 E-FIRE1 SHOWING THE LIKELIHOOD OF A WILDFIRE ESCAPING CONTAINMENT AS A FUNCTION OF BY SMOKE COLOUR AND BUILDUP INDEX WITH SHADING REPRESENTING THE MODEL’S 95% CONFIDENCE INTERVALS FOR SMOKE COLOUR. THE EARLY TERMINATION OF THE CONFIDENCE INTERVAL FOR BLACK GREY SMOKE REFLECTS THE HIGHEST RECORDED BUI VALUE IN THE DATASET FOR THAT SMOKE COLOUR.	51
FIGURE 17 PROBABILITY OF A WILDFIRE ESCAPING CONTAINMENT ACCORDING TO ITS LIDAR STRUCTURE CLASS AS A FUNCTION OF RELATIVE HUMIDITY AND BUILDUP INDEX. Sb REPRESENTS BLACK SPRUCE, AND Aw REPRESENTS TREMBLING ASPEN. NOTE THAT VERY TALL, COMPLEX ASPEN STANDS ARE NOT SHOWN DUE TO THE LACK OF FIRE ESCAPES.	58
FIGURE 18 C-FIRE1: PROBABILITY OF A SUPPRESSION CREW ARRIVING TO A FIRE THAT HAS ALREADY EXCEEDED 0.5 HA PRIOR TO BEGINNING SUPPRESSION. FIRES ARE GROUPED BY SMOKE CONTINUITY AND CROWN INVOLVEMENT AND DRAWN TO THE 0.95 CONFIDENCE INTERVAL FOR CROWN INVOLVEMENT.	64
FIGURE 19 LIKELIHOOD OF A WILDFIRE EXCEEDING 0.5 HA PRIOR TO SUPPRESSION CREW ARRIVAL AS A FUNCTION OF TEMPERATURE, BUI HAZARD RANK, AND ASSESSOR-ASSIGNED FIRE TYPE.	72
FIGURE 20 EXAMPLE PHOTO OF STRUCTURE CLASS 7, OPTICALLY ASSESSED AS DENSITY3 CLOSED, SUCCESSFULLY CONTAINED, NO CHALLENGE.	75

FIGURE 21 EXAMPLE COMPARISON BETWEEN (A) STRUCTURE CLASS 2 (SHORT, OPEN CANOPY BLACK SPRUCE, OPTICAL ASSESSMENT DENSITY3 CLOSED, SUCCESSFULLY CONTAINED, NO CHALLENGE), AND (B) STRUCTURE CLASS 3 (OPTICAL ASSESSMENT DENSITY3 CLOSED, SUCCESSFULLY CONTAINED, CHALLENGING FIRE).76

FIGURE 22 AN ARRIVAL PHOTO WITH AN INTERNAL COCKPIT REFLECTION. THE HELICOPTER PORTHOLE IS IN VIEW AND A REFLECTION OF A CREW MEMBER IN THE FRONT PASSENGER SEAT CAN BE SEEN.81

FIGURE 23 WILDFIRE WITH FUEL CLASSIFIED AS WATER BY THE PROVINCIAL FUEL GRID. PHOTO COURTESY OF ALBERTA WILDFIRE.....83

FIGURE 24 WILDFIRE FUEL TYPE CLASSIFIED AS WATER BY THE PROVINCIAL FUEL GRID. PHOTO COURTESY OF ALBERTA WILDFIRE.....84

FIGURE 25 ANDREW STACK ON THE BANKS OF THE ATHABASCA RIVER, HORSE RIVER FIRE 2016. PHOTO CREDIT: LEIGHTON LINDSAY. ..87

List of Tables

TABLE 1 TABULAR DISTRIBUTION OF WILDFIRE IGNITION SOURCES IN THE STUDY AREA AND THEIR CUMULATIVE AREAS BURNT FROM 2006-2018.	15
TABLE 2 WILDFIRES AND THEIR RESPECTIVE SIZE CLASSIFICATIONS WITHIN THE STUDY AREA BETWEEN 2006 AND 2018, INCLUSIVE. THE PERCENTAGE IN BRACKETS INDICATES THE PERCENT ATTRIBUTION OF IGNITION CAUSE AND SIZE CLASS WITH RESPECT TO TOTAL FIRES.	16
TABLE 3 STAND DENSITY CATEGORIES, DESCRIPTIONS, AND CONTEXTUAL INFORMATION.	27
TABLE 4 FLAME CATEGORIES OBSERVED AT THE FIRE EDGE, DESCRIPTION AND CONTEXTUAL INFORMATION.	29
TABLE 5 CROWN FIRE INVOLVEMENT CATEGORIES, DESCRIPTIONS, AND CONTEXTUAL INFORMATION.	32
TABLE 6 SMOKE COLUMN CATEGORIES, DESCRIPTION AND ASSOCIATED CONTEXTUAL INFORMATION.	35
TABLE 7 SMOKE CONTINUITY AND THEIR RELATIONSHIPS TO FIRE BEHAVIOUR.	37
TABLE 8 SMOKE ANGLE DESCRIPTIONS.	39
TABLE 9 EVALUATED VARIABLES FOR THE ESCAPED AND CHALLENGE FIRE ANALYSES. RANKED VALUES REFER TO THE QUALITATIVE “LOW,” “MODERATE,” “HIGH,” “VERY HIGH,” AND “EXTREME” FWI SYSTEM OUTPUT GROUPINGS AS DEFINED BY ALBERTA WILDFIRE.	42
TABLE 10 FIRE COUNTS GROUPED BY FWI SYSTEM HAZARD LEVEL AND CONTAINMENT OUTCOME. PROPORTIONS AS A FUNCTION OF COLUMN TOTALS ARE SHOWN IN BRACKETS.	46
TABLE 11 SUMMARY STATISTICS OF SELECT ESCAPED FIRE VARIABLES. GENERAL VARIABLE SIGNIFICANCE WAS EVALUATED WITH A WILCOXON RANK SUM TEST WHERE SIGNIFICANT DIFFERENCES ARE HIGHLIGHTED IN BOLD.	48
TABLE 12 THE TOP TEN ESCAPED FIRE GLMS ORDERED BY DECREASING C-STATISTIC. CALLS WITH SIGNIFICANT DENSITY VARIABLE CHI-SQUARE SCORES FOR THE DENSITY VARIABLE ARE IN DISPLAYED IN BOLD.	49
TABLE 13 COUNT OF CONTAINED AND ESCAPED FIRES BY LIDAR-DERIVED FOREST STRUCTURE CLASS AS DEFINED GUO ET AL. (2017). STRUCTURE 5 DID NOT OVERLAP WITH ANY WILDFIRES AND WAS OMITTED.	52
TABLE 14 DISTRIBUTION OF CONTAINED AND ESCAPED FIRE FWI VALUES AS BOTH RAW COUNTS AND PROPORTIONS OF THEIR RESPECTIVE ESCAPED AND CONTAINED FWI CLASSES, SHOWN IN BRACKETS.	53
TABLE 15 GENERAL SUMMARY STATISTICS OF FIRE ATTRIBUTES SORTED BY CONTAINED AND ESCAPED FIRES. GENERAL VARIABLE SIGNIFICANCE WAS EVALUATED WITH A WILCOXON RANK SUM TEST WHERE SIGNIFICANT DIFFERENCES ARE HIGHLIGHTED IN BOLD.	54
TABLE 16 THE ESCAPED FIRE GLMS ORDERED BY DECREASING C-STATISTIC. WINNING CALLS WITH SIGNIFICANT CHI-SQUARE SCORES FOR THE 100 M BUFFERED LIDAR STRUCTURE VARIABLE ARE HIGHLIGHTED IN BOLD.	55
TABLE 17 DISTRIBUTION OF WILDFIRES WITH CHALLENGE AND NO-CHALLENGE STATUS, THAT ALSO WERE SUCCESSFULLY CONTAINED OR EXCEEDED 2 HECTARES.	59
TABLE 18 COUNTS OF FIRES BY CHALLENGE STATUS AND FWI SYSTEM RANK. PROPORTIONS OF FWI MOISTURE CODE AND BEHAVIOUR CODE FOR TOTAL RESPECTIVE “NO CHALLENGE,” AND “CHALLENGING” STATUS ARE REPRESENTED IN BRACKETS.	59
TABLE 19 GENERAL STATISTICS FOR THE NUMERICAL VARIABLES IN THE CONTAINMENT CHALLENGE FIRE MODEL USING OPTICALLY ASSESSED FIRE BEHAVIOUR AND DENSITY. GENERAL VARIABLE SIGNIFICANCE WAS EVALUATED WITH A WILCOXON RANK SUM TEST WHERE SIGNIFICANT DIFFERENCES ARE HIGHLIGHTED IN BOLD.	61
TABLE 20 UNIQUE GLMS PRODUCED BY THE ESCAPED FIRE ANALYSIS. NO DENSITY VARIABLES WERE IDENTIFIED IN ANY OF THE RESULTING EQUATIONS.	62
TABLE 21 DISTRIBUTION OF FIRES AMONG THE 8 STRUCTURAL CLASSES AND THEIR RESPECTIVE NUMBER OF CHALLENGING, AND NON-CHALLENGING FIRE DISTRIBUTIONS. BRACKETED NUMBERS INDICATE PROPORTION OF ROW TOTALS.	65
TABLE 22 MATRIX OF FIRES THAT WERE IDENTIFIED AS POSING CONTAINMENT CHALLENGES VERSUS AND IF THEY EXCEEDED 2 HA.	65
TABLE 23 FIRE COUNTS GROUPED BY FWI SYSTEM HAZARD LEVEL AND CHALLENGE CLASSIFICATION. PROPORTIONS AS A FUNCTION OF COLUMN TOTALS ARE SHOWN IN BRACKETS.	66
TABLE 24 GENERAL NUMERICAL VARIABLE STATISTICS FOR THE EXPANDED CHALLENGE FIRE ANALYSIS. GENERAL VARIABLE SIGNIFICANCE WAS EVALUATED WITH A WILCOXON RANK SUM TEST WHERE SIGNIFICANT DIFFERENCES ARE HIGHLIGHTED IN BOLD.	67

TABLE 25 THE 14 CHALLENGE FIRE GLMs ORDERED BY DECREASING C-STATISTIC. WINNING CALLS WITH SIGNIFICANT CHI-SQUARE SCORES FOR THE STRUCTURE CLASSIFICATION VARIABLE ARE IN DISPLAYED IN BOLD.68

TABLE 26 EXTENDED STATISTICS FOR THE E-FIRE1 GLM MODEL. LOGIT VARIABLES ARE PROBABILITY COEFFICIENTS RELATIVE TO THE INTERCEPT VARIABLE, LOG ODDS ARE THE EXPONENT OF THE LOGIT VARIABLE AND REPRESENT ODDS RELATIVE TO THE INTERCEPT VARIABLE. STATISTICAL SIGNIFICANCE OF MODEL PARAMETERS AND THEIR LEVELS WERE TESTED USING CHI SQUARE TESTS.....103

TABLE 27 EXPANDED STATISTICS FOR EL-FIRE1 AND ASSOCIATED PARAMETERS. LOGIT VARIABLES ARE PROBABILITY COEFFICIENTS RELATIVE TO THE INTERCEPT VARIABLE, LOG ODDS VARIABLES ARE ODDS RELATIVE TO THE INTERCEPT VARIABLE. STATISTICAL SIGNIFICANCE OF MODEL PARAMETERS AND THEIR LEVELS WERE TESTED USING CHI SQUARE TESTS.104

TABLE 28 EXPANDED STATISTICS FOR THE C-FIRE1 GENERALIZED LINEAR MODEL. LOGIT VARIABLES ARE PROBABILITY COEFFICIENTS RELATIVE TO THE INTERCEPT VARIABLE, LOG ODDS VARIABLES ARE ODDS RELATIVE TO THE INTERCEPT VARIABLE. STATISTICAL SIGNIFICANCE OF MODEL PARAMETERS AND THEIR LEVELS WERE TESTED USING CHI SQUARE TESTS.106

TABLE 29 EXPANDED STATISTICS FOR CL-FIRE1. LOGIT VARIABLES ARE PROBABILITY COEFFICIENTS RELATIVE TO THE INTERCEPT VARIABLE, LOG ODDS VARIABLES ARE ODDS RELATIVE TO THE INTERCEPT VARIABLE. STATISTICAL SIGNIFICANCE OF MODEL PARAMETERS AND THEIR LEVELS WERE TESTED USING CHI SQUARE TESTS.107

List of Equations

$EY = g - 1X\beta\beta_0 + \beta_1x_1 + \beta_2x_2 + \dots + \beta_mx_m$	EQUATION 1.....	23
$E-FIRE1\gamma = 11 + e - (-6.4330 + \alpha + 0.0225BUI + 0.1195PRECIP + \gamma)$	EQUATION 2,.....	50
$EL-FIRE1\gamma = 11 + e - (0.2 + \alpha + \beta + \gamma - 0.02693RH + \varepsilon)$	EQUATION 3.....	55
$C-FIRE1\gamma = 11 + e - (-3.79 + \alpha + \beta + 0.07WIND)$	EQUATION 4.....	63
$CL-FIRE1\gamma = 11 + e - (-0.49122 + \alpha + \beta + \gamma + \varepsilon + 0.04273WIND + 0.039TEMP)$	EQUATION 5,.....	69

Chapter 1: Introduction

1.1 Fire in Canada's Boreal Forest

Extending across the width of the country and measuring over 3 million square kilometers, Canada's Boreal Forest is regularly altered by natural disturbances (Natural Resources Canada, 2005). Through time, the Boreal Forest has evolved diverse adaptations to these disturbances to maintain their diversity and resilience, and in the case of wildland fire, incorporate them into their natural succession (Rowe, 1970). Wildland fire is a rapid exothermic chemical reaction that consumes plant material and is a natural process in the terrestrial carbon cycle (Falkowski et al., 2000). Fires in the Boreal Forest ecoregion fragment the landscape into smaller, diverse stands of varying age, composition, and ecological function, often resembling a huge patchwork quilt. The properties of these patches can inhibit fire growth; cycle grazing habitats for foraging animals, and by extension their predators; remove congestion and woody debris on the forest floor to create room for new growth successions; and promote diversity of plant species of different ages, improving a forest's resistances to other disturbances such as insect attacks and disease (Wright and Heinselman, 2014).

Alberta's Forest Protection Area (FPA) covers roughly 39 million hectares, the majority of which lies within the Boreal Forest ecoregion. Between 2006 and 2018, inclusive, 19 844 fires within the FPA have been documented in a published database that is available to the public (Alberta Wildfire, 2020). Within this period, approximately 2.71 million hectares have been burned, equivalent to 0.5% or 208 000 ha of the FPA annually (Figure 1). Wildland fire ignition in Alberta can be effectively divided into two categories: lightning-caused and human-caused. Within the FPA, between 2006 and 2018, lightning was attributed as the cause for 36% of fires, but nearly 52% of total area burnt. By contrast, 64% of fires were human caused and accounted for 48% of total area burnt.

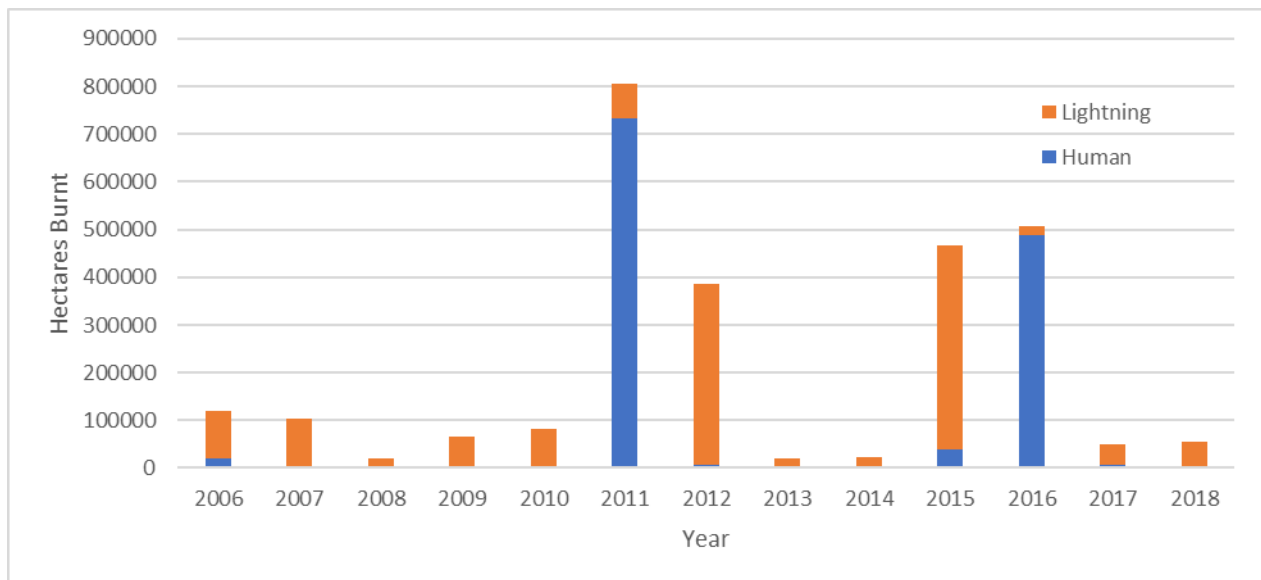


Figure 1 Total hectares burnt each year within Alberta's Forest Protection Area, from 2006-2018, inclusive, sorted by ignition cause.

The Boreal Forest is comprised of a mix of conifer and deciduous trees, and around the edges of Alberta's abundant bogs, tamarack can also be found (Kelsall et al., 1977). Conifers in this region include white spruce (*Picea glauca*) and jack pine (*Pinus banksiana*) in the drier, upland regions of the forest; and black spruce (*Picea mariana*) dominating the wetter lowlands. Deciduous trees are a mix of balsam poplar (*Populus balsamifera*), aspen poplar (*Populus tremuloides*) and paper birch (*Betula papyrifera*) which are commonly found in, but not exclusive to, the drier uplands (Kelsall et al., 1977). Pure forest stands tend to return to their pre-disturbance composition following wildfire, such that deciduous stands remain deciduous and coniferous remain coniferous; however, mixed stands aggressively regenerate deciduous trees first, followed by the slower growing, more shade-tolerant conifers (Rowe, 1970).

1.2 A Brief Summary of Wildfire Management in Alberta

Wildfire management began in Alberta with Indigenous groups applying fire to the landscape before European settlement. Alberta's landscape is a challenging environment to inhabit, with relentless insects

in the snow-free months and cold, harsh winters. The advantage of choosing when fire is applied to the landscape, versus the stochastic process of lightning ignition, is that wildfire outcomes can be tailored to match the needs of the applicants (Pyne and Wynn, 2008). In a review of Indigenous land management practices, Christianson (2022) notes that fire served a wide variety of objectives, from insect management, landscape modification, protection around communities, agricultural use, religious, cultural, and aesthetic purposes. Westward expansion of productive forestry operations and economic development imposed constraints on cultural burning practices, which were considered destructive to valuable resources. Eventually, cultural burning was officially banned in Alberta in 1910 (Pyne and Wynn, 2008), although discreet and open flaunting of the law continued in the following decades. Throughout the evolution of Alberta's wildfire management program, major changes to both law and policy often followed in the wake major wildfire seasons. Following the intense wildfire season of 1950, a law was introduced in 1952 effectively mandating suppression of all ignitions (Tymstra et al., 2016). Expansion of the wildfire management program was recommended in 1954 for both capability and legal reach, and in 1956 forest protection was designated its own branch in the Alberta Government.

1.3 The Canadian Forest Fire Danger Rating System

As populations grew, wildfire management groups across Canada had to develop a greater understanding of wildfire behaviour and occurrence. Wildfire science in Canada began in the mid-1920s with J. G. Wright's development of a research program to study the influence of weather and fuel moisture on wildfire behaviour (Forestry Canada Fire Danger Group, 1992). In the late 1960s, a working group of researchers from the Canadian Forest Service developed the first iteration of the Canadian Forest Fire Danger Rating System (CFFDRS) (Stocks et al., 1989). The CFFDRS is a collection of modules designed to report fire hazard in the wildlands and was initialized in the late 1980's. The CFFDRS received some updates in 2009 and is still in use today (Wotton et al., 2009).

The Canadian Forest Fire Weather Index (FWI) System is one of two major components of the CFFDRS and is used to interpret the short- and long-term effects of weather on fuels, the ease of ignition, fire sustainability, and containment challenges (Van Wagner, 1974). The FWI System takes inputs of temperature, relative humidity, wind speed, and rain accumulation over the previous 24 hours from weather measurements taken at noon, local standard time (Lawson and Armitage, 2008); in Alberta, these inputs are gathered by a network of dedicated fire weather stations deployed across Alberta (Government of Alberta, 2024). Outputs produced by the FWI System are for the peak burning period of each day, approximately 1700 h LDT, where temperature is the highest and relative humidity is lowest. The FWI System also serves as a bookkeeping system of fuel moisture levels, as previous FWI System outputs affect subsequent forecasts. When used in conjunction with local knowledge and by experienced wildfire managers, the FWI System is employed to inform placement of suppression resources across the landscape to maximize coverage in response to the ever-evolving wildfire hazard.

The Canadian Forest Fire Behaviour Prediction (FBP) System is the second major module of the CFFDRS and is designed to output predictions of fuel-specific fire behaviour (Forestry Canada Fire Danger Group, 1992). The FBP System has 16 original benchmark fuel types, and has received some revisions and updates which were published in 2009 (Wotton et al., 2009). For each fuel type, the FBP outputs fire behaviour predictions based on inputs that include the outputs of the FWI System, wind speed and direction, topographic attributes, and foliar moisture content. Predicted fire behaviour includes the fire's rate of spread, intensity of energy released, fuel consumption, amount of crown involvement, direction of growth, and fire size. Fuel inputs in Alberta are derived from a 100 x 100 m resolution raster map of the province that tracks fuel types in annually released updates that document disturbances such as wildfire, harvesting, and changes along the boundaries of communities in the wildland urban interface ("Fire Behavior Prediction (FBP) Fuel Types," 2023). The FBP System follows a series of assumptions, including the uniformity and lateral continuity of fuel types, and a representative fuel type

selected during initial assessment by suppression personnel (Forestry Canada Fire Danger Group, 1992). This presents a drawback of the System in its current form, because the fuel inputs of the FBP System are fixed, and do not account for the effect of different structure and density changes that occur in a stand, which can dramatically alter a fire's behaviour.

1.4 Effects of Forest Density on Fire Behaviour

The energy output per unit length of fireline is directly proportional to the quantity of fuel consumed and a fire's rate of spread (Byram, 1959). The quantity and arrangement of fuel in a stand affect how a fire grows and behaves. Stand density, expressed as stems per hectare, defines the concentration of trees in a forested area. Density plays a crucial role in wildfire behaviour, where a higher forest density has more fuel available for combustion both on the forest floor and in the canopy in the form of increased needle litter production, dead and down woody debris on the forest floor, and live twigs and foliage in the canopy (Van Wagner, 1977a). Wildfires first ignite on the forest floor and begin to release energy in the form of radiative, convective, and conductive heat and light as they grow. If a surface fire releases enough energy to ignite the lowest branches of the canopy, defined as the critical surface intensity, the fire becomes engaged in the overstory (Van Wagner, 1977a). The crowns in black spruce stands are standardized to 1.5 m in the FBP System, but may reach the forest floor, which makes the critical surface intensity lower than most other conifer fuels, and therefore rather volatile (Forestry Canada Fire Danger Group, 1992). Overstory fuel load is expressed by a stand's crown bulk density in kilograms per cubic meter, which is the amount of burnable fuel in the canopy (Van Wagner, 1977a). Crown bulk density can be averaged across a stand or expressed in different layers to reflect the heterogeneity and structural changes within a stand itself. Should fire that has climbed into the canopy have sufficient radiant energy to contribute to the preheating of adjacent crown and surface fuels in advance of the flaming front, active crowning is achieved, resulting in an exponential increase in energy output.

1.5 A Brief Overview of Initial Attack Wildfire Fighting in Alberta

Wildfires detected within Alberta's Forest Protection Area (FPA) are aggressively fought by suppression personnel with explicit emphasis on firefighter safety (Government of Alberta, 2016). The Alberta Wildfire Management Branch within the Ministry of Forestry and Parks is responsible for wildfire management in the province and engages wildfire on the landscape with two primary objectives: 1) initiate suppression prior to the wildfire exceeding 2 hectares (ha); and 2) successfully contain the perimeter by 1000 h the following morning (Government of Alberta, 2024). Wildfire response is coordinated by 10 regional wildfire centres distributed within the FPA in conjunction with the provincial Alberta Wildfire Coordination Centre (AWCC). Regional wildfire centres preposition initial attack (IA) crews based on wildfire hazard levels using a combination of computer-generated maps and local knowledge to minimize crew response times when new wildfires are reported (MNP LLP, 2020).

A typical IA crew consists of three wildfire crew members and a crew leader, who collectively form a Helitack (HAC) crew. HAC crews use trucks and rotary wing aircraft to travel to, and assess, the suppression needs of new wildfires, prioritizing incidents in the event of multiple starts in proximity to each other or values at risk (VARs), requesting additional resources if needed, and suppressing the fire. New wildfires are assessed prior to suppression and situational details are reported directly to the regional fire centre via radio transmission (Government of Alberta, 2016). Assessment details include the date and time of assessment and start of suppression, location of the fire in dominion land survey coordinates or latitude and longitude, wildfire type defined as ground, surface, or crown, overhead weather conditions, namely clear, cloudy, rainshowers, dry cumulonimbus, and wet cumulonimbus, values at risk such as homes, cabins, and infrastructure, and assigning an FBP System fuel type that best represents the burning fuel complex. In addition to textual information, a visual record of the incident is documented with photographs taken by the crew. In the case of airborne assessment, photographs

capture landscape-level contextual information on observed wildfire behaviour and associated fuel type (Figure 2 and Figure 3). Once documentation is complete, the HAC crew moves in to begin suppression.



Figure 2 Example oblique aerial photo showcasing diversity of Alberta's forests, observed wildfire behaviour, and IA photography. Photo Courtesy of Alberta Wildfire.



Figure 3 Example oblique aerial photo showcasing diversity of Alberta's forests, observed wildfire behaviour, and IA photography. Photo Courtesy of Alberta Wildfire.

1.6 Thesis Overview

New technology has enabled expansion of CFFDRS capability in response to a growing need for more advanced fire intelligence (Canadian Forest Service Fire Danger Group, 2021). Fuel stand characteristics affect how fires grow, behave, and propagate into forest crowns (Beverly et al., 2020; Cruz et al., 2005). Technology capable of analyzing forest structure, such as light detection and ranging (LiDAR), can characterize forest structure and identify specific structures where wildfire is a dominant environmental disturbance (Cameron, 2020; Guo et al., 2017). White (2016) established that aerial ocular estimates, also known as ocular assessment, ocular inspection, or ocular examination, is a method of data collection that uses the expertise of a trained analyst to coarsely estimate features of interest in a forest

without the use of specific measurement equipment; the method is inexpensive, very fast, and appropriate for when high statistical precision is not necessary for an analysis.

Given that aerial ocular assessment for coarse statistical analysis of forest structure and the understanding that forest structure has an effect on wildfire behaviour (Government of Alberta, 2016; Phelps et al., 2022), aerial ocular assessments performed by trained assessors may provide a valuable source of data for understanding and modeling fire behaviour. Therefore, can aerial ocular assessment of forest density sufficiently determine if a wildfire is more or less likely to exceed pre-established boundaries? Aerial ocular assessment of forest structure, in lieu of more intensive measurement techniques, is appealing because it accommodates the rapid decision making and time pressures associated with IA operations. As such, the overarching objective of this thesis is to investigate the potential link between ocularly-assessed forest structure wildfire behaviour.

Data collection by researchers during an active wildfire scenario is constrained by potential threats to safety and the incompatibility of having a civilian presence potentially interfering with emergency response operations. However, oblique aerial imagery obtained during response operations by wildfire assessors provides a data source that documents contextual wildfire behaviour, forest density, and other potential information. This opportunistic dataset documents wildfire behaviour across a broad spectrum of conditions and alleviates the need for on-site data collection. I chose to investigate the relationship between ocularly assessed fuel structure and fire behaviour in black spruce forests in Alberta, identified by the FBP System as the benchmark fuel type C-2. To perform my analysis, I created a database of potential predictors of wildfire behaviour using FWI System data, Alberta fire weather station data, publicly available wildfire incident data, and wildfire behaviour observed and catalogued from oblique aerial photos taken during the assessment phase of wildfire suppression. To analyze the effects of ocularly assessed forest density on fire behaviour, I defined and investigated two scenarios: 1)

The likelihood of a fire escaping a pre-established containment size of 2 ha, and 2) the likelihood of a wildfire suppression crew experiencing difficulty containing the fire based on the work by Beverly (2017). I also performed a parallel assessment of the two scenarios using a LiDAR forest structure classification of Alberta, in lieu of using ocularly assessed wildfire photography, which was provided by the Nicholas Coops Lab from the University of British Columbia (Guo et al., 2017).

Chapter two of this thesis documents the study methods. It includes a description of the study area and the role of fire as a disturbance, descriptive summaries of wildfires in the study area, steps taken to process and clean the photography archive to select appropriate wildfire imagery for analysis, how generalized linear models (GLM) were used to determine significance of forest density and other examined variables on fire behaviour, as well definitions of observed wildfire behaviour derived from the oblique aerial photography. The descriptive attributes of wildfire behaviour derived from the oblique aerial imagery, as well as the rationale for including each attribute, are explored in depth. Documented photo attributes include forest density, surface fire intensity, crown fire involvement, smoke angle, smoke colour, and smoke continuity. The descriptive attributes selected for this study were inspired by existing wildfire definitions, some of which are formalized in the literature and expanded upon, and other terms which are commonly used by agency personnel during response and suppression operations. Visual examples of each descriptive attribute are provided along with abridged and extended definitions.

Chapter three presents the results of the statistical analysis. General findings are noted and GLMs selected from the analysis are presented with their discriminate accuracy scores, significance of the respective model parameters, and predictive capability using leave-one-out cross validation.

In the final chapter, chapter four, the implications of the results are discussed. Limitations of the data, approach, and results are disseminated, the implications of this research for wildfire management, and recommendations for future research are introduced.

Chapter 2: Methods

2.1 Study Area

2.1.1 The Boreal Forest and Foothills Natural Regions

A comprehensive description of Alberta's natural regions and natural subregions is made available by the Natural Regions Committee (2006). The study area for this thesis, and the wildfires therein are found in the Boreal Forest and Foothills natural regions. Together, their combined area totals 447 482 km², accounting for 68% of Alberta's land coverage. These two natural regions occupy most of Alberta's northern half but also extend well into the southern end of the province to approximately 260 km from the Canada-US border (Figure 4).

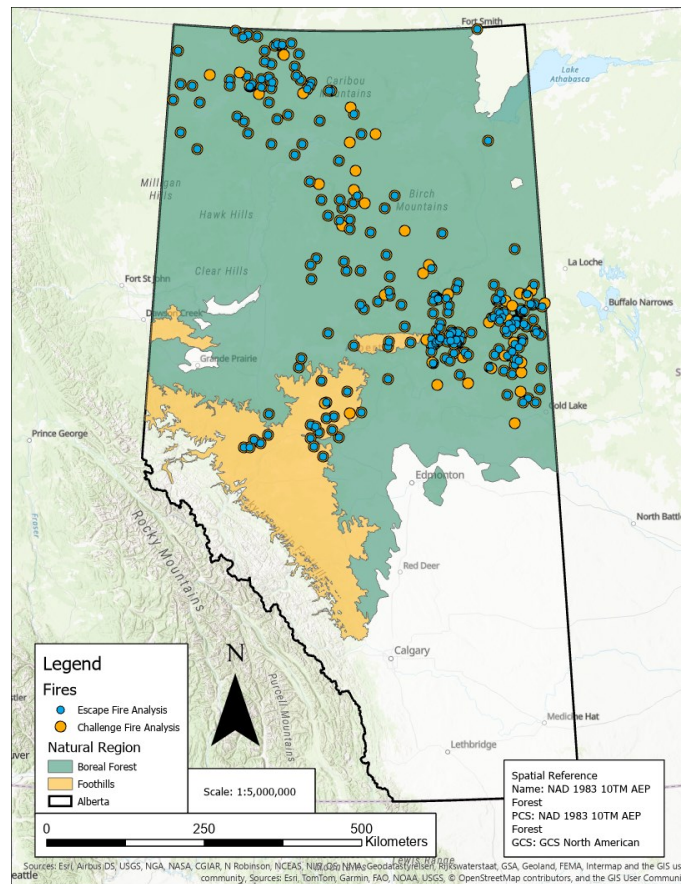


Figure 4 The geographical extent of the Boreal Forest and Foothills Natural Regions across Alberta and locations of the fires used in the escape fire and the challenging fire oblique photo analysis. Note that some fires were used for in both analyses.

The Boreal Forest natural region ranges from approximately 150 m elevation in the north to 1100 m near the British Columbia border in the west. The regional geomorphology of the Boreal Forest features rolling hills, plains, plateaus, and river valleys, but is mostly comprised of wetlands and bog or fen environments. Within wetland environments, subtle topographic changes often delineate the difference between saturated soils, submerged soils, and well-drained soils; this effect is made further apparent during heavy rainfall periods where the lowlands are prone to flooding.

Elevation in the Foothills region ranges from 700-1700 m, with the lowest elevations in the north, and the most elevated in the south. Foothills topographical features are much more varied than the Boreal Forest region, with the upper western elevations exposing bedrock ridges adjacent to the mountains, transitioning into rolling hills to the northeast, and isolated bog or fen environments in topographical lows (Natural Regions Committee, 2006).

2.1.2 Climate

Climate in the Boreal Forest region is generally characterized by long, cold winters with average temperatures of -19°C , and short summers averaging 15°C (Natural Regions Committee, 2006). Isolated and sporadic permafrost is found in the north of the natural region, dissipating to the south (Helbig et al., 2016). Moving northward, mean annual temperature decreases to 10°C , with annual precipitation decreasing in a similar trend. Average precipitation across the Boreal Forest is 469 mm per year with peak accumulation between April and August.

Precipitation across the Foothills region averages 603 mm but has an overall higher proportion during its short growing season. Mean annual temperatures in the Foothills are milder than the Boreal Forest, with a mean high temperature of 14°C and mean winter temperature of -12°C , with an overall average of 1.7°C .

2.1.3 Vegetation Composition

Within the Boreal Forest, vegetation composition varies by latitude and drainage conditions. The far north is host to poorly drained bogs and fens with overstories composed of black spruce (*Picea mariana*), and an understory of mosses with thick organic layers (Natural Regions Committee, 2006). Well-drained fens include tamarack (*Larix laricina*). Moderately dry biomes are still dominated by black spruce, but well-elevated sites with good drainage are home to uncommon balsam poplar (*Populus balsamifera*) and aspen poplar (*Populus tremuloides*), jack pine (*Pinus banksiana*), and white spruce (*Picea glauca*) stands with understories of feathermosses, low shrubs, and lichen communities. In the south, the Boreal Forest features patchworks of deciduous, mixedwood, and coniferous stands. Uplands are composed of white spruce, balsam poplar, and aspen poplars with understories of low bushes, lichens, shrubs, and mosses. Jack pine and lodgepole pine (*Pinus contorta*) can be found throughout the subregions, in both pure and hybridized forests, giving way to black spruce in lowland bogs and fens.

Transition zones between the Boreal Forest and Foothills natural regions are marked by the presence of lodgepole pine forests (Natural Regions Committee, 2006). In drier areas, the Lower Foothills subregion is typified by deciduous and mixedwood forests containing white (paper) birch (*Betula papyrifera*), lodgepole pine, and white and black spruce. Wetland environments contain short black spruce and tamarack. The Upper Foothills are coniferous-dominated and indicated by even-aged, closed-stand pine forests with black spruce understories. Presence of mixedwood and deciduous forests is limited to southern and western aspects. Rich and poor fens of the Upper Foothills contain black spruce and tamarack, and the driest areas of the natural region which are comprised of shrubby grasslands.

2.2 Fire Regime

Alberta’s publicly available wildfire records document 19 844 fires from 2006 to 2018, of which 16 647 (84 %) occurred in the study area (Alberta Agriculture and Forestry, 2020). Fires that occurred within the study area account for 2 512 322 ha (93%) of total area burned across the province. Lightning-caused wildfires (n=6689) account for 40.18% of wildfires in the study area and are responsible for 1 223 227 ha (49%) of area burned (Figure 5).

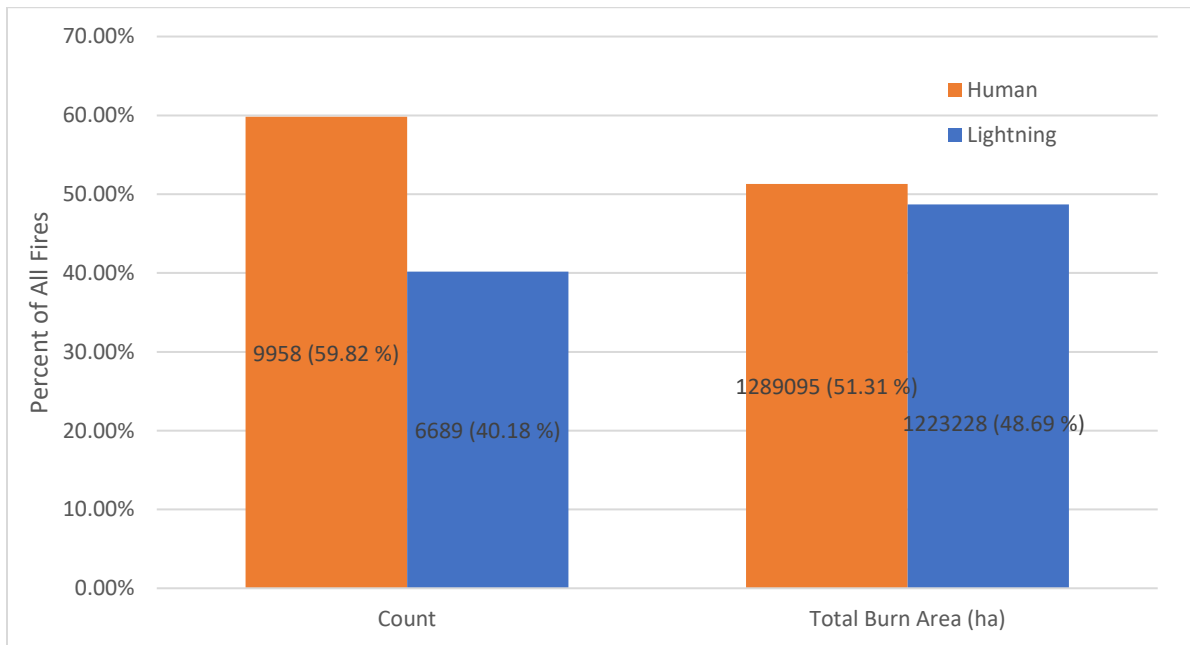


Figure 5 Distribution of wildfire ignition sources in the study area and their cumulative areas burnt from 2006-2018.

Table 1 Tabular distribution of wildfire ignition sources in the study area and their cumulative areas burnt from 2006-2018.

Cause	Count	Count Percent	Total Burn Area (ha)	Percent Total Area Burned
Human	9958	59.82%	1289094.52	51.31%
Lightning	6689	40.18%	1223227.69	48.69%
Total	16647	100.00%	2512322.21	100.00%

Fire size distribution is graphed in Figure 6 and tabulated in Table 1. Most fires in the study area tend to be small, with 93% of fires (class A, B, and C) burning less than 40 ha. The remaining 7% of fires (class D

and E), however, account for over 99% of total area burnt, and are overwhelmingly caused by lightning (5.28% lightning-caused, vs 1.59% of all fires).

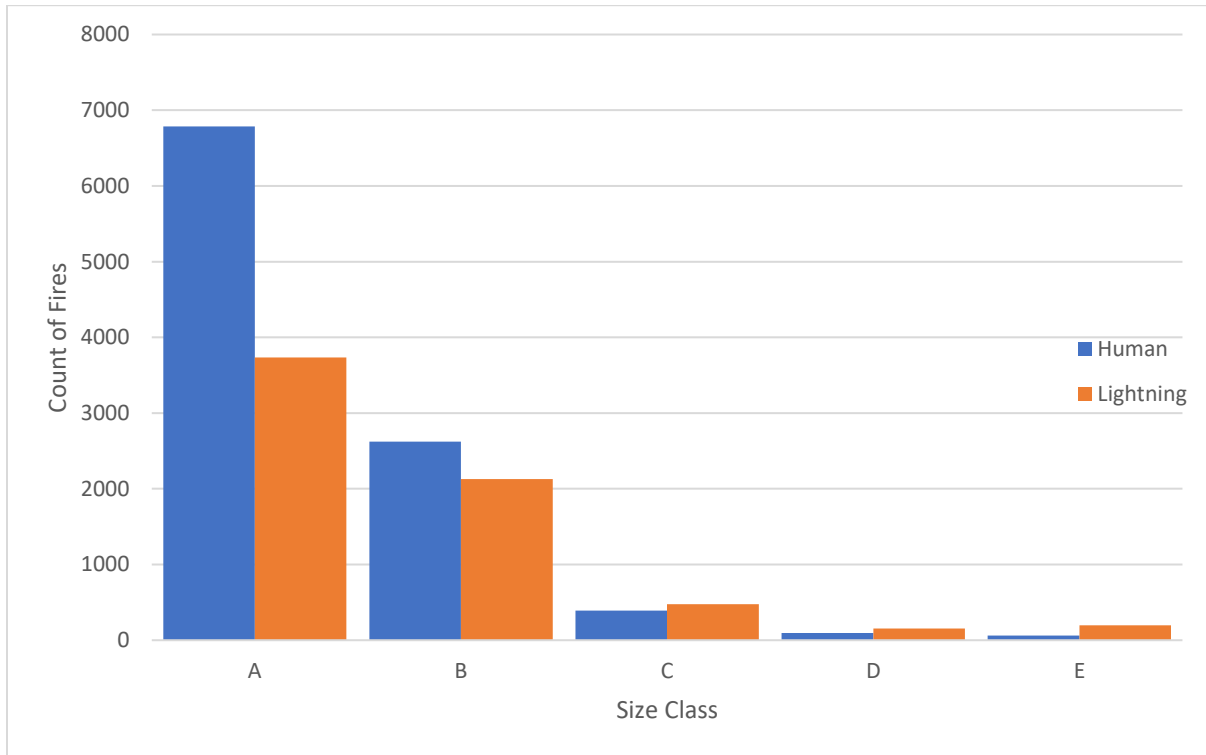


Figure 6 Distribution of wildfires and their respective size classifications within the study area between 2006 and 2018, inclusive. 1

Table 2 wildfires and their respective size classifications within the study area between 2006 and 2018, inclusive. The percentage in brackets indicates the percent attribution of ignition cause and size class with respect to total fires.

Size Class	Size Range	Human	Lightning
A	0 ha to 0.1 ha	6784 (68.13 %)	3734 (55.82%)
B	>0.1 ha to 4.0 ha	2623 (26.34 %)	2128 (31.81%)
C	>4.0 ha to 40.0 ha	392 (3.94 %)	474 (7.09%)
D	>40 ha to 200 ha	96 (0.96 %)	156 (2.33%)
E	>200 ha	63 (0.63 %)	197 (2.95%)

Fire passage invokes changes to the landscape, which fall under two major classifications: first- and second-order fire effects (Higuera, 2019). First-order fire effects occur during, or immediately, following

fire passage. First-order fire effects include fuel consumption, smoke production, spontaneous plant death, soil heating, chemical and nutrient cycling in soils, and seed release in serotinous (jack pine, lodgepole pine) and semi-serotinous (black-spruce) trees (Reinhardt et al., 2001; Wright and Heinselman, 2014). Second-order fire effects are latent downstream effects that follow first-order effects and therefore are inextricably linked (Reinhardt et al., 2001). Second order effects include delayed tree mortality, vegetation succession and biome cycling, and increased susceptibility to further disturbance from weather and insects (Reinhardt et al., 2001; Wright and Heinselman, 2014).

High intensity fires consume the live foliage suspended in the forest canopy, often leaving the larger stem and branchwood intact. This process opens the forest floor to insolation and new growth, restarting successional growth stages; this creates a mosaic of stand ages and forest successions that accomplishes multiple roles, including creating natural fire barriers, promoting vegetation diversity, limiting the spread of insect and fungal outbreaks, and creating new foraging grounds for herbivores who are pursued by their associated predators, maintaining population balances for both (Wright and Heinselman, 2014).

The Boreal Spruce fuel type, FBP System fuel type C-2, is composed of pure black spruce in both lowland and upland sites (Natural Regions Committee, 2006). This benchmark fuel type is moderately well stocked, with branches that extend near-to, or all the way to the forest floor. The forest floor is often dominated by Labrador tea (*Ledum groenlandicum* Oeder) and feather mosses but can also include sphagnum mosses (*Sphagnum* sp.), lichens, grasses, and horsetails (*Equisetum* sp.), and deep duff layers that often exceed 30 cm in depth. The C-2 fuel type is a volatile fuel type and prone to burning: Ample ladder fuels in the form of live branches, dead branches with bearded lichens (*Usnea* sp.), and flaky bark found on the stem of black spruce trees facilitate a wildfire's climb into the crown. Intermittent crowning occurs easily in this fuel type, and begins when the Buildup Index as low as 81 and an Initial

Spread Index of 2, with greater than 50% crown consumption occurring as the Initial Spread Index increases to 3 (Taylor and Alexander, 2018). The Buildup Index and Initial Spread Index are further covered in section 2.4.

Black spruce is a fire-adapted species and incorporates periodic wildfire into parts of its regeneration and succession (Viereck, 1983). Black spruce cones are semi-serotinous, and open from the heat of passing wildfire. In nutrient-poor environments, where black spruce is commonly found, nutrient recycling is slow. Fire passage consumes biomass from the forest floor and forest canopy and converts them into nutrients. The consumption of the forest floor removes insulation for the underlying permafrost and exposes it to sunlight from the removed canopy. The exposure spurs permafrost melt, increasing the active layer depth by up to 2-3 times its original depth for the next 10-15 years before it begins rebounding to its original state over the next 50 years (Viereck, 1983). Freshly deposited spruce seedlings, herbs, and shrubs, take advantage of the increased active layer and elevated nutrient pool to establish the next growth succession.

2.3 Historical Fire Database

Wildfire records for this study were obtained from a public database published by the Alberta Wildfire Management Branch. These records contain the details and timing of operational activities, as well as fire characteristics observed directly by fire management staff on arrival to the fire location and at subsequent operational milestones. Fire size (ha) was reported by ocular estimate at the time of the initial assessment of the fire, and the onset of firefighting. Fire size at formal stages of control, namely being held, under control and extinguished, was reported by ocular assessment if small, and GPS measurements or satellite mapping if large. Accuracy of ocularly assessed fire sizes becomes more difficult as fire size increases, and is influenced by many factors such as nearby reference points such as oil lease sites, which are standardized to one hectare; weather conditions; visibility of the forest floor;

experience of the assessor; and visibility of the burn, which may be obfuscated by smoke and canopy cover. Additional variables reported for each fire included the date and time of departure of fire suppression resources and information relayed by agency personnel upon arrival to the fire, such as the fire's latitude and longitude in decimal degrees and associated fire environment. Fire behaviour conditions including the assigned Canadian Forest Fire Behaviour Prediction (FBP) System fuel type, the type of fire, namely ground, surface, or crown, and overhead weather conditions defined as clear; CB wet (wet thunderstorm); CB dry (dry thunderstorm); cloudy; and rain showers. Following the incident, additional information such as the fire cause is documented.

Agency records were used to derive additional variables for analysis including dispatch delay, which was calculated as the time between the initial fire report and dispatch of suppression resources, and travel time delay, which was calculated as the time between resource dispatch and the start of fire suppression action. Finally, dispatch time delay and travel time delay were combined to create a single variable defined as total time.

2.4 Fire Weather Database

Alberta Wildfire uses a network of weather stations deployed across the provincial wildfire management area to record local weather, which is then used to predict daily wildfire behaviour. The procedure, outlined in the Development and Structure of the Canadian Forest Fire Behaviour Prediction (FBP) System (Forestry Canada Fire Danger Group, 1992), uses the previous day's fine fuel moisture code (FFMC), duff moisture code (DMC), draught code (DC), and the present day's noon local standard time (LST) inputs to predict anticipated fire behaviour for peak burning that day. The noon LST inputs are temperature, relative humidity, wind speed, and the cumulative precipitation over the previous 24 hours (Figure 7) (Van Wagner, 1987). The outputs generated by the FWI System are unitless indicators that express relative fuel moisture and general wildfire behaviour. The values for each FWI moisture

code and behaviour code are independently binned into hazard ratings of low, moderate, high, very high, and extreme, which are described in Figure 8. When combined with an FBP System fuel type, fuel-specific outputs predicting rates of fire spread, fuel consumption, crown consumption, and energy output are produced.

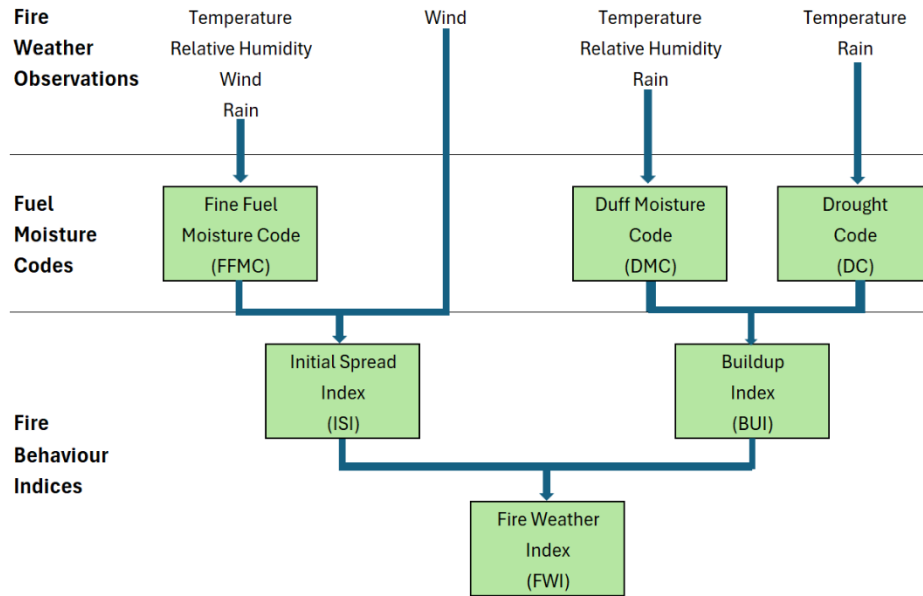


Figure 7 The Fire Weather Index (FWI) System inputs and outputs used to forecast fire behaviour. Diagram adapted from Natural Resources Canada (Van Wagner, 1987).

Fire Weather Index

Hazard Divisions

Hazard Rating	FFMC Fine Fuel Moisture Code	DMC Duff Moisture Code	DC Drought Code	ISI Initial Spread Index	BUI Buildup Index	FWI Fire Weather Index	HFI Head Fire Intensity
Low	0-76	0-21	0-79	0-1.5	0-24	0-4.5	1-2
Moderate	77-84	22-27	80-189	2-4	25-40	4.5-10.5	3
High	85-88	28-40	190-299	5-8	41-60	10.5-18.5	4
Very High	89-91	41-60	300-424	9-15	61-89	18.5-29.5	5
Extreme	92+	61+	425+	16+	90+	29.5+	6

Term

Range

Fine Fuel Moisture Code (FFMC)

0-101

An indicator of dryness of fine, easily-ignited vegetation such as twigs, leaf litter, and needles. Calculated using yesterday's FFMC and noon standard time dry bulb temperature, relative humidity, wind speed, and precipitation in the previous 24 hours.

Range

Duff Moisture Code (DMC)

0-Unlimited

An indicator of dryness for loosely-compacted vegetation beneath the surface litter and medium-sized branches. Calculated using yesterday's DMC and noon standard time dry bulb temperature, wind speed, and precipitation in the previous 24 hours.

Range

Drought Code (DC)

0-Unlimited

An indicator of dryness for deep organic layers and thick vegetation such as tree trunks. Calculated using yesterday's DC and noon standard time dry bulb temperature and precipitation in the previous 24 hours.

Range

Initial Spread Index (ISI)

0-Unlimited

A combination of FFMC and wind speed to create a numerical indicator of anticipated rate of fire spread

Range

Buildup Index (BUI)

0-Unlimited

A combination of DMC and DC to indicate the amount of fuel available to burn

Range

Fire Weather Index (FWI)

0-Unlimited

A general indicator of overall expected fire intensity. Derived from a combination of ISI and BUI

Range

Head Fire Intensity (HFI)

1-6

Classification of overall energy output of a fire's main front.

Figure 8 FWI System ranking adapted from Alberta Wildfire (Alberta Wildfire, 2023).

Each wildfire used in this study was assigned weather data from the closest active fire weather station matched to the ministry record for the date of ignition. Data attributed to each fire from the FWX system included temperature, wind speed and direction, relative humidity, the previous 24 hours of accumulated precipitation, and the 6 FWI System outputs: Fine Fuel Moisture Code (FFMC), Duff Moisture Code (DMC), Drought Code (DC), Initial Spread Index (ISI), Buildup Index (BUI), and Fire Weather Index (FWI). The Daily Severity Rating (DSR), a measure of anticipated effort required to control wildfires, was also included.

2.5 Research Questions

While flying to a fire and during initial assessment, Helitack crews are instructed to verbally describe and document fire behaviour and the fire environment, values at risk (VARs), and request needed resources in terms of personnel and equipment over the radio to the district fire centre. The information provided by the verbal description assists the Duty Officer in developing appropriate suppression strategies and allocating resource deployment, especially in the case of a multi-start fires. Operational documentation of wildfires collects textual and photographic information about the fire environment and observed fire behaviour. In this thesis, I use variables extracted from these operational archives to model fire containment outcomes. My working theory is that wildfire observations documented in operational reports and photographs can be used to model fire behaviour for augmented operational decision support, while also providing new insights about the relationship between fuel structure and fire behaviour in the C-2 FBP System fuel type. I investigated the following research questions:

- 1) Does estimated stand density significantly influence the probability of a fire escaping initial attack and exceeding two hectares?

2) Does estimated stand density influence the potential of “challenge” fires, where fires exceed 0.5 ha prior to suppression resource arrival on scene, indicating agency resources may have difficulty containing the fire?

The above questions were explored 1) using the visually estimated stand density classification assigned by IA firefighters, and 2) in an independent, larger dataset using forest structure data obtained through LiDAR surveys, in lieu of oblique aerial photos.

Given the binary outcomes of escaped fires, challenge fires, and the non-normal distribution of their covariates, I chose to use logistic regression in the form of generalized linear models (GLM) to characterize escaped fire and challenge fire probability. The general GLM formula is expressed by Equation 1 and includes the non-linear interactions between predictive variables and their binary outcomes:

$$E(Y) = g^{-1}(X\beta)\beta_0 + \beta_1x_1 + \beta_2x_2 + \dots + \beta_mx_m \quad \text{Equation 1}$$

Where $E(Y)$ describes the probability of escape, g represents a link function, and $\beta_0, \beta_1, \dots, \beta_m$ are regression coefficients.

2.6 Oblique Aerial Photo Screening

From an initial dataset of 1327 wildfires with imagery provided by Alberta Wildfire, a subset of 216 fires qualified for testing their probability of escaping containment (hereafter referred to as the “escaped fire analysis”), and 264 fires were suitable for the “challenge fire” analysis. Valid photographs for the escaped fire analysis required suppression resources to take clear oblique aerial photographs during assessment phase of firefighting and initiate suppressive action before fires exceeded 2.0 hectares in size (

Figure 9). The 2.0 ha threshold conforms with Alberta Wildfire’s published standard (Government of Alberta, 2024) as well as Beverly’s (2017) definition of escaped fire. Challenge fires were defined as fires that exceeded 0.5 hectares prior to assessment, regardless of containment outcomes. The challenge fire

threshold of 0.5 ha was selected as it was the crossover point in this study's dataset where more fires escaped containment than were contained.



Figure 9 An example arrival photo taken by suppression crews during initial assessment, prior to the wildfire exceeding 2.0 ha. Photo courtesy of Alberta Wildfire.

Drawing on my experience as a wildland firefighter, I used the operational photo archive to identify fires burning in black spruce forests, with characteristics aligning with the C-1 (Spruce-lichen woodland) and C-2 (Boreal spruce) fuel types of the Canadian Forest Fire Behaviour Prediction (FBP) System (Forestry Canada Fire Danger Group 1992). Fires burning in other conifer fuel types such as mature or immature pine, deciduous or mixedwood stands, or other land cover types were excluded from analysis. If available, supplementary documentation and in-stand photos captured by crews on the ground were used to corroborate the timing of aerial photos and the assigned fuel type. Location data from the provincial records were verified using geolocation metadata attached to fire photos and landscape features verified with Google Earth satellite imagery. Additionally, I compared my assigned fuel types with two supplementary sources to corroborate my fuel type assessment:

- 1) On-site assignment of fuel type by agency staff at the time of assessment; and
- 2) remotely sensed fuel type determined from the Alberta FBP System fuel grid.

The provincial fuel grid is a province-wide raster dataset with a 100 m x 100 m spatial resolution populated with fuel types derived from multiple sources such as the Alberta Vegetation Inventory (AVI), Alberta Ground Cover Classification (AGCC), and disturbance inventories compiled by the provincial government (“Fire Behavior Prediction (FBP) Fuel Types,” 2023). The provincial fuel grid is released annually; therefore, the year’s preceding fuel grid was referenced for fuel type comparison with the year of each respective fire. Comparing my fuel type assignments to wildfire assessor fuel typing, we agreed approximately 80% of the time with fuel type calls. In contrast, both myself and the wildfire assessors agreed with the provincial fuel grid only 50% of the time.

2.7 Fire and Fire Environment Attributes Derived From Oblique Aerial Imagery

The presence of researchers and data collection instrumentation during wildland firefighting is generally prohibited. It is possible to utilize firefighting personnel for data collection, however, such demands are typically secondary to suppression priorities; there are calls for improved data collection during wildfire operations (Filkov et al., 2018). Photos were assessed with respect to smoke column, flame (including smouldering combustion), and fuel density characteristics. Attributes were assigned to each fire using ordered categories. Some attributes and categories were custom developed for the analysis while others draw on existing definitions. For example, the Canadian Forest Fire Behaviour Prediction (FBP) System defines three categories of fires based on the amount of crown fuel involvement: surface fire (0-10% crown involvement), intermittent crown fire (11-89%), and continuous crown fire (90%+) (Hirsch, 1996); in this study, the original three categories are expanded to five categories of crown involvement.

2.7.1 Stand Density

Density was ocularly estimated with inspiration from the degree of canopy gaps and visible forest floor seen in the oblique wildfire photos. Density was estimated independently of tree height, however shorter stands and more vertical photography can be expected to increase the detection of forest floor gaps. Sikkink et al. (2009) defines a forested area as having greater than 10% tree coverage, which provides considerable latitude when establishing the lower end of the density spectrum. The picture archive contained oblique photos with varied viewing angles of the fire location, typically ranging from 10 to 30 degrees below horizontal. Fires used in this study were predominantly found on flat terrain. As such, density definitions do not account for any slope affects affecting apparent density.

Each fire was assigned a label of sparse, moderate, or dense, collectively referred to as DENSE1.

Simplified two-category groupings were also defined for modeling purposes using combinations of the three base categories: DENSE2 merges sparse and moderate density stands into one category, and DENSE3 merges moderate and dense stands into one category. Breakdowns of DENSE1, DENSE2, and DENSE3 are described in detail in Table 3.

Table 3 Stand density categories, descriptions, and contextual information.

Classification	Description	Notes
Base Density Categories		
DENSE1		
Sparse	Isolated individual trees or small clumps of about 3-5 trees. Limited to rare contact between tree crowns.	Commonly found in C-2 bog/fen environments and C-1 fuel types. Easy to mentally remove trees and describe the underlying topography and surface characteristics. The upper limit for forest density in this category is approximately 400-500 mature trees per hectare, possibly higher in bog/fen environments.
Moderate	Regular crown contact intermixed with canopy gaps showing visible forest floor.	Canopy gaps are easy to identify even at low altitude and low camera angles. Approximately 400-900 mature trees per hectare, with canopy gaps typically covering <50% of the forest.
Dense	Canopy gaps are rare to nonexistent. >90% tree crowns are touching.	Gaps are seldom larger than a few tree canopies across, if any, even in near-nadir (vertical) camera orientation. Stands are often fully mature and tall.
Grouped Density Categories		
DENSE2		
Density2 Open (Sparse + Moderate)	sparse + moderate combined	Merging sparse and moderate stand densities.
Density2 Closed (Dense)	Canopy gaps are rare to nonexistent. Nearly all tree crowns are touching.	
DENSE3		
Density3 Open (Sparse)	Isolated individual trees or small clumps of about 3-5 trees. Limited to rare contact between tree crowns.	
Density3 Closed (Moderate + Dense)	Moderate + dense combined	Merges moderate and dense stand densities.



Figure 10 Visual examples of forest density: Sparse (A), moderate (B), and dense (C). Photos Courtesy of Alberta Wildfire.

2.7.2 Perimeter Surface Flame

Flame is direct visual confirmation of energy released by a fire (Rossa et al., 2024). Byram’s equation for fireline intensity (1959) calculates the total energy output per meter length of fireline from the product of a constant heat of combustion and two inputs: rate of spread and fuel consumption. Flame length has been used to estimate fire intensity when measurements of rate of spread and fuel consumption are not available (Alexander and Cruz, 2012). It was not possible to measure the dimensions of flames visible in the photo archive. Instead, an ordinal descriptor of flame arrangement was created (Table 4). Should the head fire be obscured by smoke, flanking fire can be used as a proxy for head fire intensity by increasing the observed flank fire to the next level. Four categories were used to classify perimeter surface flame: Smouldering, sprites, isolated flame fronts, and continuous flame fronts.

Table 4 Flame categories observed at the fire edge, description and contextual information.

Classification	Description	Notes
Smouldering	Observed during a low intensity surface or ground fire. Flames may not be visible.	Flames may not be visible; however, smoke can be created from smouldering combustion.
Sprites	Small visible flames ranging from single burning branches to small campfire equivalents.	Flame is localized and possibly intermittent, without continuous linear extent. Does not convey a direction of spread.
Isolated flame fronts	Continuous, flaming linear features no more than 5 m long.	Not limited to one location and may occur in different sections of the perimeter. May have large gaps between isolated fronts and is not limited to the head fire.
Continuous flame fronts	Extensive, flaming linear features.	Longer than isolated fronts, may occur around the flanks and back of the fire in addition to the head. Associated with high-intensity, vigorous surface and crown fires. Can easily be seen through the canopy.

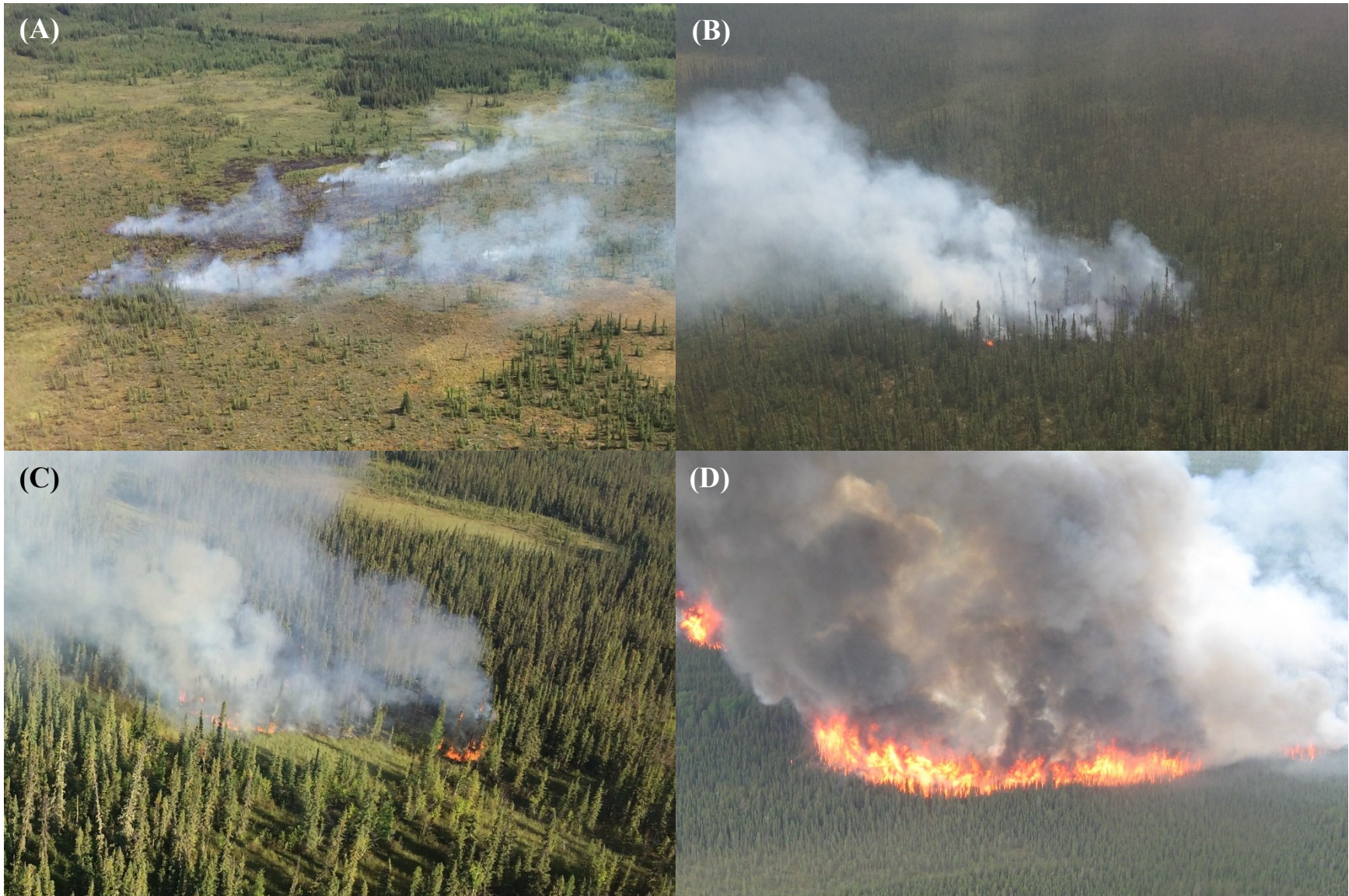


Figure 11 Visual examples of perimeter surface flame: Smouldering (A), sprites (B), isolated (C), and continuous flame (D). Photos courtesy of Alberta Wildfire.

2.7.3 Crown Involvement

Van Wagner (1977a) describes three classes of crown fire: passive, where surface fire drives movement of the flame front; active, where crown fire and surface fire link to form a single unit but are interdependent for canopy and surface pre-heating; and independent fire, where (rarely) the crown can self-ignite and propagate independent of surface fuels. The Canadian Forest Fire Behaviour Prediction (FBP) System defines three fire types based on the amount of crown fuel involved in combustion: surface fires (0-9%), intermittent crown fires (10-89%), and continuous crown fires ($\geq 90\%$ crown consumption) (Forestry Canada Fire Danger Group, 1992). In this study, the original three terms were expanded, and fires were assigned one of five ordinal categories of crown involvement (Table 5) based on visible flame characteristics observed in the: none, light candling, heavy torching, intermittent crowning, and continuous crowning. In cases where the advancing flame front was not visible in the photograph, the presence and amount of crown fraction burned was used to assign a crown involvement category.

Table 5 Crown fire involvement categories, descriptions, and contextual information.

Classification	Description	Notes
None	No evidence of crown involvement.	No visible flame in the canopy, no partial or completely burned crowns visible.
Light candling	Individual trees rarely being partially or completely consumed by fire.	Conforms to the surface fire definition of the FBP with <10% of canopy involvement in the fire (Hirsch, 1996). No more than one tree candling at a time. Ample spacing between candles. Typical of low-intensity surface fire. Does not include single tree lightning fires.
Heavy torching	Candling but more than one tree simultaneously, or clumps of tree crowns burning. 10-65% CFB	Some fire connectivity between canopies if trees are close enough. Dependent on surface fire for propagation, <65% crown consumption.
Intermittent crowning	Discontinuous crowning up to several meters wide. CFB 65-89%	Multiple trees torching in proximity but still dependent on vigorous surface fire for preheating. Consumes 65-89% of the canopy. Canopy fire is several tree widths across but laterally discontinuous.
Continuous crowning	Flame front and canopy fire advances as a singular unit $\geq 90\%$ CFB	Extreme fire activity in which the crown fire is advancing through the canopy in a continuous, connected fire front. Flame heights can extend well above two times tree height, with >90% canopy consumption.



Figure 12 Example photographs associated with crown involvement categories: (A) light candling; (B) heavy torching; (C) intermittent crowning; and (D) continuous crowning. Photos Courtesy of Alberta Wildfire.

2.7.4 Smoke Colour

Smoke is a product of incomplete combustion. Wildfire smoke can be used to visually identify wildfire activity from more than 40 km away and is a key feature in wildfire detection. As fire intensity increases, carbon-based particulate matter ejected into the atmosphere becomes denser and larger, blocking sunlight from passing through the column. The scattering of light through the convective column, an optical property referred to as Mie scattering, progressively darkens the fire's convective column from grey, to brown, to black as a result (Patterson and McMahon, 1984). Smoke colour has long been used in operational fire response as an indicator of fire intensity and the potential for fire suppression challenges: The Alberta Wildfire Crew Leader Training Manual advises crew leaders to report smoke column activity as soon as it is visible, noting smoke colour and lean (angle) (Government of Alberta, 2016). According to the manual, dense white smoke signifies very moist fuels and low fire behaviour; grey smoke indicates moist fuel and low to moderate behaviour; black smoke represents dry or manufactured fuels and high fire behaviour; and copper-bronze indicates very dry fuels with high to extreme fire behaviour, or manufactured fuels. In this study, the darkest smoke colour visible in the photograph archive was used to assign each fire one of three possible smoke colour categories based: light grey, brown grey, and black grey (Table 6). The copper-bronze smoke colour is seen in extreme wildfire behaviour and that occurs beyond the scope of initial attack as defined in this thesis, so it was not included.

Table 6 Smoke column categories, description and associated contextual information.

Classification	Description	Notes
Light grey	White to light grey.	Associated with low-intensity fires.
Brown grey	Light beige to yellow brown.	Commonly observed along the fireline with higher intensity fire, notably once the canopy becomes involved with candling and torching. Colour darkens with increasing fire intensity and may be found within a predominantly light grey column.
Black grey	Dark grey to black, also includes the bronze/copper extreme fire behaviour condition.	Associated with significant canopy involvement and intense wildfire behaviour. Indicative of incomplete combustion and live vegetation contributing a significant component of burning material (Patterson and McMahon, 1984).

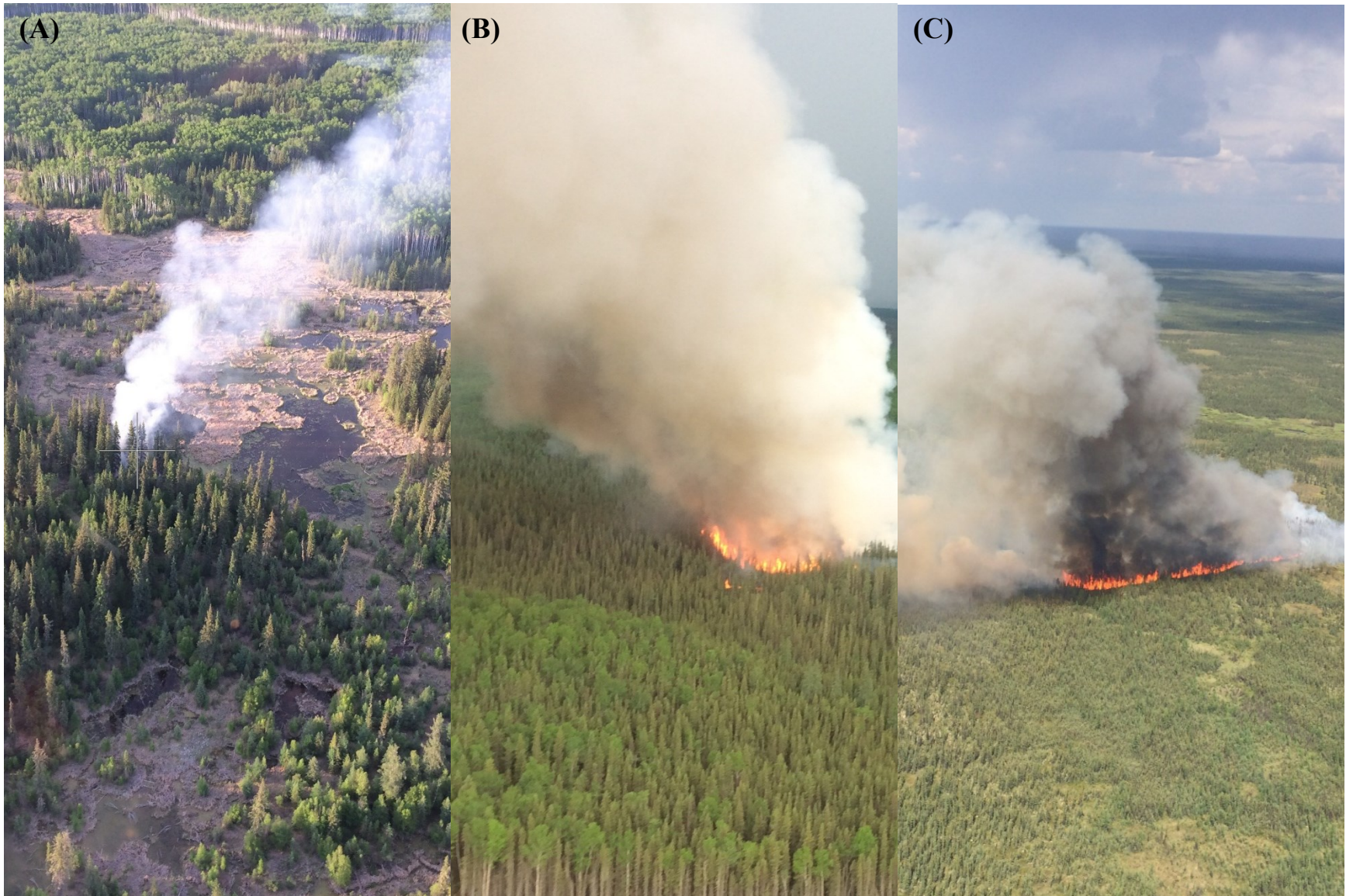


Figure 13 Example photos associated with smoke colour categories: (A) Light grey, (B) brown grey, and (C) black grey. Photos courtesy of Alberta Wildfire.

2.7.5 Smoke Continuity

A rating of smoke continuity was used to document the overall length and opaqueness of the smoke column. The upper extent of the column was defined as the location where the column begins to break up and disperse. Smoke plume size is positively correlated to wildfire intensity (Williamson et al., 2013). Three categories were used to document smoke continuity: puffer, continuous, and heavy (Table 7).

Table 7 Smoke continuity and their relationships to fire behaviour.

Class	Definition	Notes
Puffer	Light, wispy, lacks continuity.	Will be affected by local weather conditions, may be contained within the canopy by winds aloft. Upon leaving the canopy, the column will quickly disperse.
Continuous	Smoke rises equal to at least double average tree height before dispersing.	Column may be several trees wide but can still be seen through. Column is contiguous beyond several tree heights above the canopy.
Heavy	Column is opaque regardless of width	Dense column that cannot be seen through. Not limited by colour of smoke.

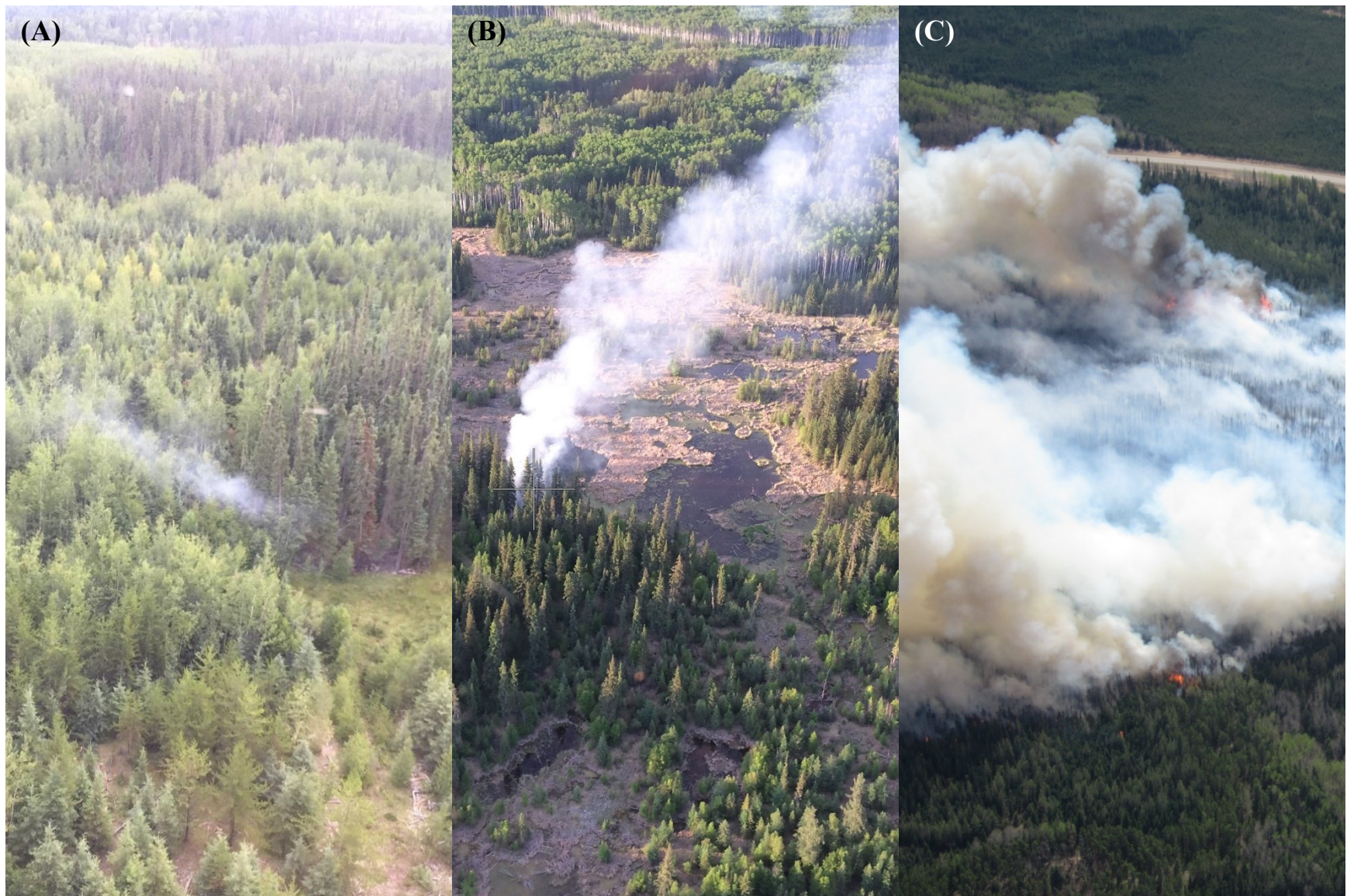


Figure 14 Visual examples of smoke continuity: Puffer (A), continuous (B), and heavy (B).

2.7.6 Smoke Angle

Smoke angle is the result of interactions between the convective gasses in the smoke column and the lower atmosphere. Column angle was determined by the approximate midline of the main column where smoke is most dense, typically in the region of the head fire. After accounting for parallax from the photos to estimate true smoke angle, four categories were identified: vertical, light, moderate, and steep (Table 8).

Table 8 Smoke angle descriptions.

Classification	Description	Notes
Vertical	Smoke column rises straight up	
Light	Non-vertical to approximately 60° above the horizon	
Moderate	Mean angle of 45°	Angle may range between 20° - 60°
Steep	Below 20°	In many circumstances, the column maintains contact with the top of the forest canopies.



Figure 15 Visual examples of column angle: Vertical (A), light (B), moderate (C), and steep (D). Photos Courtesy of Alberta Wildfire.

2.8 Data analysis: Probability of Escaped Fire and Challenge Fire

In total, 33 variables were analyzed in the escaped fire and challenge fire analysis. To decrease multidimensionality of the analysis and alleviate multicollinearity errors, the 33 variables were grouped into 6 categories as seen in Table 9, where for each test only one subset of terms within each group was selected. For example, a given test could not include numerical moisture values + categorical moisture values, such as an FFMC of 90 and a categorical FFMC of “Very High”, numerical moisture values and numerical fire behaviour values such as Duff Moisture Code and Build-Up Index, and categorical fire behaviour values and categorical fire behaviour index, such as Initial Spread Index and Fire Weather Index. Combining numerical fuel moisture values, ocularly assessed fire behaviour, and ocularly assessed forest density, for example, would produce a valid test. Containment milestones that report fire size, specifically being held, under control, and extinguished, were excluded from the analysis as they were directly linked to the response variables. Following the criteria stated above, 512 independent tests containing up to 13 terms were created for evaluation of both escaped fire and for challenge fire GLMs, respectively. An additional 28 combinations were created for the parallel LiDAR data analysis.

Table 9 Evaluated variables for the escaped and challenge fire analyses. Ranked values refer to the qualitative “low,” “moderate,” “high,” “very high,” and “extreme” FWI System output groupings as defined by Alberta Wildfire.

Group	Variables
FWI System Values	
Numerical fuel moisture values	FFMC, DMC, DC
Numerical fire behaviour values	ISI, BUI
Numerical FWI value	FWI
Ranked fuel moisture values	FFMC (ranked), DMC (ranked), DC (ranked)
Ranked fire behaviour values	ISI (ranked), BUI (ranked)
Ranked FWI value	FWI (ranked)

Ocularly assessed fire behaviour	
Ocularly assessed fire behaviour	Perimeter flame, crown fire involvement, smoke colour, smoke plume angle, and smoke continuity
Suppression crew observations	
Suppression crew observations	Crew fire type, and observed overhead weather
Dispatch time variables	
Independent time variables	Crew departure, travel time
Merged time variables	Crew departure + travel time
Weather variables	
Weather variables	Temperature, relative humidity, wind speed, wind direction, 24-hour precipitation
C-1 and C-2 fuel density variants	
Standard	Sparse, moderate, dense
Density2	(sparse + moderate) and dense
Density3	Sparse and (moderate + dense)

2.8.1 Simplifying Test GLMs

Simplification of the GLM input parameters was achieved using a bidirectional stepwise regression with statistical modeling software “R,” version 4.0.2 (R Core Team, 2017). A bidirectional GLM test works as follows: For each test, a starter term is added to the GLM, which was then evaluated for its Akaike Information Criterion (AIC) against a baseline formula. AIC employs the parsimonious concept of optimal model fitting by penalizing increasing model complexity, selecting the best-fitting model using the least

number of parameters (Burnham and Anderson, 2002). In practice, between two GLM tests, if test two has a lower AIC score than test 1 (the baseline formula), that means the second test is better. Terms were added and evaluated until the AIC no longer decreased relative to the baseline formula, signifying the completion of the test, and the final output was recorded.

2.8.2 Model Building

The results of the GLM tests were ordered by decreasing C-statistic. The C-Statistic is a measure of model fit, called the receiver operating characteristic (ROC) curve, and quantifies the predictive accuracy of a given GLM (Westreich et al., 2011). The value of an ROC curve ranges from 0 to 1, with a higher ROC curve value indicating higher predictive accuracy; an ROC curve below 0.5 indicates poor accuracy, where a value of 0.9 or higher indicates strong predictive accuracy. Model accuracy and predictive capability for selected models were then evaluated using leave-one-out cross validation (Celisse, 2014).

Identifying if a variable was significant in a model output was achieved by analyzing the logit ratios of a model's terms. By comparing the logit ratios of each model's terms using a Chi-Square statistic, a variable's statistical significance is established if the p-value is $p < 0.05$ (Westreich et al., 2011). To facilitate understanding of the impact of each variable relative to the model intercept, taking the logarithm of the model's logit terms converts the model from a probability-based model to a likelihood-based model. This changes the term coefficient to an easier-to-understand decimal value indicating how much more or less likely a fire is to escape containment or present suppression challenges referred to the log odds. Models were then visualized using the sjplot package (Lüdecke, 2020).

2.8.3 Comparing Photograph Density Estimations Against LIDAR-Derived Forest Structure

LIDAR (LIght Detection and Ranging) is an active remote sensing technique that uses precisely-timed laser pulses emitted from a scanner to determine the distances of objects (Wehr and Lohr, 1999). When combined with high-accuracy GPS and mounted to a moving platform such as an airplane, researchers

can create highly-detailed point clouds that provide both vertical and lateral structural information of a forest (Lim et al., 2003). This distance data can be used to generate intricate and highly detailed 3D maps of forested areas.

The parallel LiDAR-based forest structure data was provided by the Coops Lab at the University of British Columbia. The data was originally developed for comparing forest structure and ecological diversity in Alberta's Boreal Forest (Guo et al., 2017), but was repurposed to cross-examine the effects of forest structure on wildfire. The dataset consisted of a province-wide, 30 m spatial resolution raster layer acquired between 2003 and 2014 that were classified into eight distinct structural arrangements.

Fires that were classified as lightning ignitions in C-2 fuels by wildfire assessors in provincial records, and classified by Guo et al. (2017) at least one year prior to ignition, were considered valid for testing. The LiDAR structure classification measures were applied to the escaped fire and challenge fire tests using two approaches:

- 1) The location of the individual 30m structure classification pixel and fire location coordinates.
- 2) The highest count of structure classification pixels within a 100 m radius around each ignition location.

Scenarios were modeled and graphed the same way as the escaped and challenge fire tests, but in this case, forest density and wildfire behaviour derived from the oblique photo dataset were replaced by LiDAR-assessed forest structure and wildfire assessor-documented overhead weather (clear, dryCB, wetCB, overcast, and rainshowers) and observed fire type (ground, surface, crown).

Chapter 3: Results

3.1 Modeling the Probability of Fire Escape with Ocularly Assessed Forest Density

3.1.1 Comparing Attributes of Contained and Escaped Fire Groups

Of the 216 fires that satisfied the conditions for analysis, sixteen exceeded 2 hectares and were classified as escaped. Seventy-six percent of wildfires occurred within 30 km of the nearest active fire weather (FWX) station, increasing to 95% within 40 km. Table 10 shows counts and proportions for both escaped and contained fires arranged by their FWI System hazard level. In general, the proportion of fire escapes increased as FWI System values increased. A Chi-square test of proportions between contained and escaped fire FWI System hazard ranks showed no significant difference between groups.

Table 10 Fire counts grouped by FWI System hazard level and containment outcome. Proportions as a function of column totals are shown in brackets.

Rank	FFMC		DMC		DC	
	Contained	Escaped	Contained	Escaped	Contained	Escaped
Low	40 (0.20)	3 (0.19)	88 (0.44)	3 (0.19)	6 (0.03)	1 (0.06)
Moderate	43 (0.22)	3 (0.19)	21 (0.11)	3 (0.19)	39 (0.20)	4 (0.25)
High	76 (0.38)	5 (0.31)	42 (0.21)	4 (0.25)	73 (0.37)	3 (0.19)
Very High	38 (0.19)	5 (0.31)	30 (0.15)	4 (0.25)	59 (0.30)	4 (0.25)
Extreme	3 (0.02)	0 (0.00)	19 (0.10)	2 (0.13)	23 (0.12)	4 (0.25)

Rank	ISI		BUI		FWI	
	Contained	Escaped	Contained	Escaped	Contained	Escaped
Low	3 (0.26)	(0.25)	52 (0.26)	2 (0.13)	55 (0.28)	4 (0.25)
Moderate	61 (0.38)	6 (0.31)	51 (0.26)	3 (0.19)	54 (0.27)	4 (0.25)
High	51 (0.31)	4 (0.38)	78 (0.26)	9 (0.38)	61 (0.31)	3 (0.19)
Very High	75 (0.05)	5 (0.06)	9 (0.18)	0 (0.19)	26 (0.13)	5 (0.31)
Extreme	10 (0.02)	1 (0.00)	10 (0.05)	2 (0.13)	4 (0.02)	0 (0.00)

Mean, median, standard deviation, and range values of quantitative fire attributes are shown in Table 11 for both contained and escaped fire groups. FWI System values were not included in this table, as single digit increases or decreases in FWI System values are not linear and are more impactful as hazard increases. Attributes that reflect fire size were intuitively significantly different between the two groups, which is expected given that successful containment was determined by fire size; all fire size variables

were excluded from the analysis for this reason. Temperature and 24-hour precipitation were found to be significant between contained and escaped fire groups, however in both cases mean and median values for escaped fires had more rain and lower temperatures than contained fires. Mean response times were not significantly different between contained and escaped fire groups.

Table 11 Summary statistics of select escaped fire variables. General variable significance was evaluated with a chi square test where significant differences are highlighted in bold.

	Mean		Median		Standard Dev.		Range		Chi Square Score
	Contained = 200	Escaped = 16	Contained	Escaped	Contained	Escaped	Contained	Escaped	
Wind Speed (km/h)	9.66	9.81	9.00	8.50	5.56	5.66	0.0 - 32.0	0.0 - 20.0	0.91
Assessment Hectares (ha)	0.29	0.82	0.10	1.00	0.42	0.42	0.0 - 1.8	0.1 - 1.5	0.0014**
Departure Time	0.57	0.87	0.08	0.11	2.56	2.54	0.0 - 22.4	0.0 - 10.2	0.184
Crew Travel Time	1.05	0.77	0.53	0.61	2.31	0.60	-0.1 - 17.2	0.1 - 2.1	0.16
Departure Time + Crew Travel Time	1.62	1.63	0.71	0.75	3.39	2.72	0.0 - 22.6	0.2 - 11.1	0.199
Firefighting Start size (ha)	0.27	1.14	0.10	1.00	0.40	0.55	0.0 - 2.0	0.1 - 2.0	<0.0001***
Fire Being Held Size (ha)	0.33	21.98	0.10	4.50	0.46	37.03	0.0 - 2.0	2.5 - 120.7	<0.0001***
Fire Under Control Size (ha)	1.90	21.53	0.10	5.39	20.00	36.86	0.0 - 281.0	2.1 - 120.7	<0.0001***
Fire Extinguished Size (ha)	1.49	19.89	0.10	5.66	14.40	34.31	0.0 - 200.7	1.2 - 120.1	<0.0001***
Temperature (C)	22.01	21.38	22.00	20.25	3.48	4.51	10.4 - 32.0	14.0 - 29.5	0.0092**
Relative Humidity (%)	52.07	46.75	51.00	44.75	13.32	16.48	17.7 - 100.0	27.6 - 79.2	0.685
24-Hour Precipitation (mm)	1.20	2.23	0.00	0.25	3.88	4.45	0.0 - 28.2	0.0 - 17.2	0.0004***

Significance codes: p<0.001=*** (v. strong sig.) p<0.01=** (strong sig.) p<0.05=* (significant) p<0.10 =. (weak sig.)

3.1.2 Logistic Regression Analysis

The escaped fire analysis produced 30 unique models with C-statistics ranging from 0.607 to 0.911, containing up to 5 predictor variables, and as few as 1. The top 10 models in decreasing order of C-Statistic are shown in Table 12. In tests 73 and 33, Density3 played a significant role in predicting containment outcome with Chi-square p-values of 0.04029 and 0.04838, respectively. In tests 53 and 13, DENSE1 was weakly significant (p= 0.07119, p= 0.08222). DENSE2 was retained in two of the models, contributing to overall model performance, but was not statistically significant in either.

Table 12 The top ten escaped fire GLMs ordered by decreasing C-statistic. Calls with significant density variable Chi-square scores for the density variable are in displayed in bold.

Test	Winning call (Terms ordered by reduction in overall model AIC)	C-stat	AIC Reduction	Density Sig. (Chi-sq.)
Test 43	Smoke Colour + BUI + Smoke Continuity + Precipitation + RH	0.9108	21.7903	NA
Test 3	Smoke Colour + DMC + Precipitation + Smoke Continuity + RH	0.9073	21.6736	NA
Test 73 (E-FIRE1)	Smoke Colour + BUI + Smoke Continuity + Precipitation + DENSE3	0.9020	23.7396	0.04029*
Test 53	Smoke Colour + BUI + Smoke Continuity + Precipitation + Density	0.9009	22.8189	0.07119.
Test 33	Smoke Colour + DMC + Precipitation + Smoke Continuity + DENSE3	0.8984	23.1485	0.04838*
Test 13	Smoke Colour + DMC + Precipitation + Smoke Continuity + Density	0.8961	22.2486	0.08222.
Test 63	Smoke Colour + BUI + DENSE2 + Smoke Continuity + Precipitation	0.8919	22.7980	0.12482
Test 71	Smoke Colour + BUI + Smoke Continuity + DENSE3	0.8898	20.5762	0.11873
Test 31	Smoke Colour + DMC + Smoke Continuity + DENSE3	0.8878	20.1424	0.1313
Test 23	Smoke Colour + DENSE2 + DMC + Smoke Continuity + Precipitation	0.8848	22.4334	0.10072

Significance codes: p<0.001=*** (v. strong sig.), p<0.01=** (strong sig.), p<0.05=*(significant), p<0.10 =. (weak sig.)

3.1.3 Contribution of Stand Density Attributes to the Probability of a Fire Escaping Containment

Test 73 and test 33 were identified as the two best-performing models that included a density input.

Both models reported accuracy scores of 0.93 and kappa statistics of 0.1. Smoke continuity as a term in both models reported high standard error where removal of the term resulting in test 33 losing density as significant predictor variable, and test 73's (hereafter E-FIRE1) density term to only report weak significance ($p = 0.08$). Model terms are ordered by their decreasing influence on the model's AIC score relative to a general intercept formula of $y = 1$. Model E-fire1 is as follows:

$$\text{E-FIRE1 } y = \frac{1}{1 + e^{-(-6.4330 + \alpha + 0.0225\text{BUI} + 0.1195\text{PRECIP} + \gamma)}} \quad \text{Equation 2,}$$

Where α is a smoke colour term with values of 0 for light grey smoke, 1.8395 for brown grey smoke, and 3.6384 for black grey smoke; BUI is the reported FWI system value; PRECIP is the number of millimeters of rain in the previous 24 hours; and γ describes DENSE3 where open is 0 and closed canopy is 1.3389.

Of all the attributes derived from ocular assessments of wildfire photographs, smoke colour was the most influential variable with respect to the probability of a wildfire exceeding 2 ha, with a general variable p-value of 3.987e-06. Log odds for E-FIRE1 shows that a wildfire with grey-black smoke is 38 times more likely to escape containment than a wildfire with a light grey smoke column. Stand density was weakly significant ($p = 0.082$). Fires burning in stands with closed canopies, as defined by DENSE3, are over three times more likely to escape containment than fires burning in stands with open canopies.

The Buildup Index had weak significance in E-FIRE1 ($p=0.086$). The expanded statistics for E-FIRE1 are shown in Table 26 in the appendix and is graphically illustrated in Figure 16 .

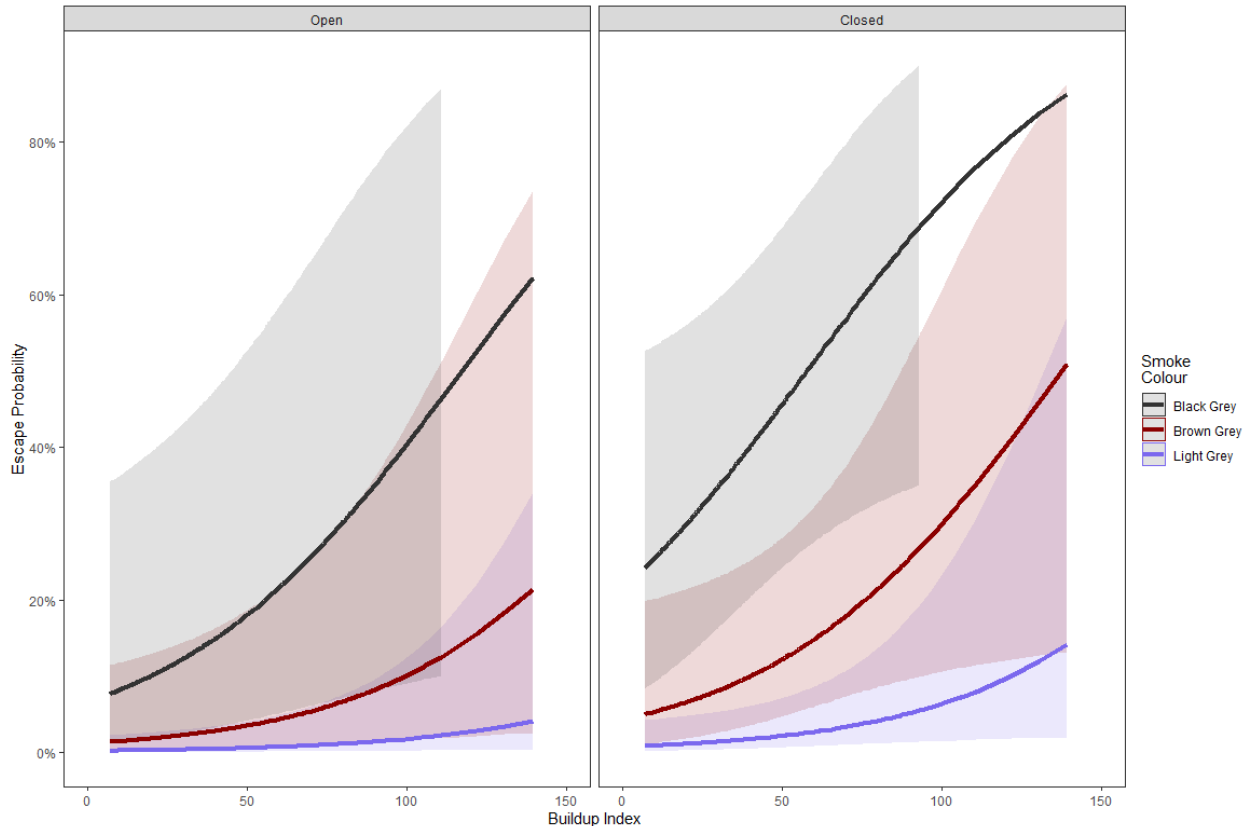


Figure 16 E-FIRE1 showing the likelihood of a wildfire escaping containment as a function of by smoke colour and Buildup index with shading representing the model’s 95% confidence intervals for smoke colour. The early termination of the confidence interval for black grey smoke reflects the highest recorded BUI value in the dataset for that smoke colour.

3.2 Modeling the Probability of Fire Escape with forest LiDAR Structure Classification

3.2.1 Comparing Contained and Escaped Fire Groups

All fires used in the LiDAR structure analysis were classified as C-2 during assessment by wildfire crews at the scene of the fire. Credence was given to the fuel type assigned by the wildfire assessors over the LiDAR structural classification as fuel typing was done based on the physical presence of Boreal spruce, whereas the LiDAR structural classification is an association with a particular forest type and not species specific. When compared to the LiDAR forest structure classification developed by Guo et al. (2017), 52% of wildfires were classified as short, open canopy black spruce stands (Table 13); these stands also had

the highest proportion of escaped fires of the 8 structural classifications, with 8% of fires exceeding the 2 ha threshold. From the analysis, 10 unique GLMs were produced, all of which had significant forest structure variables with C-statistics ranging from 0.771 to 0.674 (Table 16).

Table 13 Count of contained and escaped fires by LiDAR-derived forest structure class as defined Guo et al. (2017). Structure 5 did not overlap with any wildfires and was omitted.

Structure	Description	Count (proportion of structure class)		
		Contained	Escaped	Total
1	Short, medium canopy cover stand (Aw)	126 (0.95)	6 (0.05)	132 (1.00)
2	Short, open canopy stand (Sb)	704 (0.92)	61 (0.08)	765 (1.00)
3	Very short, dense canopy cover stand (Sb)	110 (0.97)	3 (0.03)	113 (1.00)
4	Very tall, complex stand (Sb)	83 (1.00)	0 (0.00)	83 (1.00)
5	N/A	N/A	N/A	N/A
6	Tall, dense canopy cover stand (Aw)	242 (0.96)	10 (0.04)	252 (1.00)
7	Short, closed canopy stand (Aw+Sb)	99 (0.95)	5 (0.05)	104 (1.00)
8	Very tall, closed canopy stand (Aw)	11 (1.00)	0 (0.00)	11 (1.00)
	Total	1375 (0.94)	85 (0.06)	1460 (1.00)

FWI System values for escaped and contained fires are noted in Table 14. Overall, very high and extreme FWI System classes are associated with higher proportions of escaped fires than those associated with low and moderate fire weather conditions (Table 14). Chi-squared analysis of FWI System values showed no significant differences between probability of escaped and contained fires for either FWI System components or FWI System behaviour codes.

Table 14 Distribution of contained and escaped fire FWI values as both raw counts and proportions of their respective escaped and contained FWI classes, shown in brackets.

Rank	FFMC		DMC		DC	
	Contained	Escaped	Contained	Escaped	Contained	Escaped
Low	236 (0.17)	6 (0.07)	520 (0.38)	28 (0.33)	54 (0.04)	1 (0.01)
Moderate	260 (0.19)	14 (0.16)	188 (0.14)	6 (0.07)	240 (0.17)	15 (0.18)
High	439 (0.32)	33 (0.39)	353 (0.26)	19 (0.22)	474 (0.34)	23 (0.27)
Very High	359 (0.26)	27 (0.32)	225 (0.16)	21 (0.25)	387 (0.28)	28 (0.33)
Extreme	81 (0.06)	5 (0.06)	89 (0.06)	11 (0.13)	220 (0.16)	18 (0.21)

Rank	ISI		BUI		FWI	
	Contained	Escaped	Contained	Escaped	Contained	Escaped
Low	314 (0.23)	10 (0.12)	239 (0.17)	11 (0.13)	313 (0.23)	11 (0.13)
Moderate	439 (0.32)	22 (0.26)	411 (0.30)	25 (0.29)	339 (0.25)	22 (0.26)
High	451 (0.33)	39 (0.46)	411 (0.30)	16 (0.19)	417 (0.30)	27 (0.32)
Very High	155 (0.11)	14 (0.16)	237 (0.17)	24 (0.28)	247 (0.18)	21 (0.25)
Extreme	16 (0.01)	0 (0.00)	77 (0.06)	9 (0.11)	59 (0.04)	4 (0.05)

Consistent with results reported in Section 4.1, size-based fire attributes were significant with respect to fire escape, as well as temperature (Table 15). Contained fires had a median suppression start size of 0.2 ha, whereas escaped fires had a median suppression start size of 0.89 ha. In summary, compared with contained fires, escaped fires were larger by the time suppression crews began actioning the fire, and were associated with weather conditions that tended to be hotter, drier, and windier.

Table 15 General summary statistics of fire attributes sorted by contained and escaped fires. General variable significance was evaluated with a chi square test where significant differences are highlighted in bold.

	Mean		Median		Standard Dev.		Range		Chi Square p-value
	Contained	Escaped	Contained	Escaped	Contained	Escaped	Contained	Escaped	
Contained = 1375									
Escaped = 85									
Wind Speed	9.72	10.32	9.00	10.00	5.60	4.48	0.00 - 42.00	4.00 - 26.00	0.1191
Assessment Size	0.22	0.88	0.10	0.70	0.41	0.90	0.01 - 6.00	0.01 - 5.00	<0.0001 ***
Crew Departure Time	1.19	0.73	0.07	0.10	9.31	2.77	0.00 - 263.25	0.00 - 17.93	0.5522
Crew Travel Time	2.58	0.99	0.58	0.52	7.99	2.26	0.00 - 116.68	0.00 - 17.05	0.9952
Crew Departure Time +Crew Travel time	3.77	1.72	0.75	0.70	12.50	3.61	0.00 - 263.78	0.07 - 19.55	0.8729
Fire Fighting Start size	0.20	0.87	0.10	1.00	0.32	0.48	0.01 - 1.80	0.04 - 1.80	<0.0001 ***
Being Held Size	0.23	430.11	0.10	3.80	0.40	2600.72	0.01 - 3.40	0.10 - 18620.40	<0.0001 ***
Under Control size	0.23	604.30	0.10	4.60	0.39	3027.84	0.01 - 3.40	1.00 - 19280.00	<0.0001 ***
Extinguished Size	0.22	580.24	0.10	5.40	0.34	2933.70	0.01 - 2.00	2.08 - 19280.00	<0.0001 ***
Temperature	21.29	22.44	22.00	23.00	4.77	4.68	0.50 - 32.50	-4.60 - 29.50	0.007276**
RH	50.49	44.92	48.02	45.00	14.33	12.24	17.00 - 100.00	19.00 - 72.00	0.965
Precip	1.19	0.54	0.00	0.00	4.49	1.40	0.00 - 77.40	0.00 - 8.12	0.9319

Significance codes: p<0.001=*** (v. strong sig.), p<0.01=** (strong sig.), p<0.05=*(significant), p<0.10=. (weak sig.)

3.2.2 Logistic Regression Analysis

The analysis produced 10 unique models with C-statistics ranging from 0.67 – 0.79. The number of terms in the models ranged from two to five, with the 100 m structural LiDAR term having strong significance on the successful containment or containment failure for all models (Table 16). Significance of the 100 m density term in the 10 GLMs ranged from 0.0008 – 0.002 and relative AIC reductions of 20.26 - 56.1 relative to a baseline equation of $y = 1$.

Table 16 The escaped fire GLMs ordered by decreasing C-statistic. Winning calls with significant Chi-square scores for the 100 m buffered LiDAR structure variable are highlighted in bold.

Test	Winning call (Terms ordered by reduction in overall model AIC)	C-Stat	AIC Reduc.	Density Sig. (Chi-sq.)
Test 6 (EL-FIRE1)	Fire Type + Weather Overhead + LiDAR 100m Structure + RH + BUI Rank	0.791	56.118	0.001974**
Test 5	Fire Type + Weather Overhead + LiDAR 100m Structure + RH + DMC Rank	0.786	54.492	0.001974**
Test 1	Fire Type + Weather Overhead + LiDAR 100m Structure + RH + DMC	0.782	56.748	0.001974**
Test 2	Fire Type + Weather Overhead + LiDAR 100m Structure + RH + BUI	0.780	56.059	0.001974**
Test 3	Fire Type + Weather Overhead + LiDAR 100m Structure + RH	0.777	54.408	0.001974**
Test 12	RH + LiDAR 100m Structure + DMC Rank + FFMC Rank	0.717	21.285	0.0008413***
Test 13	RH + LiDAR 100m Structure + BUI Rank	0.709	22.363	0.0008413***
Test 8	RH + LiDAR 100m Structure + DMC	0.687	21.589	0.0008413***
Test 9	RH + LiDAR 100m Structure + BUI	0.685	21.293	0.0008413***
Test 10	RH + LiDAR 100m Structure	0.674	20.261	0.0008413***

Significance codes: $p < 0.001 = ***$ (v. strong sig.), $p < 0.01 = **$ (strong sig.), $p < 0.05 = *$ (significant), $p < 0.10 = .$ (weak sig.)

3.2.3 Contribution of Stand Structure to the Probability of a Fire Exceeding 2.0 Hectares

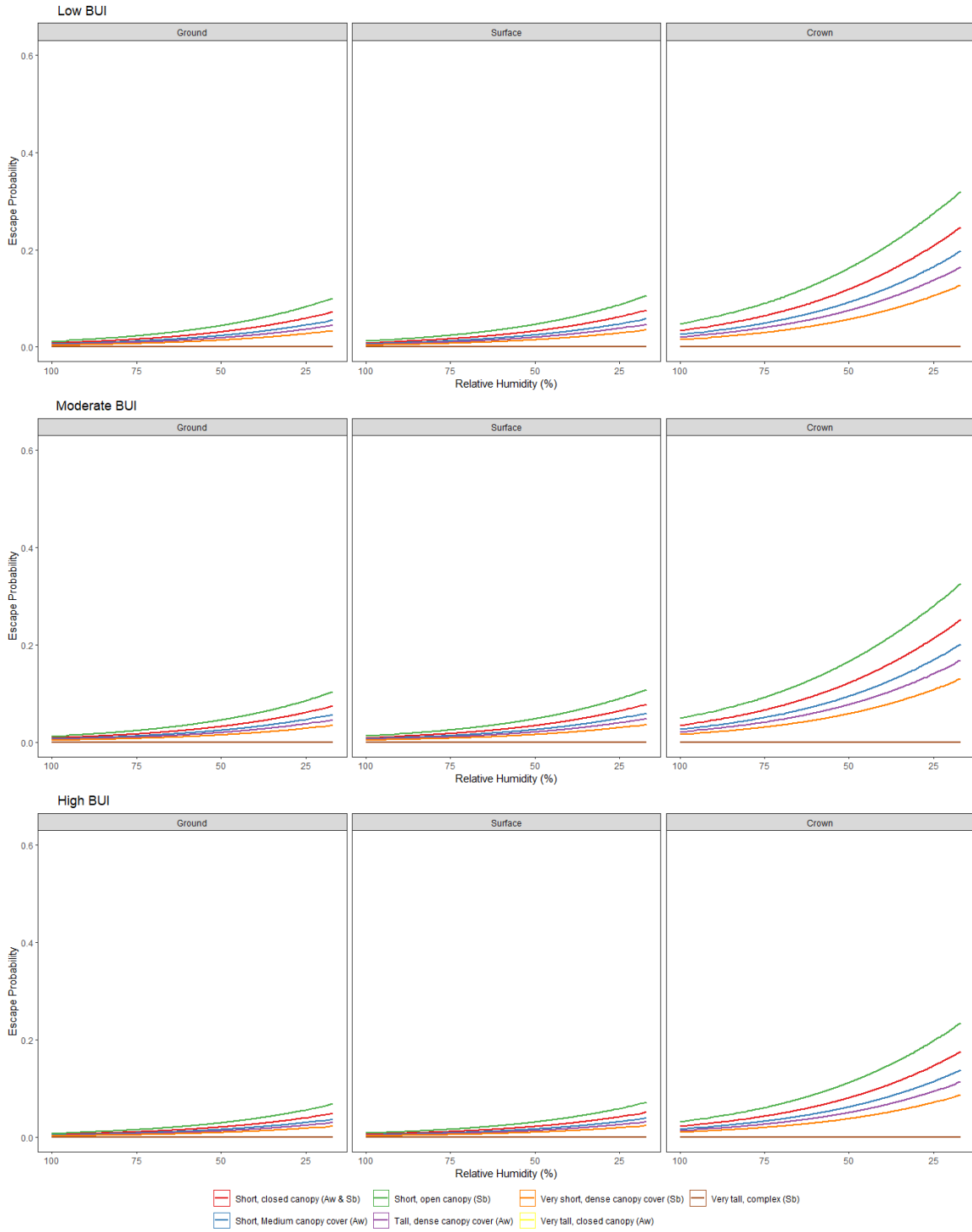
Test 6 (hereafter EL-FIRE1) reported the highest C-statistic of 0.79, an accuracy score of 0.94, and a kappa statistic of -0.004, is expressed by Equation 3, below:

$$\text{EL-FIRE1 } y = \frac{1}{1 + e^{-(0.2 + \alpha + \beta + \gamma - 0.02693RH + \epsilon)}} \quad \text{Equation 3}$$

Where α is a term for fire type, with values of 0 for crown fire, ground fire is -1.434, and surface fire is -1.378; β is a term for weather observed over the fire, where CBDry is 0, CBWet is -1.575, clear skies is 0.1079, cloudy is -0.6479, and raining is -1.021; γ represents LiDAR forest classification, where structure 1 is 0, structure 2 is 0.6479, structure 3 is -0.5207, structure 4 is -15.39, structure 6 is -0.2197, structure 7 is 0.2861, and structure 8 is -15.27; RH is the percent relative humidity expressed as a decimal; and ε denotes Buildup index hazard level, with values where extreme BUI is 0, very high BUI is 0.01179, high BUI is -0.9751, moderate BUI is -0.5193, and low BUI is -0.5455.

Fire type had a significant influence on the probability of a fire exceeding 2 ha. When a fire was classified as a crown fire, it increased the probability of a fire escaping compared with a surface fire classification by a factor of 4 (Table 27). Coefficients are expressed relatively to the factor chosen by the calculation as the intercept; for example, if Dry CB (dry cumulonimbus, alternatively, dry lightning) is the overhead weather factor chosen as the default, a fire experiencing rain showers would be less likely to exceed the 2 ha threshold by a factor of 2.4. Forest structure had a significant influence on the probability of a fire escaping ($p= 0.003$). Relative to Structure 1 (medium canopy aspen stand), Structure 2 (open canopy black spruce stand) is 1.9 times as likely to escape containment given otherwise equivalent conditions. When the LiDAR analysis was rerun with just spruce-based classes (3, 4, and 7), forest structure remained significant.

The model containing stand structure, overhead weather, and RH predictors is shown graphically in Figure 17. Fires burning in stands classified as Structure 2 have the greatest likelihood of escaping containment. The relative effects of overhead weather, noted in the expanded statistics below, show that fire escapes are more likely under clear conditions than overcast conditions; and fire escapes are more likely under overcast conditions than wet conditions. Fire will also be more likely to escape containment as fire crew-assigned crown involvement increases.



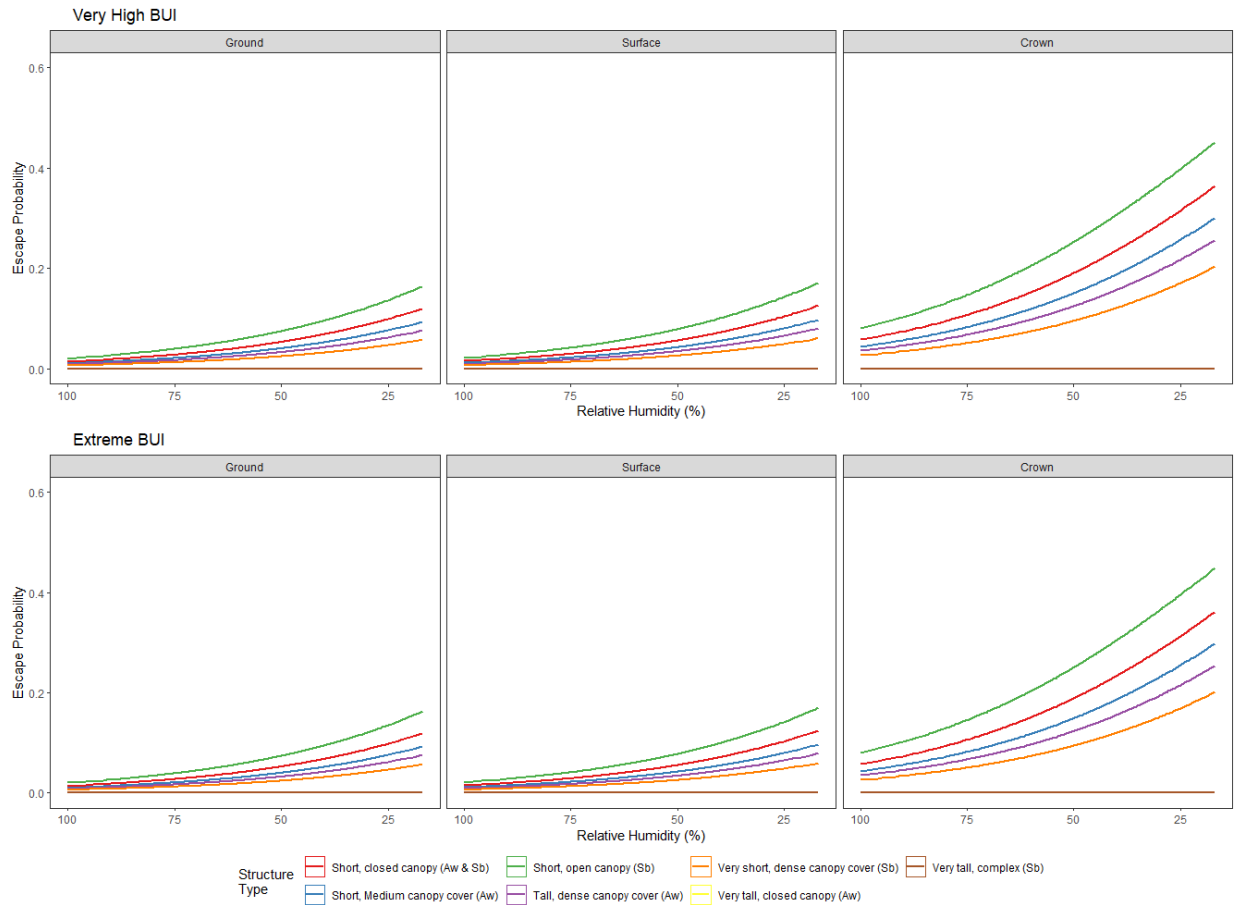


Figure 17 Probability of a wildfire escaping containment according to its LiDAR structure class as a function of relative humidity and Buildup index. Sb represents black spruce, and Aw represents trembling aspen. Note that very tall, complex aspen stands are not shown due to the lack of fire escapes.

3.3 Probability of a Crew Arriving to a Challenge Fire Using Ocularly Assessed Forest Density

3.3.1 Comparison of Attributes Between Challenge and No-Challenge Fire Groups

From the oblique aerial image dataset, 264 fires qualified for analysis. Of these 264 fires, 189 were assessed before they surpassed the 0.5 ha “challenge fire” threshold, and 75 fires had exceeded 0.5 ha prior to suppression resource arrival. When suppression began prior to a fire exceeding 0.5 ha, 98% of fires were contained before they exceeded 2 ha. In contrast, 44 of the 75 (59%) fires that exceeded 0.5 ha prior to the start of suppression also eventually exceeded 2 ha. (Table 17).

Table 17 Distribution of wildfires with challenge and no-challenge status, that also were successfully contained or exceeded 2 hectares.

	Count of fires (proportion)		
	No Challenge	Challenge	Total
Contained	186 (0.98)	31 (0.41)	217 (0.82)
Escaped	3 (0.02)	44 (0.59)	47 (0.18)
Total	189 (0.72)	75 (0.28)	264 (1.00)

Differences in FWI System values between no challenge and challenge fires were minimal, within 3-5%, but as high as 9% for respective FWI System moisture codes and behaviour codes (Table 18). Challenge fires begin to overtake no-challenge fires at a very high and extreme danger levels, however, Chi-square testing of FWI System components suggested differences were not significant.

Table 18 Counts of fires by challenge status and FWI System rank. Proportions of FWI moisture code and behaviour code for total respective “no challenge,” and “challenging” status are represented in brackets.

Rank	FFMC		DMC		DC	
	No Challenge	Challenge	No Challenge	Challenge	No Challenge	Challenge
Low	35 (0.19)	13 (0.17)	82 (0.43)	33 (0.44)	5 (0.03)	2 (0.03)
Moderate	39 (0.21)	14 (0.19)	19 (0.10)	8 (0.11)	35 (0.19)	13 (0.17)
High	72 (0.38)	27 (0.36)	40 (0.21)	12 (0.16)	70 (0.37)	29 (0.39)
Very High	40 (0.21)	16 (0.21)	28 (0.15)	18 (0.24)	56 (0.30)	20 (0.27)
Extreme	3 (0.02)	5 (0.07)	20 (0.11)	4 (0.05)	23 (0.12)	11 (0.15)

Rank	ISI		BUI		FWI	
	No Challenge	Challenge	No Challenge	Challenge	No Challenge	Challenge
Low	44 (0.23)	19 (0.25)	48 (0.06)	16 (0.18)	18 (0.21)	49 (0.25)
Moderate	73 (0.39)	21 (0.28)	47 (0.09)	23 (0.18)	18 (0.31)	50 (0.25)
High	57 (0.30)	25 (0.33)	76 (0.11)	29 (0.29)	21 (0.17)	59 (0.26)
Very High	12 (0.06)	7 (0.09)	8 (0.02)	4 (0.03)	13 (0.27)	26 (0.19)
Extreme	3 (0.02)	3 (0.04)	10 (0.01)	3 (0.04)	5 (0.04)	5 (0.05)

Chi-square testing of mean wildfire size at assessment and containment milestones, temperature, and 24-hour rainfall were significant between the two groups (i.e., challenge and no challenge). Total time between wildfire detection and crew travel time to an incident, in contrast to the escaped fire analysis, are higher for challenge fires than fires where crews would likely face no containment challenges by

approximately 3 minutes. Rainfall over the previous 24 hours was also, on average, counter-intuitively higher for a crew facing containment challenges by over a 1.1 mm, which is sufficient to begin lowering the FFMC in circumstances where there is no canopy interception to reduce precipitation hitting the ground (Table 19); this is further explored in the discussion section.

Table 19 General statistics for the numerical variables in the containment challenge fire model using optically assessed fire behaviour and density. General variable significance was evaluated with a chi square test where significant differences are highlighted in bold.

	Mean		Median		Standard Dev.		Range		Chi Square p-value
	No Challenge	Challenge	No Challenge	Challenge	No Challenge	Challenge	No Challenge	Challenge	
Wind Speed (km/h)	9.66	9.81	9	8.5	5.56	5.66	0.0 - 32.0	0.0 - 20.0	0.91
Assessment Hectares (ha)	0.29	0.82	0.1	1	0.42	0.42	0.0 - 1.8	0.1 - 1.5	0.0014**
Departure Time (hrs)	0.57	0.87	0.08	0.11	2.56	2.54	0.0 - 22.4	0.0 - 10.2	0.184
Crew Travel Time (hrs)	1.05	0.77	0.53	0.61	2.31	0.6	-17.3	0.1 - 2.1	0.16
Departure Time + Crew Travel Time (hrs)	1.62	1.63	0.71	0.75	3.39	2.72	0.0 - 22.6	0.2 - 11.1	0.199
Firefighting Start size (ha)	0.27	1.14	0.1	1	0.4	0.55	0.0 - 2.0	0.1 - 2.0	<0.0001***
Fire Being Held Size (ha)	0.33	21.98	0.1	4.5	0.46	37.03	0.0 - 2.0	2.5 - 120.7	<0.0001***
Fire Under Control Size (ha)	1.9	21.53	0.1	5.39	20	36.86	0.0 - 281.0	2.1 - 120.7	<0.0001***
Fire Extinguished Size (ha)	1.49	19.89	0.1	5.66	14.4	34.31	0.0 - 200.7	1.2 - 120.1	<0.0001***
Temperature (C)	22.01	21.38	22	20.25	3.48	4.51	10.4 - 32.0	14.0 - 29.5	0.0092
Relative Humidity (%)	52.07	46.75	51	44.75	13.32	16.48	17.7 - 100.0	27.6 - 79.2	0.685
24 Hour Precipitation (mm)	1.2	2.23	0	0.25	3.88	4.45	0.0 - 28.2	0.0 - 17.2	0.0004***

Significance codes: p<0.001=*** (v. strong sig.), p<0.01=** (strong sig.), p<0.05=* (significant), p<0.10 =. (weak sig.)

3.3.2 Logistic Regression Analysis

From the analysis, 9 unique models were produced using 1 to 5 predictors and reported discriminate C-statistics ranging from 0.91 to 0.62. Smoke colour was not a significant predictor; however, smoke continuity and smoke angle were significant in multiple models. FWI System moisture codes (FFMC, DMC, and DC) and fire behaviour indices (ISI, BUI, or FWI) were not significant in any models. Windspeed was significant in five of the nine models and relative humidity was significant in one model.

Table 20 Unique GLMs produced by the escaped fire analysis. No density variables were identified in any of the resulting equations.

Test	Winning call (Terms ordered by reduction in overall model AIC)	C-Stat	AIC Reduc.
Test 5	Crown Involvement + Smoke Continuity + Crew Fire Type + Wind Speed + Smoke Angle	0.909488536	117.9298292
Test 1	Crown Involvement + Smoke Continuity + Crew Fire Type + Smoke Angle	0.904797178	116.7384886
Test 3 (C-FIRE1)	Crown Involvement + Smoke Continuity + Wind Speed	0.885855379	110.754311
Test 2	Crown Involvement + Smoke Continuity	0.878624339	108.5032399
Test 10	Crew Fire Type + Wind Speed + Action Time + Departure Time	0.740458554	44.1555885
Test 8	Crew Fire Type + Wind Speed	0.72659612	40.99811319
Test 7	Crew Fire Type + Action Time + Departure Time	0.682962963	40.79999414
Test 127	Crew Fire Type	0.682786596	38.14635238
Test 9	Wind Speed + RH	0.615978836	1.54793462

3.3.3 Contribution of Stand Structure to the Probability of Containment Challenge

From the analysis, no test reported forest density as an input parameter. Test 5 had the overall highest performance with a C-statistic of 0.91 and an AIC reduction of 117.9, calling for crown involvement, smoke continuity, crew fire type, wind speed, and smoke angle. However, Test 3 (hereafter C-FIRE1) produced similar results (C-statistic 0.89, AIC of 110.6) with two fewer terms than Test 5 by omitting the assessor-assigned fire type and smoke continuity variables. C-FIRE1 reported an accuracy score of 0.86 and a kappa statistic of 0.64. The omission of the assessor fire type as a variable in C-FIRE1 also removes

potential multicollinearity conflicts with the Crown Involvement Variable. C-FIRE 1 is expressed in its general form as:

$$\text{C-FIRE1 } Y = \frac{1}{1 + e^{-(-3.79 + \alpha + \beta + 0.07WIND)}} \quad \text{Equation 4}$$

Where α is an interchangeable variable for crown involvement with surface fire as 0, light candling is 0.6, heavy torching is 1.29, intermittent crowning is 1.72, and continuous crowning is 2.80; β is an interchangeable variable for smoke continuity, with puffer smoke as 0, continuous smoke as 0.67, and heavy smoke as 2.37; and WIND is the wind speed in km/h.

Each variable in the C-FIRE1 equation is significant in predicting containment challenges for suppression crews. Crown involvement is the most significant variable, with continuous crowning indicating a 16-fold increase in the likelihood of a crew arriving to a fire posing containment challenges relative to a surface fire with no crown involvement. Smoke continuity also plays a significant role, with heavy smoke indicating a 10-fold increase in the likelihood a crew will arrive on scene to a wildfire that is over 0.5 ha and actively growing, than a fire with puffer smoke. Further breakdown of the C-FIRE1 model is presented in Table 28, and graphically represented in Figure 18. A notable takeaway from the graphical representation of C-FIRE1 is the apparent reversal of fires experiencing no crown involvement and fires with light candling; this is interpreted in the discussion section.

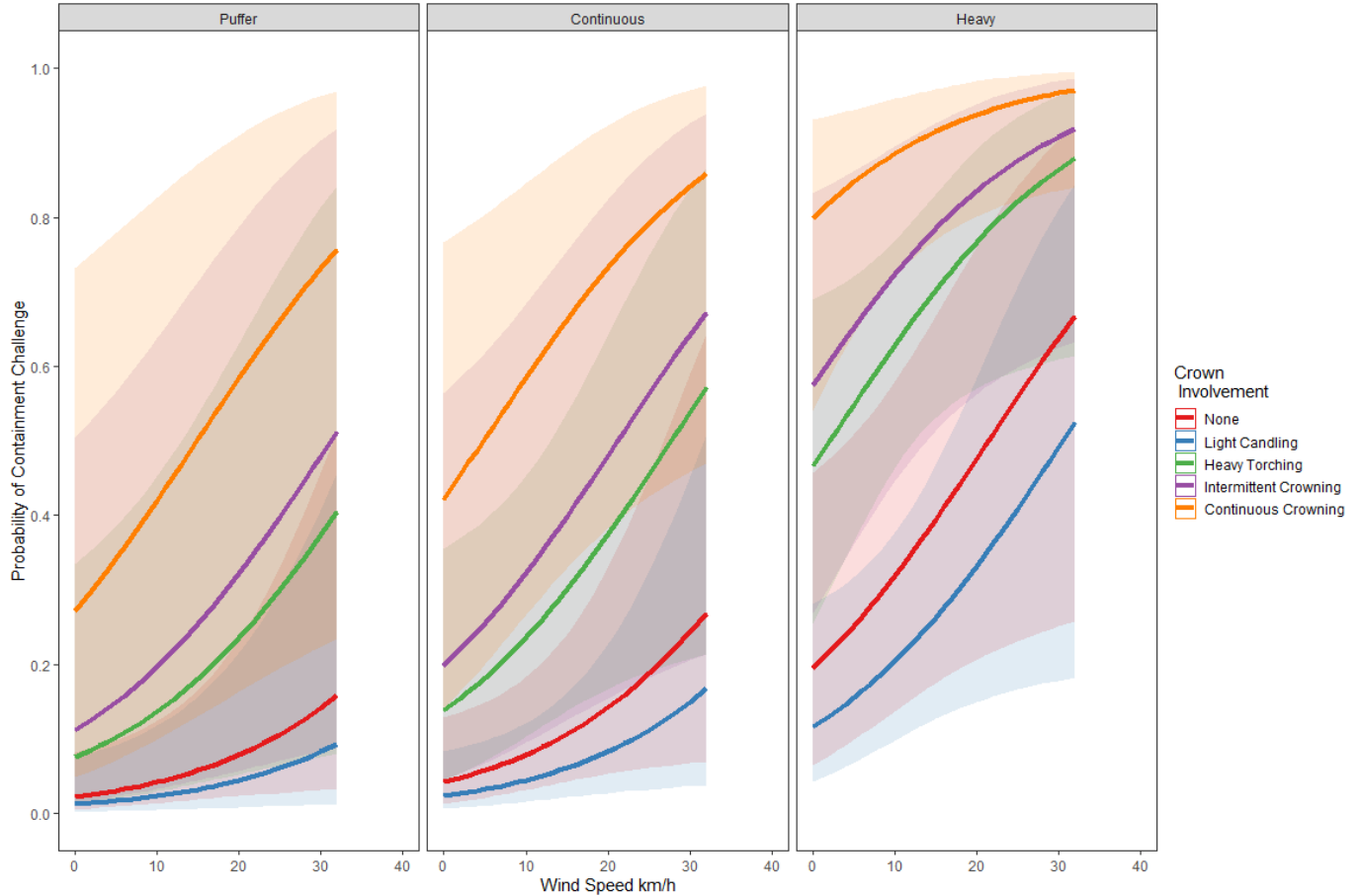


Figure 18 C-FIRE1: Probability of a suppression crew arriving to a fire that has already exceeded 0.5 ha prior to beginning suppression. Fires are grouped by smoke continuity and crown involvement and drawn to the 0.95 confidence interval for crown involvement.

3.4 Probability of a Crew Arriving to a Challenge Fire Using LiDAR-Based Forest Structure

3.4.1 Comparing Challenging and Non-Challenging Fire Groups

From the expanded wildfire dataset, 1317 fires were classified as not posing a containment challenge (no challenge), and 382 as challenge fires at the time of assessment. Fires designated as a challenge exceeded the 2 ha containment threshold in 63% of cases; in contrast, when crews began suppression prior to the fire reaching a 0.5 ha size threshold, 95% were successfully contained below 2 ha (Table 22).

Fires classified as short, open canopy black spruce stands accounted for 55% of fires in this analysis, as well as the highest proportion of challenge fires across all structure classifications.

Table 21 Distribution of fires among the 8 structural classes and their respective number of challenging, and non-challenging fire distributions. Bracketed numbers indicate proportion of row totals.

Structure	Description	No Challenge	Challenge	Total
1	Short, medium canopy cover stand (Aw)	124 (0.86)	20 (0.14)	144 (1.00)
2	Short, open canopy stand (Sb)	664 (0.71)	268 (0.29)	932 (1.00)
3	Very short, dense canopy cover stand (Sb)	103 (0.78)	29 (0.22)	132 (1.00)
4	Very tall, complex stand (Sb)	82 (0.94)	5 (0.06)	87 (1.00)
6	Tall, dense canopy cover stand (Aw)	239 (0.86)	38 (0.14)	277 (1.00)
7	Short, closed canopy stand (Aw+Sb)	95 (0.83)	20 (0.17)	115 (1.00)
8	Very tall, closed canopy stand (Aw)	10 (0.83)	2 (0.17)	12 (1.00)
	Total	1317 (0.78)	382 (0.22)	1699 (1.00)

Table 22 Matrix of fires that were identified as posing containment challenges versus and if they exceeded 2 ha.

Escape Status	No Challenge	Challenge	Grand Total
Contained	1254 (0.95)	142 (0.37)	1396 (0.82)
Escaped	63 (0.05)	240 (0.63)	303 (0.18)
Grand Total	1317 (1.00)	382 (1.00)	1699 (1.00)

Challenge fires were associated with high and extreme fire weather conditions (Table 23). When FWI System components were low, moderate, or high, fire size tended to be under the 0.5 ha threshold. A Chi-square analysis of challenge status and FWI System rankings was not independently significant for FFMC but did show significance for DMC ($p=0.01$), DC ($p=0.04$), ISI ($p= 0.0001$), BUI ($p= 0.0009$), and FWI ($p=0.002$).

Table 23 Fire counts grouped by FWI System hazard level and challenge classification. Proportions as a function of column totals are shown in brackets.

FWI System Rank	FFMC Challenge		DMC Challenge		DC Challenge	
	No	Yes	No	Yes	No	Yes
Low	239 (0.17)	44 (0.15)	525 (0.38)	97 (0.32)	55 (0.04)	3 (0.01)
Moderate	264 (0.19)	53 (0.17)	192 (0.14)	25 (0.08)	241 (0.17)	32 (0.11)
High	443 (0.32)	92 (0.30)	362 (0.26)	78 (0.26)	488 (0.35)	89 (0.29)
Very High	369 (0.26)	82 (0.27)	228 (0.16)	68 (0.22)	389 (0.28)	101 (0.33)
Extreme	81 (0.06)	32 (0.11)	89 (0.06)	35 (0.12)	223 (0.16)	78 (0.26)

FWI System Rank	ISI Challenge		BUI Challenge		FWI Challenge	
	No	Yes	No	Yes	No	Yes
Low	319 (0.23)	59 (0.19)	242 (0.17)	32 (0.11)	317 (0.23)	50 (0.17)
Moderate	445 (0.32)	74 (0.24)	415 (0.30)	87 (0.29)	345 (0.25)	72 (0.24)
High	458 (0.33)	109 (0.36)	423 (0.30)	69 (0.23)	423 (0.30)	78 (0.26)
Very High	158 (0.11)	58 (0.19)	238 (0.17)	79 (0.26)	252 (0.18)	77 (0.25)
Extreme	16 (0.01)	3 (0.01)	78 (0.06)	36 (0.12)	59 (0.04)	26 (0.09)

Wildfire size assessment and containment milestones were intuitively significant with respect to a crew arriving to a fire above or below the 0.5 ha threshold. Wind speed, elapsed time between fire discovery and time taken to dispatch suppression resources, and temperature were also found to be significant, as seen in Table 24.

Table 24 General numerical variable statistics for the expanded challenge fire analysis. General variable significance was evaluated with a chi square test where significant differences are highlighted in bold.

	Mean		Median		Std. Dev		Range		Chi Square p-Value
	No Challenge = 1317 Challenge = 382	No Challenge	No Challenge	Challenge	No Challenge	Challenge	No Challenge	Challenge	
Wind speed	9.70	11.04	9.00	10.00	5.53	6.07	0 – 42.00	0 – 40.00	0.0448*
Assessment Size	0.12	12.51	0.08	2.00	0.15	112.79	0 – 0.50	1 - 2056.00	<0.0001***
Crew Departure Time (hrs)	1.21	1.34	0.08	0.10	9.49	10.05	0 – 263.25	0 – 168.07	0.0302*
Crew Travel Time (hrs)	2.77	2.59	0.57	0.68	8.68	10.74	0 – 116.68	0 – 182.98	0.1196
Crew Departure Time + Crew Travel time (hrs)	3.98	3.93	0.75	0.85	13.09	15.36	0 – 263.78	0 – 193.93	0.1494
Fire Fighting Start size	1.03	23.57	0.10	2.00	20.59	165.41	0 – 677.18	0 – 2385.00	<0.0001***
Being Held Size	23.50	564.62	0.10	3.50	552.04	4016.78	0 – 15376.00	0 – 680.00	<0.0001***
Under Control size	23.87	742.36	0.10	3.60	552.12	4627.05	0 – 15376.00	0 – 680.00	<0.0001***
Extinguished Size	23.82	736.79	0.10	3.82	552.09	4601.66	0 – 15375.60	0 – 680.00	<0.0001***
Temperature	21.31	22.61	22.00	23.00	4.77	4.50	001 – 32.50	-005 – 32.00	0.0135*
RH	50.39	47.63	48.00	46.09	14.38	13.49	017 – 100.00	017 – 100.00	0.0275*
Precip	1.21	0.83	0.00	0.00	4.56	2.37	0 – 77.40	0 – 22.90	0.8685

Significance codes: p<0.001=*** (v. strong sig.), p<0.01=** (strong sig.), p<0.05=* (significant), p<0.10 =. (weak sig.)

3.4.2 Logistic Regression Analysis

From the analysis, 14 unique GLMs were produced with C-statistics ranging from 0.66 to 0.78 and calling for four to six input variables. For all GLMs, 100 m structural classification was strongly significant. A drop in C-statistic from 0.77 to 0.67 is noted when a GLM did not include observed overhead weather or reported fire type as a predictor variable (Table 25).

Table 25 The 14 challenge fire GLMs ordered by decreasing C-statistic. Winning calls with significant Chi-square scores for the structure classification variable are in displayed in bold.

Test	Winning call (Terms ordered by reduction in overall model AIC)	C-Stat	AIC Reduc.	Density Sig. (Chi-sq.)
Test 6	Fire Type + 100 m Structure Class + Weather overhead + BUI Rank + Wind Speed + Temp	0.78	297.40	<0.0001 ***
Test 5	Fire Type + 100 m Structure Class + Weather overhead + BUI + Wind Speed + Temp + ISI	0.78	296.39	<0.0001 ***
Test 1	Fire Type + 100 m Structure Class + Weather overhead + DMC + Wind Speed + Temp + FFMC + Precip	0.78	297.09	<0.0001 ***
Test 2	Fire Type + 100 m Structure Class + Weather overhead + DMC Rank + Wind Speed + Temp	0.78	294.29	<0.0001 ***
Test 3	Fire Type + 100 m Structure Class + Weather overhead + FWI Rank + Wind Speed + Temp + Precip	0.78	289.91	<0.0001 ***
Test 4	Fire Type + 100 m Structure Class + Weather overhead + DSR + Wind Speed + Temp	0.77	286.90	<0.0001 ***
Test 7	Fire Type + 100 m Structure Class + Weather overhead + Wind Speed + Temp	0.77	285.98	<0.0001 ***
Test 12	100 m Structure Class + BUI + Wind Speed + Temp + ISI + RH	0.67	93.08	<0.0001 ***
Test 13	100 m Structure Class + BUI Rank + Wind Speed + Temp	0.67	90.68	<0.0001 ***
Test 8	100 m Structure Class + Temp + Wind Speed + DMC Rank	0.67	86.57	<0.0001 ***
Test 9	100 m Structure Class + FWI Rank + Temp + Wind Speed + Precip	0.66	81.32	<0.0001 ***
Test 10	100 m Structure Class + Temp + Wind Speed + DC + DMC	0.66	88.38	<0.0001 ***
Test 11	100 m Structure Class + Temp + Wind Speed + RH	0.66	80.45	<0.0001 ***
Test 14	100 m Structure Class + DSR + Temp + Wind Speed	0.66	80.88	<0.0001 ***

Significance codes: p<0.001=*** (v. strong sig.), p<0.01=** (strong sig.), p<0.05=* (significant), p<0.10 =. (weak sig.)

3.4.3 Contribution of LiDAR Structure Attributes to Predictive Models

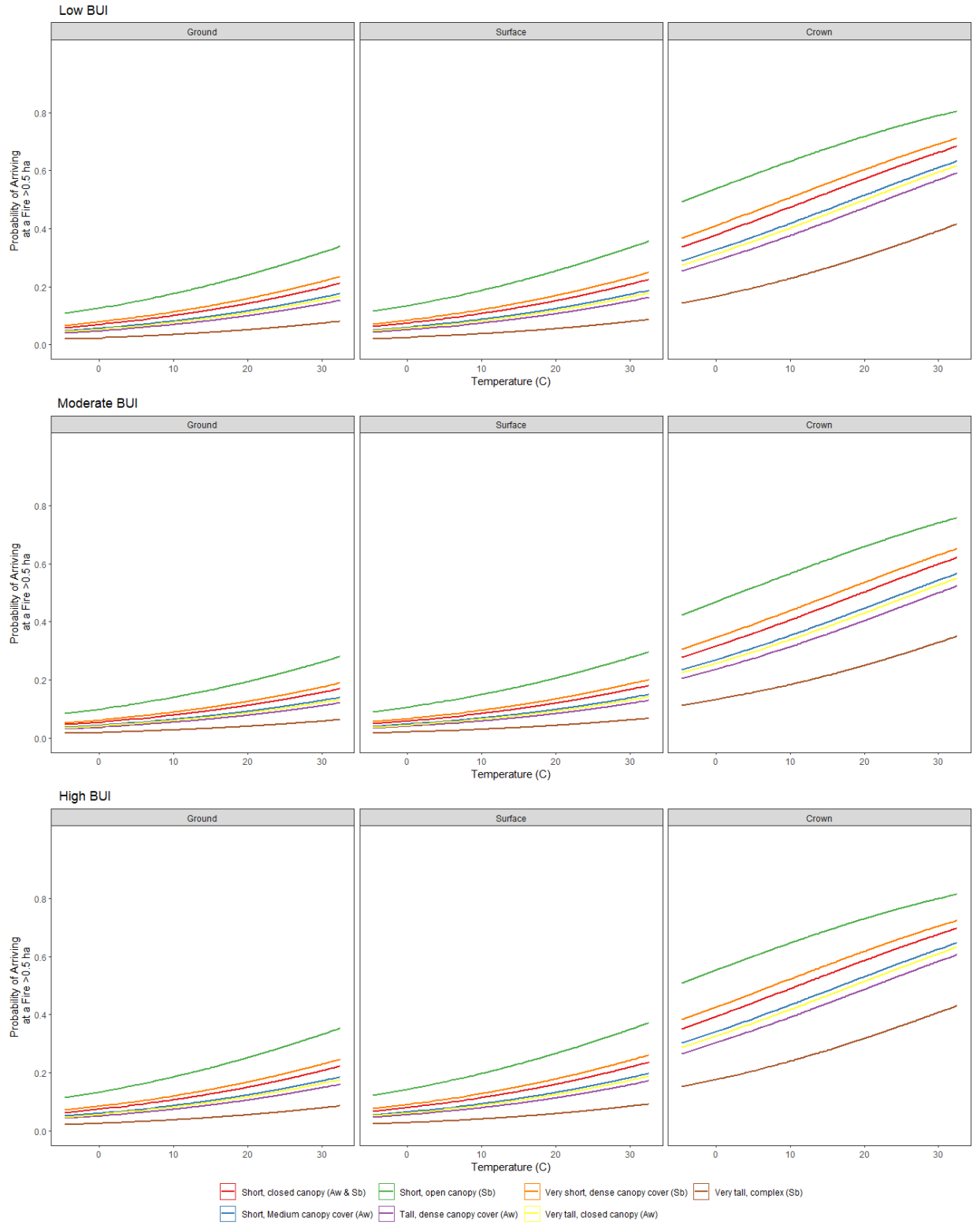
Test 6 (Hereafter CL-FIRE1) reported the highest C-statistic (0.78) and relative AIC reduction of the models produced by the analysis. CL-FIRE1 had an accuracy score of 0.81 and a kappa statistic of 0.34. Assessor-assigned fire type, 100 m LiDAR structure classification, reported overhead weather, BUI rank, wind speed, and temperature were all significant predictors ($p < 0.05$) with respect to the probability of encountering a challenge fire. CL-FIRE1 in its general form is expressed as:

$$\text{CL-FIRE1 } y = \frac{1}{1 + e^{-(-0.49122 + \alpha + \beta + \gamma + \varepsilon + 0.04273WIND + 0.039TEMP)}} \quad \text{Equation 5,}$$

Where α represents observed fire type where crown fire is 0, ground fire is -2.08368, and surface fire is -2.00677; β is 100 m LiDAR structure classification where Structure 1 is 0, structure 2 is 0.87195, structure 3 is 0.35822, Structure 4 is -0.88582, structure 5 was omitted, structure 6 is -0.17426, structure 7 is 0.22632, and structure 8 is -0.06568; γ represents observed overhead weather at the time of assessment, where CB (cumulonimbus/thunderstorm) dry is 0, CB wet is -0.80395, clear skies is 0.19876, cloudy is -0.37289, and raining is -0.69486; ε represents BUI Rank, where extreme BUI is 0, high is -0.75027, low is -0.81188, moderate is -1.0899, and very high is -0.55478; and wind speed is expressed in km/h and temperature is expressed in degrees C.

Fires burning in stands classified as Structure 2 (short, open canopy black spruce) were twice as likely to result in a challenging fire, relative to the intercept (Structure 1). With respect to temperature and wind speed, a unit increase in either variable resulted in a 1.04-fold increase in the likelihood of crews arriving to a challenge fire. Clear skies and Dry CB (thunderstorms) both increased the likelihood of encountering a challenge fire, with overcast skies and wet weather decreasing the likelihood. Further breakdown of the input variables can be found in Table 29 in the appendix. When the LiDAR analysis was rerun with just spruce-based classes (3, 4, and 7), forest structure remained significant.

Figure 19 illustrates the relationship between 100 m structure classification and likelihood of crews arriving to a challenge fire. A short, open canopy black spruce stand has the greatest likelihood of crews arriving to a challenge fire scenario. A positive relationship can be seen with increasing temperature, BUI rank, and crown involvement and the probability of arriving at a challenge fire.



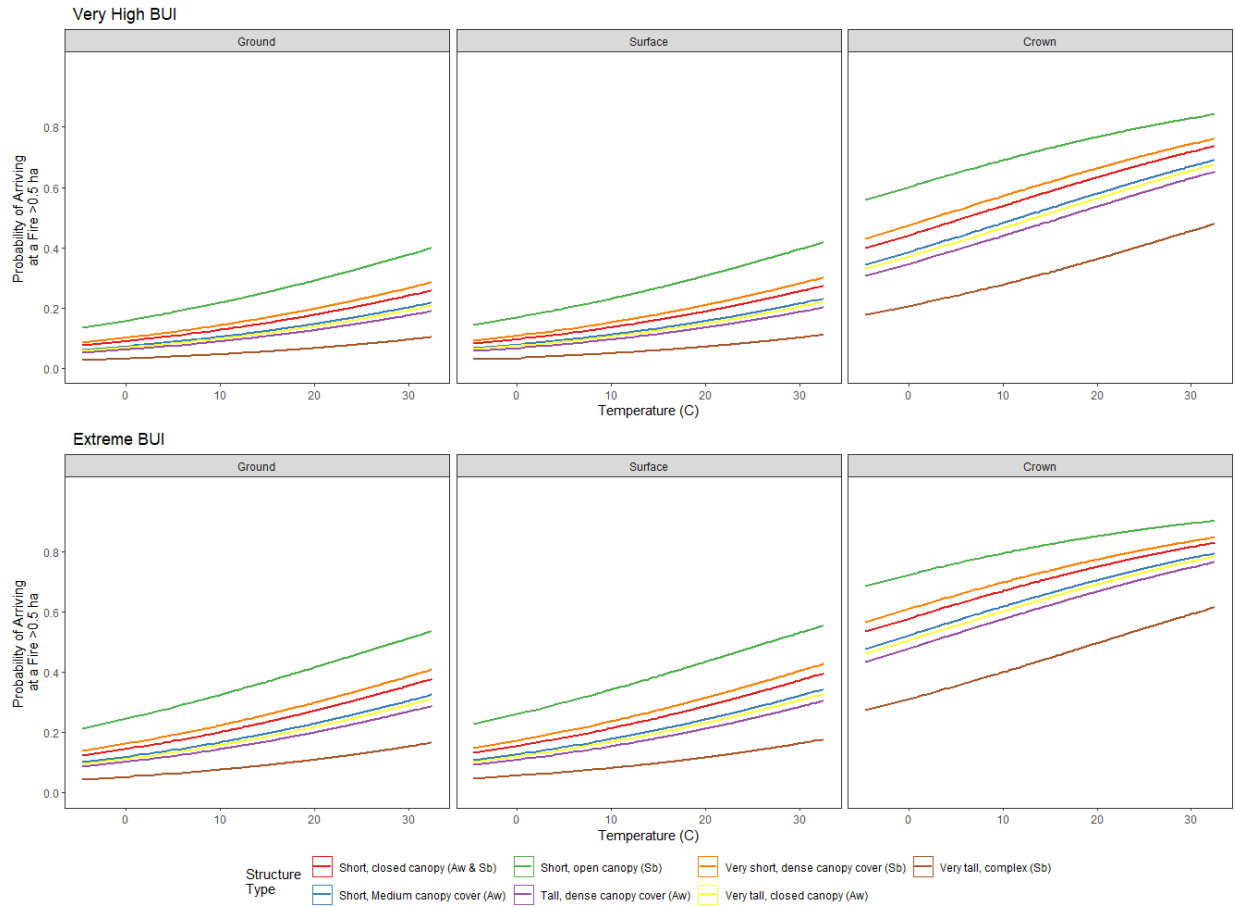


Figure 19 Likelihood of a wildfire exceeding 0.5 ha prior to suppression crew arrival as a function of temperature, BUI hazard rank, and assessor-assigned fire type.

Chapter 4: Discussion

This study demonstrates that forest structure significantly affects fire behaviour when density is evaluated using aerial ocular assessments. Selected models from the analysis performed well (C-Statistic > 0.75) but had poor to moderate predictive power. Similar studies have been done on forest density and fire behaviour interactions; however, using aerial ocular assessment is a novel approach. The effects of forest density on fire behaviour are well known: In similar work, Butler et al. (2013) identified that biomass reduction and thinning in the Boreal forest results in lower rates of spread, decreased fire intensity, and decreased burn severity relative to control plots using data collected from intensive in-stand measurements. Cameron (2020) successfully identified key forest characteristics that influence wildfire behaviour using a dedicated plane-mounted LiDAR platform. White (2016) concluded that aerial ocular estimates of stand regeneration, which are popular in stand restocking surveys, are agreeable to in-stand measurements in pure conifer stands when afforded a +/-20% buffer, but advocated for improved auditing of tree count estimates and standardization of the methodology across the industry.

4.1 Oblique Imagery Model Performance

Model accuracy was greatly improved when visual indicators of fire behaviour and overhead weather were incorporated in the GLM parameters. Fire behaviour variables include crown fire involvement, smoke colour, smoke continuity, and weather conditions observed over the fire. Visually assessed parameters raised the C-statistic by over 0.1 between E-FIRE1 and EL-FIRE1, and C-FIRE1 and CL-FIRE1, respectively. The most significant indicator of a wildfire exceeding the 2 hectare containment threshold was the presence of black grey smoke, increasing odds of escape by up to a factor of 38 relative to light grey smoke. Smoke colour is easy to assess from the air, and can be seen over 40km kilometers back from the ignition site, which compliments Alberta Wildfire's instructions to crew leaders to report

smoke characteristics (size, colour, height, lean) when performing a wildfire assessment (Government of Alberta, 2016).

Model C-FIRE1 did not include a density variable, and instead uses crown fire involvement, smoke continuity, and wind speed as input parameters. Wildfire is primarily driven by its surface fuels and must surpass a critical surface intensity before crown fuels become involved (Van Wagner, 1977a). While the fuel strata gap in C-2 fuels is effectively nonexistent as spruce crowns extend to the forest floor, the log odds for C-FIRE2 show a jump from light candling (0.55) to heavy torching (3.62), suggesting a jump in a fire's forward rate of spread once crown involvement exceeds 10%. This threshold could explain the inversion between no crown involvement and light candling, which in turn suggests light candling does not contribute to elevated pre-heating of fuels that would otherwise result in a faster rate of spread, such as crown to crown spread as noted by Cruz and Alexander (2017).

4.2 LiDAR Classification Model Performance

The parallel analyses used LiDAR-classified forest structure in lieu of wildfire photograph interpretation. From the LiDAR analysis, the conifer-dominated forest structures which demonstrated the highest likelihood of fire escape was Structure 2 (short, open canopy spruce), followed by Structure 7 (short, closed canopy mixedwood), and Structure 3 (very short, dense canopy spruce). The results of the LiDAR structural assessments appear to contradict the results of the oblique aerial study by suggesting the denser forest structure classes are less likely to challenge suppression objectives, but this comes down to a mismatch in definitions, where the closed canopy defined by Density3 has approximately the same number of stems as Structure Class 2 from the LiDAR classification, and Structure Class 3 has even higher density than defined by the ocular assessment study. In simpler terms, Structure Class 2 is roughly equivalent to Density 3 Closed, and Structure Class 3 could be considered Density3 Closed+. Visual inspection of wildfires with the conifer-dominated LiDAR structural classes that also had matching

oblique aerial photography suggests there is considerable overlap between them, however the increased density of Structure 3 relative to Structure 2 may be so excessive that it baffles air from entering the stand and inhibiting fire growth. Structure 7 typically appears to be found in older and drier upland spruce stands whereas structures 2 and 3 are both shorter in composition and in wetter lowlands (Figure 20 and Figure 21).



Figure 20 Example photo of structure class 7, optically assessed as Density3 Closed, successfully contained, no challenge.

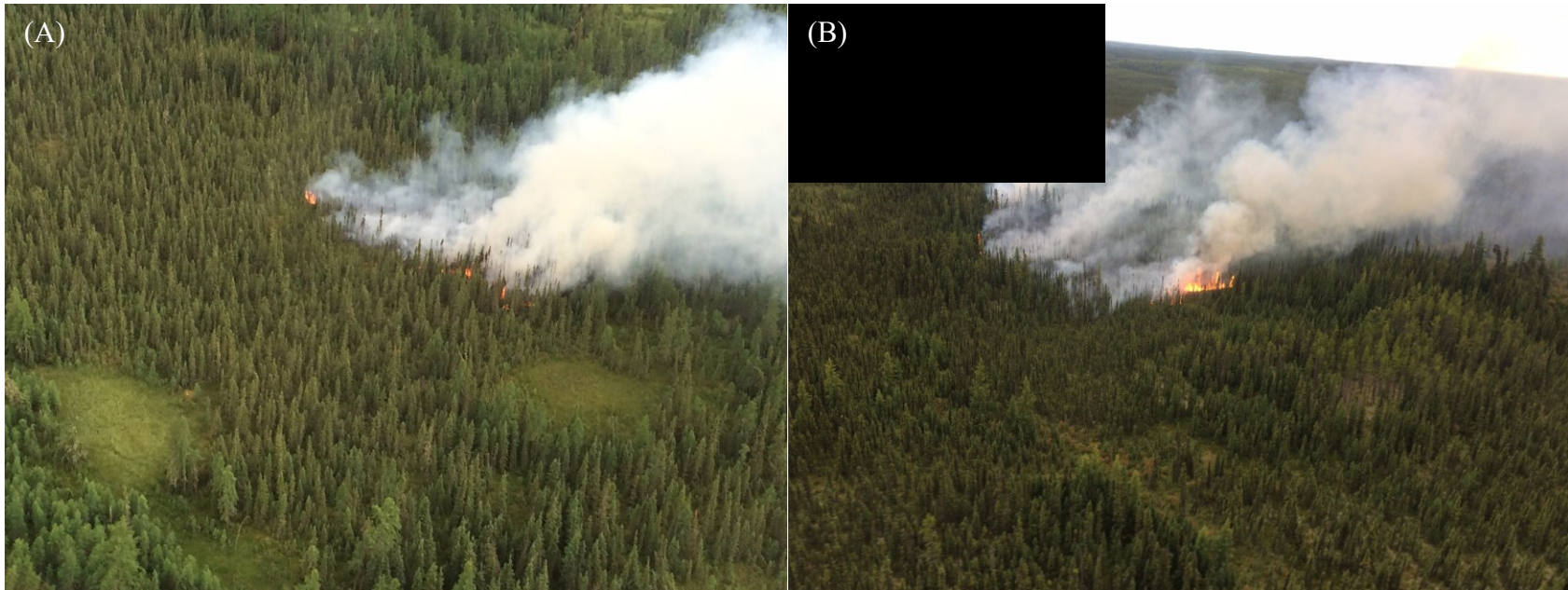


Figure 21 Example comparison between (A) structure class 2 (short, open canopy black spruce, optical assessment Density3 Closed, successfully contained, no challenge), and (B) structure class 3 (optical assessment Density3 Closed, successfully contained, challenging fire).

The FBP System fuel types assigned to each fire used in the parallel study were assigned by wildfire suppression personnel who were physically present at each ignition location. Assessors are instructed to identify the best fitting fuel type that matches the observed fire behaviour. In cases, for example, where the overstory structure may be a tall aspen stand, but the sub-dominant or understory is black spruce that is responsible for fire propagation, assessors are recommended to assign an FBP System fuel type C-2 rather than D-2 (leafed aspen).

The LiDAR classifications created by Guo et al. (2017) were generated using an unsupervised classification algorithm, which were then associated to different stand types by referencing three information sources: the first was a GIS layer of Alberta's historical wildfires, the second a polygonal anthropogenic disturbance layer created from interpretation of 1:50 000 scale Landsat imagery, and the third was a large biodiversity survey conducted by the Alberta Biodiversity Monitoring Institute that included permanent photo sample plots and detailed vegetation inventory. Guo et al. also notes that canopy density and height class between 20 and 30 m were the greatest discriminates between structure classes, which structures 2, 3, and 7 are almost entirely absent from as their height profiles fell below the 20 m height bin.

LiDAR stand structure classification varied from dense and juvenile spruce to pure, mature aspen. Disagreement between crew fuel calls and the LiDAR classifications could be due to several reasons: resolution of LiDAR-derived structure data, inaccurate fire location coordinates, inexperienced firefighting personnel classifying the fuels, typographical or data-input errors, failure of the LiDAR classification algorithm, and the fuel driving the fire may not match the LiDAR classification. Despite the aforementioned reasons, a wildfire assessor, would have been present at each incident to assign the FBP System fuel type and ultimately entered the stand itself to being suppression action. Therefore, the

likelihood of mistyping the FBP System fuel type, relative to Guo et al.'s structure association, would overall be less; it is for these reasons that the assessor-assigned FBP fuel type considered as correct.

4.3 Model Challenges and Data Limitations

The very nature of fire science is complicated, interconnected, and in a constant state of flux. Even in controlled burns, "identical" fuel complexes can be drastically different, making repeat experiments difficult to reproduce at the best of times. Several factors may have contributed to the results of the escaped fire analysis and the model's poor kappa statistic: Firstly, insufficient number of escaped fires: 93% of fires were successfully contained, which means one could theoretically predict all fires will be successfully contained and be correct 93% of the time. This bias was reflected in the confusion matrices for each experiment where successful containment was heavily favoured in all tests. Second, while the signal produced by the data is significant with respect to density and a fire escaping containment, the error from the analyses resulted in extensive overlap between factored variables such as smoke colour. This suggests that, while including visual attributes in the models increased overall accuracy, factored variables could use further refining and larger datasets to improve precision, which is evidenced by the strength of the structure classification in the LiDAR-based models. Additional consultation with other industry experts could further refine ocular definitions and their selection criteria. Lastly, other variables omitted from the analysis, whether intentionally or otherwise, may have helped further stratify model results. Smoke continuity also should be examined, as it served as a significant contributor to wildfire containment challenges but had to be dropped in the escaped fire analysis due to its excessive standard error.

4.3.1 Input Weather

Overhead weather had a significant impact on the likelihood of crews experiencing containment challenges, with clear skies having the most impactful influence. Dry lightning also represented elevated

risk, as lightning can strike outside the rain shadow of passing storm cells, and cloud cover and precipitation decreased the likelihood of wildfire crews experiencing containment challenges. These observations add credence to the understanding that direct insolation increases wildfire behaviour, but scientific literature suggests a greater understanding is needed on the effects of insolation and fire behaviour (Potter, 2012).

The weather data used in the analysis was recorded at noon local standard time, on average 20 km away but up to 60 km from the ignition location of fires; this is more than sufficient for weather to vary drastically between sites both spatially and temporally (Filkov et al., 2018), and is likely why precipitation had a positive correlation with the likelihood of fire escaping containment in the testing despite the relationship being the inverse. For example, thunderstorms may be as small as several kilometres across but dramatically change wind speed and direction, temperature, relative humidity, and precipitation over a wildfire. Effects of this are further compounded by coarse, single measurements taken once a day. In-situ weather measurement by crew leaders at the time of the wildfire assessment would have improved temperature, relative humidity, and wind speed variables for modeling purposes but such data were not available for this study. The matter of how to better account for rainfall in a specific location, however, still needs to be addressed in future work.

4.3.2 Photograph Quality

Photographs capture a moment in time, whereas wildfires are dynamic; conditions can change rapidly due to changes in fuel structure and composition, weather, and topography that may not be captured in a single photo. Videos, or a series of photos taken at regular time intervals would better capture this variability. Wildfire imagery taken during assessment is rarely used outside of forensic investigation for ignitions of suspicious origin and bespoke wildfire behaviour case studies, so altitude, distance from fires, and photo angle are not standardized. In White's (2016) recommendations for aerial optical

assessment in forest regeneration surveys, they advocate for standardization of ocular assessment techniques and protocols, as well as regular auditing of results to ensure consistency across time and assessors. In a wildfire context, standardization of helicopter altitude during wildfire assessment, distance from ignition, progress shots of suppression operations at regular intervals, and regular review of ocular assessments would provide more accuracy in the GLM results should this methodology be considered for further development. In a study by Hart et al. (2021), time-stepped oblique aerial imagery was used to successfully calculate rates of spread of five fires. From their study, they recommended that oblique aerial imagery be acquired from 650 to 2500m away, from an elevation of 350 to 1050 m using high definition cameras with georeferencing capability. Additionally, they advocated for mounting cameras with colour and infrared sensors to aircraft, so imagery could be collected in a more systematic fashion. While Heart et al.'s study used fixed-wing aircraft orbiting high above wildfire incidents and suppression crews arrive at a relatively low altitude in rotary wing aircraft, these recommendations are certainly a step in the right direction.

In many cases, photos taken by firefighting personnel traveling in a helicopter were not suitable for review due to poor quality, often disqualifying fires from the analysis. Various factors contribute to loss of photo quality including the altitude of the helicopter, the distance and angle of the camera in relation to the fire, poor focus, camera quality, weather (heavy rain or smoke), lighting conditions, and time of day. Further complications are introduced within the confined space of the aircraft such as the aircraft itself causing window glare and reflections (Figure 22). One solution to mitigate glare and reflections is to open the window port in the side of the helicopter door, but this has the potential to result in abrupt defenestration of the smartphone.



Figure 22 An arrival photo with an internal cockpit reflection. The helicopter porthole is in view and a reflection of a crew member in the front passenger seat can be seen.

4.4 Implications for Wildfire Management

This study reinforces the value of documenting smoke, forest density, and other properties during the assessment process. While the predictive capabilities of the models require more refinement, the link between smoke colour and fire intensity can still inform decision making at the incident level (Patterson and McMahan, 1984). While not currently standardized, it would be prudent for wildfire agencies to develop a protocol for wildfire assessors to document fire and fuel structure during assessment, when safe to do so. This, in turn, would reduce error in future models, as well as models for other FBP System fuel types, should wildfire agencies continue to develop this methodology. In addition, compiling standardized oblique aerial photography into a compendium organized by fuel complex would serve as an excellent resource for training new wildfire assessors, refreshing veteran firefighter knowledge, and an excellent starter database for AI-based image analysis.

Absent fire, aerial ocular assessment of fuel complexes can be used to help prioritize fuel treatment areas around communities when establishing landscape level tactical plans (British Columbia), wildfire preparedness guides (Alberta), and other wildfire risk mitigation programs. Beverly and Forbes (2023) developed a method to define fuel pathways into communities using 100 x 100 m FBP System raster fuel maps. The current FBP System uses fixed values for its parameters (Forestry Canada Fire Danger Group, 1992), therefore in conjunction with assessment by oblique aerial imagery, those fuel pathways could be further sub-divided into high and low priority zones for mitigation treatments responding to changing forest density. Large forest areas can be rapidly assessed by inexpensive micro drones to validate ground-based sample plots and satellite imagery. For example, a 50 000 hectare area of interest can be completed as quickly as a week to ten days. Aerial wildfire photography could also help verify the validity of the provincial fuel grid and reduce classification errors. For example, in 2 cases fires in the oblique photo analysis were classified as water by the provincial fuel grid (Figure 23 and Figure 24), which could be easily corrected to a more appropriate fuel type with photo evidence.



Figure 23 Wildfire with fuel classified as water by the provincial fuel grid. Photo courtesy of Alberta Wildfire.



Figure 24 Wildfire fuel type classified as water by the provincial fuel grid. Photo courtesy of Alberta Wildfire.

4.5 Areas for future research

The oblique aerial photographs used in this study were graciously provided by Alberta Wildfire and made for an excellent opportunistic dataset. Standardization of how assessment photos are taken could further improve fire behaviour predictions in scenarios where more precise technology, such as LiDAR and boots-on-the-ground data collection, are not available to assess forest structure due to not having the equipment present, nor the time for post-processing. Advancements in object-based image recognition and artificial intelligence could potentially be applied to wildfire applications with sufficient training data (on the order of 100's of gigabytes) (Challa, 2023; LABED et al., 2023). Startup companies using AI image analysis are developing automated smoke research detection algorithms, although they currently do not exceed the abilities of a qualified watchtower person (Hsieh, 2023). Additional fuel types can be compiled so long as there are sufficient training data for both escaped and contained fires.

Using a data analytics approach, such as the k-means cluster analysis used in the Guo et al. (2017) study, may also produce novel fuel types or add novel structural elements to existing fuel types. The next generation of Canadian Forest Fire Danger Rating System (CFFDRS) is projected to have 16 inputs in its new fuel type raster layer (Canadian Forest Service Fire Danger Group, 2021) and a form of image analysis could aid in the data collection and verification of these inputs.

Fires used in this study were on flat terrain and therefore did not contain any significant topographic changes. Further research could include topographic influences on density thresholds or develop an appropriate modifier like slope and aspect adjusted FFMC (Taylor and Alexander, 2018). Assumptions made in this study included all fuels within the 2 ha escape threshold were homogenous and continuous in the direction of fire growth. Interactions between fuel type and attribute boundaries such as density could be further explored, such as wind penetration into a given stand. This study applied the FWI values for peak burning regardless of the time suppression crews arrived at a fire. Future applications of this work could apply either diurnally adjusted FWI values (Lawson et al., 1996; Van Wagner, 1977b), or more stand-specific modifiers such as the approach by Wotton and Beverly (2007).

Delving into some world building and theory crafting, the idealized vision of this research is eventual development of a tool that could be used by wildfire assessors to rapidly assess wildfire escape probability. Eventually, this tool could evolve into a fully automated data product that can take video recorded by assessors and have it analyzed in real time to be livestreamed back to a Duty Room via a satellite internet feed. Various telemetry could be broadcast with the live feed advising of changing weather conditions, dry bulb temperature, wind speed and direction, barometric pressure and so on. Other data could include automatically calculated escape probabilities, forward rate of spread, and highlight potential values at risk with the calculated time to intercept by expanding on Hart's monoplotting technique (2021). To take the concept one step further, an unmanned aerial system, such

as a fixed wing drone, could be released to maintain a high orbit above the fire and tanker operations, taking full advantage of restricted airspace provisions during suppression for data collection.

4.6 Conclusion

The opportunistic data created from oblique aerial photography taken by wildfire suppression personnel presented the opportunity to explore ocularly assessed density and its connection to wildfire behaviour.

Ocularly-assessed density attributes of black spruce fuel types were shown to be significant in determining the likelihood of a wildfire escaping containment during assessment but were not significant in determining the likelihood of suppression crews arriving to challenge fire scenarios.

Ocularly assessed attributes used as input variables were superior when comparing GLM discriminate scores to those without. LiDAR-derived attributes of forest structure tested on an expanded dataset of wildfires in Alberta were found to have also have significant impact for containment and suppression challenge thresholds and performed best when including assessor-documented incident overhead weather and fire type.

During this study, wildfire smoke plume attributes, most notably smoke colour, were found to have the greatest impact in determining the likelihood of a wildfire escaping containment, further reinforcing current training practices for wildfire assessment personnel. Smoke observation serves as a good proxy for wildfire behaviour, even when observed some distance away from a wildfire. While the results of this study identified a moderately significant signal on the impacts of optically assessed forest density on fire escape, the poor predictability scores mandate further refinement before this tool can potentially integrated into suppression operations. However, with the foundational groundwork laid out in this thesis, it represents a key milestone as proof-of-concept for future iterations of this work that can be applied in both the wildfire suppression and wildfire risk mitigation space.



Figure 25 Andrew Stack on the banks of the Athabasca River, Horse River Fire 2016. Photo Credit: Leighton Lindsay.

Works Cited

- Alberta Agriculture and Forestry, 2020. Historical Wildfire Data: 2006 to 2018 [WWW Document]. Wildfire Maps Data. URL <https://open.alberta.ca/opendata/wildfire-data-2006-2018#summary>
- Alberta Wildfire, 2023. Fire Weather Index Legend [WWW Document]. Gov. Alberta. URL <https://open.alberta.ca/publications/fire-weather-index-legend>
- Alberta Wildfire, 2020. Historical Wildfire Database [WWW Document]. Alberta Wildfire Rec. URL <https://wildfire.alberta.ca/resources/historical-data/historical-wildfire-database.aspx> (accessed 5.8.20).
- Alexander, M.E., Cruz, M.G., 2012. Graphical aids for visualizing byram's fireline intensity in relation to flame length and crown scorch height. *For. Chron.* 88, 185–190. <https://doi.org/10.5558/tfc2012-035>
- Beverly, J.L., 2017. Time since prior wildfire affects subsequent fire containment in black spruce. *Int. J. Wildl. Fire* 26, 10. <https://doi.org/10.1071/WF17051>
- Beverly, J.L., Forbes, A.M., 2023. Assessing directional vulnerability to wildfire. *Nat. Hazards* 117, 831–849. <https://doi.org/10.1007/s11069-023-05885-3>
- Beverly, J.L., Leverkus, S.E.R., Cameron, H., Schroeder, D., 2020. Stand-level fuel reduction treatments and fire behaviour in Canadian boreal conifer forests. *Fire* 3, 1–23. <https://doi.org/10.3390/fire3030035>
- Burnham, K.P., Anderson, D.R., 2002. *Model Selection and Multimodel Inference*, 2nd ed. Springer New York, New York, NY. <https://doi.org/10.1007/b97636>

- Butler, B.W., Ottmar, R.D., Rupp, T.S., Jandt, R., Miller, E., Howard, K., Schmoll, R., Theisen, S., Vihnanek, R.E., Jimenez, D., 2013. Quantifying the effect of fuel reduction treatments on fire behavior in boreal forests. *Can. J. For. Res.* 43, 97–102. <https://doi.org/10.1139/cjfr-2012-0234>
- Byram, G.M., 1959. Combustion of forest fuels, in: Davis, K.P. (Ed.), *Forest Fire: Control and Use*. NY: McGraw-Hill, New York, pp. 61–89. <https://doi.org/10.2307/1932261>
- Cameron, H., 2020. Predicting Fuel Characteristics of Black Spruce Stands Using Airborne Laser Scanning (ALS) in the Province of Alberta, Canada 1–121.
- Canadian Forest Service Fire Danger Group, 2021. An overview of the next generation of the Canadian Forest Fire Danger Rating System. (Information Report GLC-X-26).
- Celisse, A., 2014. Optimal cross-validation in density estimation with the L2-loss. *Ann. Stat.* 42, 1879–1910. <https://doi.org/10.1214/14-AOS1240>
- Challa, N., 2023. Artificial Intelligence for Object Detection and its Metadata 2, 121–133. <https://doi.org/10.17605/OSF.IO/FG3SQ>
- Christianson, A.C., Sutherland, C.R., Moola, F., Gonzalez Bautista, N., Young, D., MacDonald, H., 2022. Centering Indigenous Voices: The Role of Fire in the Boreal Forest of North America. *Curr. For. Reports* 8, 257–276. <https://doi.org/10.1007/s40725-022-00168-9>
- Cruz, M.G., Alexander, M.E., 2017. Modelling the rate of fire spread and uncertainty associated with the onset and propagation of crown fires in conifer forest stands. *Int. J. Wildl. Fire* 26, 413–426. <https://doi.org/10.1071/WF16218>
- Cruz, M.G., Alexander, M.E., Wakimoto, R.H., 2005. Development and testing of models for

predicting crown fire rate of spread in conifer forest stands. *Can. J. For. Res.* 35, 1626–1639. <https://doi.org/10.1139/x05-085>

Falkowski, P., Scholes, R.J., Boyle, E., Canadell, J., Canfield, D., Elser, J., Gruber, N., Hibbard, K., Hogberg, P., Linder, S., Mackenzie, F.T., Moore, B., Pedersen, T., Rosental, Y., Seitzinger, S., Smetacek, V., Steffen, W., 2000. The global carbon cycle: A test of our knowledge of earth as a system. *Science* (80-). 290, 291–296.
<https://doi.org/10.1126/science.290.5490.291>

Filkov, A.I., Duff, T.J., Penman, T.D., 2018. Improving fire behaviour data obtained from wildfires. *Forests* 9, 1–21. <https://doi.org/10.3390/f9020081>

Fire Behavior Prediction (FBP) Fuel Types, 2023.

Forestry Canada Fire Danger Group, 1992. Development of the Canadian Forest Fire Behavior Prediction System. Inf. Rep. ST-X-3.

Government of Alberta, 2024. How We Fight Wildfires [WWW Document]. URL <https://www.alberta.ca/how-we-fight-wildfires> (accessed 6.1.24).

Government of Alberta, 2016. Wildfire Crew Leader Training Manual.

Guo, X., Coops, N.C., Tompalski, P., Nielsen, S.E., Bater, C.W., John Stadt, J., 2017. Regional mapping of vegetation structure for biodiversity monitoring using airborne lidar data. *Ecol. Inform.* 38, 50–61. <https://doi.org/10.1016/j.ecoinf.2017.01.005>

Hart, H., Perrakis, D.D.B., Taylor, S.W., Bone, C., Bozzini, C., 2021. Georeferencing Oblique Aerial Wildfire Photographs: An Untapped Source of Fire Behaviour Data. *Fire* 4, 81.
<https://doi.org/10.3390/fire4040081>

Helbig, M., Pappas, C., Sonnentag, O., 2016. Permafrost thaw and wildfire: Equally important drivers of boreal tree cover changes in the Taiga Plains, Canada. *Geophys. Res. Lett.* 43, 1598–1606. <https://doi.org/10.1002/2015GL067193>

Higuera, P.E., 2019. First- and Second-Order Fire Effects, in: *Encyclopedia of Wildfires and Wildland-Urban Interface (WUI) Fires*. Springer International Publishing, Cham, pp. 1–3. https://doi.org/10.1007/978-3-319-51727-8_258-1

Hirsch, K.G., 1996. Canadian Forest Fire Behavior Prediction (FBP) System: user's guide. Special Report 7. Edmonton, Alberta.

Hsieh, R., 2023. Alberta Wildfire Detection Challenge: Operational Demonstration of Six Wildfire Detection Systems.

Kelsall, J.P., Telfer, E.S., Wright, T.D., 1977. The effects of fire on the ecology of the boreal forest, with particular reference to the Canadian north: a review and selected bibliography, Occasional Paper 32.

LABED, S., TOUATÌ, H., HERÌDA, A., KERBAB, S., SAÌRÌ, A., 2023. An AI-based Image Recognition System for Early Detection of Forest and Field Fires. *Eur. J. For. Eng.* 9, 48–56. <https://doi.org/10.33904/ejfe.1322396>

Lawson, B.D., Armitage, O.B., 2008. Weather Guide Canadian Forest Fire Danger Rating System, Canadian Forest Service Northern Forestry Centre.

Lawson, B.D., Armitage, O.B., Hoskins, W.D., 1996. Diurnal Variation in the Fine Fuel Moisture Code: Tables and Computer Source Code. Victoria, BC.

Lim, K., Treitz, P., Wulder, M., St-Onge, B., Flood, M., 2003. LiDAR remote sensing of forest

- structure. *Prog. Phys. Geogr.* 27, 88–106. <https://doi.org/10.1191/0309133303pp360ra>
- Lüdecke, D., 2020. *sjPlot: Data Visualization for Statistics in Social Science*.
<https://doi.org/10.5281/zenodo.1308157>
- MNP LLP, 2020. *Spring 2019 Wildfire Review*.
- Natural Regions Committee, 2006. *Natural Regions and Subregions of Alberta*, Pub. No. T/852.
Government of Alberta.
- Natural Resources Canada, 2005. *The State of Canada's Forests 2004-2005: The Boreal Forest*.
Canadian Forest Service, Headquarters, Planning, Operations and Information Branch,
Ottawa.
- Patterson, E.M., McMahon, C.K., 1984. Absorption characteristics of forest fire particulate
matter. *Atmos. Environ.* 18, 2541–2551. [https://doi.org/10.1016/0004-6981\(84\)90027-1](https://doi.org/10.1016/0004-6981(84)90027-1)
- Phelps, N., Cameron, H., Forbes, A.M., Schiks, T., Schroeder, D., Beverly, J.L., 2022. The
Alberta Wildland Fuels Inventory Program (AWFIP): data description and reference tables.
Ann. For. Sci. 79, 1–16. <https://doi.org/10.1186/s13595-022-01144-w>
- Potter, B.E., 2012. Atmospheric interactions with wildland fire behaviour I. Basic surface
interactions, vertical profiles and synoptic structures. *Int. J. Wildl. Fire* 21, 779–801.
<https://doi.org/10.1071/WF11128>
- Pyne, S.J., Wynn, G., 2008. *Awful Splendour, Awful Splendour*. University of British Columbia
Press. <https://doi.org/10.59962/9780774855853>
- R Core Team, 2017. *R: A language and environment for statistical computing*.

- Reinhardt, E.D., Keane, R.E., Brown, J.K., 2001. Modeling fire effects. *Int. J. Wildl. Fire* 10, 373–380. <https://doi.org/10.1071/wf01035>
- Rossa, C.G., Davim, D.A., Sil, Â., Fernandes, P.M., 2024. Field-based generic empirical flame length-fireline intensity relationships for wildland surface fires. *Int. J. Wildl. Fire* 33. <https://doi.org/10.1071/WF23127>
- Rowe, S., 1970. Spruce and Fire in Northwest Canada and Alaska 245–254.
- Sikkink, P.G., Lutes, D.C., Keane, R.E., 2009. *Field Guide for Identifying Fuel Loading Models*. Fort Collins, CO.
- Stocks, B.J., Lynham, T.J., Lawson, B.D., Alexander, M.E., Wagner, C.E. Van, McAlpine, R.S., Dubé, D.E., 1989. The Canadian Forest Fire Danger Rating System: An Overview. *For. Chron.* 65, 450–457. <https://doi.org/10.5558/tfc65450-6>
- Taylor, S.W., Alexander, M.E., 2018. *Field guide to the Canadian Forest Fire Behavior Prediction (FBP) System, 3rd Edition., 3rd ed.* Natural Resources Canada, Edmonton, Alberta.
- Tymstra, C., Rogeau, M.-P., Wang, D., 2016. Alberta wildfire regime analysis. *Alberta wildfire regime Anal. /*. <https://doi.org/10.5962/bhl.title.113828>
- Van Wagner, C.E., 1987. Development and structure of the Canadian forest fire weather index system, *Forestry*.
- Van Wagner, C.E., 1977a. Conditions for the start and spread of crown fire. *Can. J. For. Res.* 7, 23–34. <https://doi.org/10.1139/x77-004>

- Van Wagner, C.E., 1977b. A method of computing fine fuel moisture content throughout the diurnal cycle. Canadian Forestry Service. Petawawa Forest Experiment Station, Information Report PS-X-69. Chalk River, Ontario.
- Van Wagner, C.E., 1974. Structure of the Canadian forest fire weather index. Dep. Environ. - Can. For. Serv. Publ. 37 pp.
- Viereck, L.A., 1983. The Effects of Fire in Black Spruce Ecosystems. Role Fire North. Cirumpolar Ecosyst. 201–220.
- Wehr, A., Lohr, U., 1999. Airborne laser scanning - An introduction and overview. ISPRS J. Photogramm. Remote Sens. 54, 68–82. [https://doi.org/10.1016/S0924-2716\(99\)00011-8](https://doi.org/10.1016/S0924-2716(99)00011-8)
- Westreich, D., Cole, S.R., Funk, M.J., Brookhart, M.A., Stürmer, T., 2011. The role of the c - statistic in variable selection for propensity score models. Pharmacoepidemiol. Drug Saf. 20, 317–320. <https://doi.org/10.1002/pds.2074>
- White, R.G., 2016. Aerial ocular assessments of forest regeneration in northwestern Ontario: A case study. Peterborough, ON.
- Williamson, G.J., Price, O.F., Henderson, S.B., Bowman, D.M.J.S., 2013. Satellite-based comparison of fire intensity and smoke plumes from prescribed fires and wildfires in southeastern Australia. Int. J. Wildl. Fire 22, 121–129. <https://doi.org/10.1071/WF11165>
- Wotton, B.M., Alexander, M.E., Taylor, S.W., 2009. Updates and revisions to the 1992 Canadian Forest Fire Behavior Prediction System, Information Report GLC-X-10. Natural Resources Canada Canadian Forest Service, Great Lakes Forestry Centre.
- Wotton, B.M., Beverly, J.L., 2007. Stand-specific litter moisture content calibrations for the

Canadian Fine Fuel Moisture Code. *Int. J. Wildl. Fire* 16, 463.

<https://doi.org/10.1071/WF06087>

Wright, H.E., Heinselman, M.L., 2014. The Ecological Role Of Fire In Natural Conifer Forests Of Western And Northern North America—Introduction. *Fire Ecol.* 10, 4–13.

<https://doi.org/10.4996/fireecology.1003001>

Alberta Agriculture and Forestry, 2020. Historical Wildfire Data: 2006 to 2018 [WWW Document].

Wildfire Maps Data. URL <https://open.alberta.ca/opendata/wildfire-data-2006-2018#summary>

Alberta Wildfire, 2023. Fire Weather Index Legend [WWW Document]. Gov. Alberta. URL

<https://open.alberta.ca/publications/fire-weather-index-legend>

Alberta Wildfire, 2020. Historical Wildfire Database [WWW Document]. Alberta Wildfire Rec. URL

<https://wildfire.alberta.ca/resources/historical-data/historical-wildfire-database.aspx> (accessed 5.8.20).

Alexander, M.E., Cruz, M.G., 2012. Graphical aids for visualizing byram’s fireline intensity in relation to flame length and crown scorch height. *For. Chron.* 88, 185–190. <https://doi.org/10.5558/tfc2012-035>

Beverly, J.L., 2017. Time since prior wildfire affects subsequent fire containment in black spruce. *Int. J.*

Wildl. Fire 26, 10. <https://doi.org/10.1071/WF17051>

Beverly, J.L., Forbes, A.M., 2023. Assessing directional vulnerability to wildfire. *Nat. Hazards* 117, 831–

849. <https://doi.org/10.1007/s11069-023-05885-3>

Beverly, J.L., Leverkus, S.E.R., Cameron, H., Schroeder, D., 2020. Stand-level fuel reduction treatments

and fire behaviour in Canadian boreal conifer forests. *Fire* 3, 1–23.

<https://doi.org/10.3390/fire3030035>

Burnham, K.P., Anderson, D.R., 2002. Model Selection and Multimodel Inference, 2nd ed. Springer New York, New York, NY. <https://doi.org/10.1007/b97636>

Butler, B.W., Ottmar, R.D., Rupp, T.S., Jandt, R., Miller, E., Howard, K., Schmoll, R., Theisen, S., Vihnanek, R.E., Jimenez, D., 2013. Quantifying the effect of fuel reduction treatments on fire behavior in boreal forests. *Can. J. For. Res.* 43, 97–102. <https://doi.org/10.1139/cjfr-2012-0234>

Byram, G.M., 1959. Combustion of forest fuels, in: Davis, K.P. (Ed.), *Forest Fire: Control and Use*. NY: McGraw-Hill, New York, pp. 61–89. <https://doi.org/10.2307/1932261>

Cameron, H., 2020. Predicting Fuel Characteristics of Black Spruce Stands Using Airborne Laser Scanning (ALS) in the Province of Alberta, Canada 1–121.

Canadian Forest Service Fire Danger Group, 2021. An overview of the next generation of the Canadian Forest Fire Danger Rating System. (Information Report GLC-X-26).

Celisse, A., 2014. Optimal cross-validation in density estimation with the L2-loss. *Ann. Stat.* 42, 1879–1910. <https://doi.org/10.1214/14-AOS1240>

Challa, N., 2023. Artificial Intelligence for Object Detection and its Metadata 2, 121–133. <https://doi.org/10.17605/OSF.IO/FG3SQ>

Christianson, A.C., Sutherland, C.R., Moola, F., Gonzalez Bautista, N., Young, D., MacDonald, H., 2022. Centering Indigenous Voices: The Role of Fire in the Boreal Forest of North America. *Curr. For. Reports* 8, 257–276. <https://doi.org/10.1007/s40725-022-00168-9>

Cruz, M.G., Alexander, M.E., 2017. Modelling the rate of fire spread and uncertainty associated with the onset and propagation of crown fires in conifer forest stands. *Int. J. Wildl. Fire* 26, 413–426.

<https://doi.org/10.1071/WF16218>

Cruz, M.G., Alexander, M.E., Wakimoto, R.H., 2005. Development and testing of models for predicting crown fire rate of spread in conifer forest stands. *Can. J. For. Res.* 35, 1626–1639.

<https://doi.org/10.1139/x05-085>

Falkowski, P., Scholes, R.J., Boyle, E., Canadell, J., Canfield, D., Elser, J., Gruber, N., Hibbard, K., Hogberg, P., Linder, S., Mackenzie, F.T., Moore, B., Pedersen, T., Rosental, Y., Seitzinger, S., Smetacek, V., Steffen, W., 2000. The global carbon cycle: A test of our knowledge of earth as a system. *Science* (80-). 290, 291–296. <https://doi.org/10.1126/science.290.5490.291>

Filkov, A.I., Duff, T.J., Penman, T.D., 2018. Improving fire behaviour data obtained from wildfires. *Forests* 9, 1–21. <https://doi.org/10.3390/f9020081>

Fire Behavior Prediction (FBP) Fuel Types, 2023.

Forestry Canada Fire Danger Group, 1992. Development of the Canadian Forest Fire Behavior Prediction System. Inf. Rep. ST-X-3.

Government of Alberta, 2024. How We Fight Wildfires [WWW Document]. URL <https://www.alberta.ca/how-we-fight-wildfires> (accessed 6.1.24).

Government of Alberta, 2016. Wildfire Crew Leader Training Manual.

Guo, X., Coops, N.C., Tompalski, P., Nielsen, S.E., Bater, C.W., John Stadt, J., 2017. Regional mapping of vegetation structure for biodiversity monitoring using airborne lidar data. *Ecol. Inform.* 38, 50–61. <https://doi.org/10.1016/j.ecoinf.2017.01.005>

Hart, H., Perrakis, D.D.B., Taylor, S.W., Bone, C., Bozzini, C., 2021. Georeferencing Oblique Aerial Wildfire Photographs: An Untapped Source of Fire Behaviour Data. *Fire* 4, 81.

<https://doi.org/10.3390/fire4040081>

Helbig, M., Pappas, C., Sonnentag, O., 2016. Permafrost thaw and wildfire: Equally important drivers of boreal tree cover changes in the Taiga Plains, Canada. *Geophys. Res. Lett.* 43, 1598–1606.

<https://doi.org/10.1002/2015GL067193>

Higuera, P.E., 2019. First- and Second-Order Fire Effects, in: *Encyclopedia of Wildfires and Wildland-Urban Interface (WUI) Fires*. Springer International Publishing, Cham, pp. 1–3.

https://doi.org/10.1007/978-3-319-51727-8_258-1

Hirsch, K.G., 1996. Canadian Forest Fire Behavior Prediction (FBP) System: user's guide. Special Report 7. Edmonton, Alberta.

Hsieh, R., 2023. Alberta Wildfire Detection Challenge: Operational Demonstration of Six Wildfire Detection Systems.

Kelsall, J.P., Telfer, E.S., Wright, T.D., 1977. The effects of fire on the ecology of the boreal forest, with particular reference to the Canadian north: a review and selected bibliography, Occasional Paper 32.

LABED, S., TOUATÍ, H., HERÍDA, A., KERBAB, S., SAİRÍ, A., 2023. An AI-based Image Recognition System for Early Detection of Forest and Field Fires. *Eur. J. For. Eng.* 9, 48–56.

<https://doi.org/10.33904/ejfe.1322396>

Lawson, B.D., Armitage, O.B., 2008. Weather Guide Canadian Forest Fire Danger Rating System, Canadian Forest Service Northern Forestry Centre.

Lawson, B.D., Armitage, O.B., Hoskins, W.D., 1996. Diurnal Variation in the Fine Fuel Moisture Code: Tables and Computer Source Code. Victoria, BC.

- Lim, K., Treitz, P., Wulder, M., St-Onge, B., Flood, M., 2003. LiDAR remote sensing of forest structure. *Prog. Phys. Geogr.* 27, 88–106. <https://doi.org/10.1191/0309133303pp360ra>
- Lüdecke, D., 2020. sjPlot: Data Visualization for Statistics in Social Science. <https://doi.org/10.5281/zenodo.1308157>
- MNP LLP, 2020. Spring 2019 Wildfire Review.
- Natural Regions Committee, 2006. Natural Regions and Subregions of Alberta, Pub. No. T/852. Government of Alberta.
- Natural Resources Canada, 2005. The State of Canada's Forests 2004-2005: The Boreal Forest. Canadian Forest Service, Headquarters, Planning, Operations and Information Branch, Ottawa.
- Patterson, E.M., McMahon, C.K., 1984. Absorption characteristics of forest fire particulate matter. *Atmos. Environ.* 18, 2541–2551. [https://doi.org/10.1016/0004-6981\(84\)90027-1](https://doi.org/10.1016/0004-6981(84)90027-1)
- Phelps, N., Cameron, H., Forbes, A.M., Schiks, T., Schroeder, D., Beverly, J.L., 2022. The Alberta Wildland Fuels Inventory Program (AWFIP): data description and reference tables. *Ann. For. Sci.* 79, 1–16. <https://doi.org/10.1186/s13595-022-01144-w>
- Potter, B.E., 2012. Atmospheric interactions with wildland fire behaviour I. Basic surface interactions, vertical profiles and synoptic structures. *Int. J. Wildl. Fire* 21, 779–801. <https://doi.org/10.1071/WF11128>
- Pyne, S.J., Wynn, G., 2008. *Awful Splendour, Awful Splendour*. University of British Columbia Press. <https://doi.org/10.59962/9780774855853>
- R Core Team, 2017. R: A language and environment for statistical computing.

- Reinhardt, E.D., Keane, R.E., Brown, J.K., 2001. Modeling fire effects. *Int. J. Wildl. Fire* 10, 373–380.
<https://doi.org/10.1071/wf01035>
- Rossa, C.G., Davim, D.A., Sil, Â., Fernandes, P.M., 2024. Field-based generic empirical flame length-fireline intensity relationships for wildland surface fires. *Int. J. Wildl. Fire* 33.
<https://doi.org/10.1071/WF23127>
- Rowe, S., 1970. Spruce and Fire in Northwest Canada and Alaska 245–254.
- Sikkink, P.G., Lutes, D.C., Keane, R.E., 2009. *Field Guide for Identifying Fuel Loading Models*. Fort Collins, CO.
- Stocks, B.J., Lynham, T.J., Lawson, B.D., Alexander, M.E., Wagner, C.E. Van, McAlpine, R.S., Dubé, D.E., 1989. The Canadian Forest Fire Danger Rating System: An Overview. *For. Chron.* 65, 450–457.
<https://doi.org/10.5558/tfc65450-6>
- Taylor, S.W., Alexander, M.E., 2018. *Field guide to the Canadian Forest Fire Behavior Prediction (FBP) System*, 3rd Edition., 3rd ed. Natural Resources Canada, Edmonton, Alberta.
- Tymstra, C., Rogeau, M.-P., Wang, D., 2016. Alberta wildfire regime analysis. *Alberta wildfire regime Anal. /* <https://doi.org/10.5962/bhl.title.113828>
- Van Wagner, C.E., 1987. Development and structure of the Canadian forest fire weather index system, *Forestry*.
- Van Wagner, C.E., 1977a. Conditions for the start and spread of crown fire. *Can. J. For. Res.* 7, 23–34.
<https://doi.org/10.1139/x77-004>
- Van Wagner, C.E., 1977b. A method of computing fine fuel moisture content throughout the diurnal cycle. Canadian Forestry Service. Petawawa Forest Experiment Station, Information Report PS-X-

69. Chalk River, Ontario.

Van Wagner, C.E., 1974. Structure of the Canadian forest fire weather index. Dep. Environ. - Can. For. Serv. Publ. 37 pp.

Viereck, L.A., 1983. The Effects of Fire in Black Spruce Ecosystems. Role Fire North. Cirumpolar Ecosyst. 201–220.

Wehr, A., Lohr, U., 1999. Airborne laser scanning - An introduction and overview. ISPRS J. Photogramm. Remote Sens. 54, 68–82. [https://doi.org/10.1016/S0924-2716\(99\)00011-8](https://doi.org/10.1016/S0924-2716(99)00011-8)

Westreich, D., Cole, S.R., Funk, M.J., Brookhart, M.A., Stürmer, T., 2011. The role of the c -statistic in variable selection for propensity score models. Pharmacoepidemiol. Drug Saf. 20, 317–320. <https://doi.org/10.1002/pds.2074>

White, R.G., 2016. Aerial ocular assessments of forest regeneration in northwestern Ontario: A case study. Peterborough, ON.

Williamson, G.J., Price, O.F., Henderson, S.B., Bowman, D.M.J.S., 2013. Satellite-based comparison of fire intensity and smoke plumes from prescribed fires and wildfires in south-eastern Australia. Int. J. Wildl. Fire 22, 121–129. <https://doi.org/10.1071/WF11165>

Wotton, B.M., Alexander, M.E., Taylor, S.W., 2009. Updates and revisions to the 1992 Canadian Forest Fire Behavior Prediction System, Information Report GLC-X-10. Natural Resources Canada Canadian Forest Service, Great Lakes Forestry Centre.

Wotton, B.M., Beverly, J.L., 2007. Stand-specific litter moisture content calibrations for the Canadian Fine Fuel Moisture Code. Int. J. Wildl. Fire 16, 463. <https://doi.org/10.1071/WF06087>

Wright, H.E., Heinselman, M.L., 2014. The Ecological Role Of Fire In Natural Conifer Forests Of Western

And Northern North America—Introduction. *Fire Ecol.* 10, 4–13.

<https://doi.org/10.4996/fireecology.1003001>

Appendix

Table 26 Extended statistics for the E-FIRE1 GLM model. Logit variables are probability coefficients relative to the intercept variable, log odds are the exponent of the logit variable and represent odds relative to the intercept variable. Statistical significance of model parameters and their levels were tested using chi square tests.

Model: E-FIRE1

Call: Smoke Colour + BUI + Precipitation + Smoke Continuity + DENSE3

C-Statistic: 0.90203125 AIC Reduction: 23.73958326

Accuracy: 0.930556 Kappa: 0.1916168

General Variable

Significance (ANOVA)	Deg Freedom	Deviance	Resid. Deviance	Pr(>Chi)
Smoke colour	2	24.865	114.070	<0.0001 ***
BUI	1	2.9395	89.205	0.08644 .
Precipitation	1	2.3281	86.266	0.12706
DENSE3	1	3.0173	80.921	0.08238 .

Logit Breakdown

Variable	Estimate	Std. Error	Z-Value	Pr(> z)
(Intercept)	-6.433	1.2694	-5.07	<0.0001 ***
Brown-grey smoke	1.8395	0.7883	2.33	0.0196 *
Black-grey smoke	3.6384	0.7989	4.55	<0.0001 ***
BUI	0.0225	0.0109	2.07	0.0384 *
Precipitation	0.1195	0.0576	2.07	0.038 *
DENSE3 closed	1.3389	0.8555	1.57	0.1176

Log Odds Breakdown

Variable	Estimate	Std. Error	Z-Value	
(Intercept)	0.001607604	3.55861	0.006295776	-
Brown-grey smoke	6.293222444	2.199557	10.31500236	-
Black-grey smoke	38.02910814	2.222992	95.05583588	-
BUI	1.022791191	1.010943	7.929798288	-
Precipitation	1.12689879	1.059279	7.960794759	-
DENSE3 closed	3.814980904	2.352519	4.783227588	-

Significance codes: p<0.001=*** (v. strong sig.), p<0.01=** (strong sig.), p<0.05=*(significant), p<0.10=. (weak sig.)

Table 27 Expanded statistics for EL-FIRE1 and associated parameters. Logit variables are probability coefficients relative to the intercept variable, log odds variables are odds relative to the intercept variable. Statistical significance of model parameters and their levels were tested using chi square tests.

Model: EL-FIRE1

Call: Crew Fire call + Weather Overhead + 100 m Structure Class + RH + BUI Rank

C-Statistic: 0.790613904 **AIC Reduction:** 56.11787199

Accuracy: 0.94 **Kappa:** -0.004

General Variable	Deg Freedom	Deviance resid.	Resid. Deviance	Pr(>Chi)
Significance (ANOVA)				
Crew Fire type	2	25.2898	623.06	<0.0001 ***
Weather Overhead	4	26.1302	596.93	<0.0001 ***
LiDAR 100 m Structure Class	6	20.8224	576.11	0.001974 **
RH	1	10.1653	565.95	0.001431 **
BUI Rank	4	9.7103	556.24	0.045601 *

Logit Breakdown

Variable	Estimate	Std. Error	Z-Value	Pr(> z)
(Intercept)	0.2492	0.8	0.3	0.749533
Ground Fire	-1.434	0.4	-3.8	0.000155 ***
Surface fire	-1.378	0.3	-4.8	<0.0001 ***
CB Wet	-1.575	0.5	-3.3	0.000814 ***
Clear skies	0.1079	0.3	0.3	0.736979
Cloudy	-0.6479	0.4	-1.8	0.073174 .
Raining	-1.021	0.6	-1.7	0.084725 .
Structure2	0.6479	0.5	1.4	0.156479
Structure 3	-0.5207	0.7	-0.7	0.482219
Structure 4	-15.39	681.2	0.0	0.981977
Structure 6	-0.2197	0.5	-0.4	0.68745
Structure 7	0.2861	0.6	0.4	0.656027
Structure 8	-15.27	1923.0	0.0	0.993663
RH	-0.02693	0.0	-2.8	0.005855 **
High BUI	-0.9751	0.5	-2.1	0.033712 *
Low BUI	-0.5455	0.5	-1.1	0.278258
Moderate BUI	-0.5193	0.4	-1.2	0.235989
Very High BUI	0.01179	0.4	0.0	0.978566

Log Odds Breakdown

Variable	Estimate	Std. Error	Z-Value	
(Intercept)	1.28	2.18	1.38	-
Ground Fire	0.24	1.46	0.02	-
Surface fire	0.25	1.33	0.01	-
CB Wet	0.21	1.60	0.04	-

Clear skies	1.11	1.38	1.40	-
Cloudy	0.52	1.44	0.17	-
Raining	0.36	1.81	0.18	-
Structure2	1.91	1.58	4.12	-
Structure 3	0.59	2.10	0.50	-
Structure 4	0.00	Inf	0.98	-
Structure 6	0.80	1.73	0.67	-
Structure 7	1.33	1.90	1.56	-
Structure 8	0.00	Inf	0.99	-
RH	0.97	1.01	0.06	-
High BUI	0.38	1.58	0.12	-
Low BUI	0.58	1.65	0.34	-
Moderate BUI	0.59	1.55	0.31	-
Very High BUI	1.01	1.55	1.03	-

Significance codes: p<0.001=*** (v. strong sig.), p<0.01=** (strong sig.), p<0.05=*(significant), p<0.10 =. (weak sig.)

Table 28 Expanded statistics for the C-FIRE1 generalized linear model. Logit variables are probability coefficients relative to the intercept variable, log odds variables are odds relative to the intercept variable. Statistical significance of model parameters and their levels were tested using chi square tests.

C-FIRE1

Call: Crown Involvement + Smoke Continuity + Wind Speed

C-Statistic: 0.885855379 **AIC Reduction:** 110.754311

Accuracy: 0.86 **Kappa:** 0.64

General Variable	Significance (ANOVA)	Deg. Freedom	Deviance resid.	Resid. Deviance	Pr(>Chi)
NULL				315.1	
Crown Involvement		4	107.849	207.25	<0.0001 ***
Smoke Continuity		2	14.654	192.59	0.0006575 ***
Wind Speed		1	4.251	188.34	0.0392256 *

Logit Breakdown

Variable	Estimate	Std. Error	Z-Value	Pr(> z)
(Intercept)	-3.79	0.71	-5.37	<0.0001 ***
Light Candling	-0.60	0.64	-0.94	0.35
Heavy Torching	1.29	0.60	2.16	0.030924 *
Intermittent Crowning	1.72	0.82	2.11	0.035023 *
Continuous Crowning	2.80	0.76	3.70	0.000218 ***
Continuous Smoke	0.67	0.77	0.88	0.38
Heavy Smoke	2.37	0.81	2.93	0.003412 **
Wind Speed	0.07	0.03	2.06	0.039173 *

Log Odds Breakdown

Variable	Estimate	Std. Error	Z-Value	
(Intercept)	0.02	2.02	0.00	-
Light Candling	0.55	1.90	0.39	-
Heavy Torching	3.62	1.81	8.65	-
Intermittent Crowning	5.58	2.26	8.23	-
Continuous Crowning	16.52	2.13	40.35	-
Continuous Smoke	1.96	2.15	2.40	-
Heavy Smoke	10.70	2.25	18.69	-
Wind Speed	1.07	1.03	7.86	-

Significance codes: p<0.001=*** (v. strong sig.), p<0.01=** (strong sig.), p<0.05=*(significant), p<0.10=. (weak sig.)

Table 29 Expanded statistics for CL-FIRE1. Logit variables are probability coefficients relative to the intercept variable, log odds variables are odds relative to the intercept variable. Statistical significance of model parameters and their levels were tested using chi square tests.

Model: CL-FIRE1

Call: Fire Type + 100 m Structure Class + Weather overhead + BUI Rank + Wind Speed + Temp

C-Statistic: 0.781244658 **AIC Reduction** 297.3959887

Accuracy: 0.81 **Kappa:** 0.34

General Variable significance

Variable	Deg Freedom	Deviance resid.	Resid. Deviance	Pr(>Chi)
Fire Type	2	204.242	1606.8	<0.0001 ***
100 m Structure Class	6	48.691	1558.1	<0.0001 ***
Weather Overhead	4	39.549	1518.5	<0.0001 ***
BUI Rank	4	23.947	1494.6	<0.0001 ***
Wind Speed	1	12.495	1482.1	0.000408 ***
Temp	1	6.471	1475.6	0.010963 *

Logit Breakdown

Variable	Estimate	Std. Error	Z-Value	Pr(> z)
(Intercept)	-0.49122	0.56152	-0.875	0.381683
Ground Fire	-2.08368	0.21499	-9.692	<0.0001 ***
Surface Fire	-2.00677	0.1605	-12.503	<0.0001 ***
Structure 2	0.87195	0.27975	3.117	0.001828 **
Structure 3	0.35822	0.35806	1	0.31709
Structure 4	-0.88582	0.55088	-1.608	0.107835
Structure 6	-0.17426	0.32708	-0.533	0.594178
Structure 7	0.22632	0.38383	0.59	0.555432
Structure 8	-0.06568	0.91527	-0.072	0.942793
CB Wet	-0.80395	0.23018	-3.493	0.000478 ***
Clear Skies	0.19876	0.19655	1.011	0.311887
Cloudy	-0.37289	0.20919	-1.783	0.074651 .
Raining	-0.69483	0.33418	-2.079	0.037597 *
BUI High	-0.75027	0.25396	-2.954	0.003133 **
BUI Low	-0.81188	0.28795	-2.82	0.004809 **
BUI Moderate	-1.0899	0.25977	-4.196	<0.0001 ***
BUI Very High	-0.55479	0.26479	-2.095	0.036150 *
Wind Speed	0.04273	0.01125	3.797	0.000146 ***
Temp	0.039	0.01559	2.502	0.012353 *

Log Odds Breakdown

Variable	Estimate	Std. Error	Z-Value	
(Intercept)	0.6118807	1.753336	4.17E-01	-
Ground Fire	0.1244717	1.239856	6.18E-05	-
Surface Fire	0.1344224	1.174103	3.72E-06	-
Structure 2	2.3915741	1.322801	2.26E+01	-
Structure 3	1.4307781	1.430545	2.72E+00	-
Structure 4	0.4123751	1.734786	2.00E-01	-
Structure 6	0.8400744	1.386911	5.87E-01	-

Structure 7	1.2539779	1.467894	1.80E+00	-
Structure 8	0.9364302	2.497451	9.31E-01	-
CB Wet	0.4475561	1.258833	3.04E-02	-
Clear Skies	1.2198932	1.217194	2.75E+00	-
Cloudy	0.6887384	1.232673	1.68E-01	-
Raining	0.499159	1.396793	1.25E-01	-
BUI High	0.4722379	1.289114	5.21E-02	-
BUI Low	0.4440231	1.333687	5.96E-02	-
BUI Moderate	0.3362511	1.296638	1.51E-02	-
BUI Very High	0.5741911	1.303154	1.23E-01	-
Wind Speed	1.0436554	1.011317	4.46E+01	-
Temp	1.0397715	1.015711	1.22E+01	-

Significance codes: p<0.001=*** (v. strong sig.), p<0.01=** (strong sig.), p<0.05=*(significant), p<0.10 =. (weak sig.)